ISTANBUL TECHNICAL UNIVERSITY ★ ENERGY INSTITUTE

CARBON NANOTUBE SYNTHESIS WITH DIFFERENT CATALYSTS

M.Sc. Thesis by
Ezgi DÜNDAR TEKKAYA

Department : Energy Institute

Programme : Energy Science & Technology

JUNE 2011

İSTANBUL TECHNICAL UNIVERSITY ★ ENERGY INSTITUTE

CARBON NANOTUBE SYNTHESIS WITH DIFFERENT CATALYSTS

M.Sc. Thesis by
Ezgi DÜNDAR TEKKAYA
(301091047)

Date of submission :   06 May 2011
Date of defence examination: 07 June 2011

Supervisor (Chairman) :	**Assoc. Prof. Dr. Nilgün KARATEPE YAVUZ (ITU)**
Members of the Examining Committee :	**Assoc. Prof. Dr. Nilgün BAYDOĞAN (ITU)**
	Assoc. Prof. Dr. Yeşim HEPUZER GÜRSEL (ITU)

JUNE 2011

İSTANBUL TEKNİK ÜNİVERSİTESİ ★ ENERJI ENSTİTÜSÜ

FARKLI KATALİZÖRLERLE KARBON NANOTÜP SENTEZİ

YÜKSEK LİSANS TEZİ
Ezgi DÜNDAR TEKKAYA
(301091047)

Tezin Enstitüye Verildiği Tarih :   06 Mayıs 2011
Tezin Savunulduğu Tarih :   07 Haziran 2011

Tez Danışmanı :   Doç. Dr. Nilgün KARATEPE YAVUZ
(İTÜ)
Diğer Jüri Üyeleri :   Doç. Dr. Nilgün BAYDOĞAN
(İTÜ)
Doç. Dr. Yeşim HEPUZER GÜRSEL
(İTÜ)

HAZİRAN 2011

FOREWORD

May 2011

Ezgi Dündar Tekkaya
Metallurgical and Materials Engineer

TABLE OF CONTENTS

ABBREVIATIONS

CNT	: Carbon Nanotube
CVD	: Chemical Vapour Deposition
CCVD	: Catalytic Chemical Vapour Deposition
SWCNT	: Single Wall Carbon Nanotube
MWCNT	: Multi Wall Carbon Nanotube
TGA	: Thermal Gravimetric Analysis
TEM	: Transmission Electron Microscope
RBM	: Radial Breathing Mode
Synt.	: synthesised

LIST OF TABLES

LIST OF FIGURES

CARBON NANOTUBE SYNTHESIS WITH DIFFERENT CATALYSTS

SUMMARY

The discovery of carbon nanotubes (CNTs) in 1991 attracted a great deal of attention. CNTs are today one of the key elements of nanotechnology and are among most intensively investigated materials. CNTs with their high mechanical, electrical, thermal and chemical properties are regarded as promising materials for many different potential applications. Having unique properties they can be used in a wide range of fields such as electronic devices, electrodes, drug delivery systems, batteries, hydrogen storage, textile etc.

Catalytic chemical vapor deposition (CCVD) is a common method of CNT synthesis especially for mass production. Catalyst impregnated on a suitable substrate is important for synthesis with chemical vapor deposition (CVD) method. Different catalyst and substrate materials are used in CNT synthesis by CCVD method.

In this study, CNTs were synthesized by CCVD with carbon source of acetylene (C_2H_2) on magnesium oxide (MgO) powder substrate impregnated by different catalyst materials such as iron (Fe), cobalt (Co), nickel (Ni), and vanadium (V), respectively. In this study, CNT syntheses were performed under different conditions. Catalysts were prepared with catalyst to MgO ratios of 1:100, 5:100 and 10:100. The duration of syntheses were selected as 30 and 60 minutes. The syntheses temperature was selected to be 500 and 800 °C for definite weight ratios of catalysts depending on the results of the conducted experiments. In order to evaluate interaction between metal catalysts during CNT synthesis binary catalysts of Fe and Co couple is examined. The synthesized CNTs were characterized by thermal gravimetric analysis (TGA), transmission electron microscopy (TEM) and Raman spectroscopy. Thus, the carbon efficiencies of synthesized CNTs with different catalysts were determined and compared.

FARKLI KATALİZÖRLERLE KARBON NANOTÜP SENTEZLENMESİ

ÖZET

Karbon nanotüplerin 1991 yılında keşfedilmeleri büyük ilgi uyandırmıştır. Karbon nanotüpler günümüzde nano teknolojinin vazgeçilmez unsurlarındandır ve yoğun olarak araştırılan malzemelerdir. Mekanik, kimyasal, ısıl ve elektriksel özelliklerinin çok iyi olması sebebiyle karbon nanotüpler birçok farklı potansiyel uygulama için umut vaat etmektedir. Sahip oldukları eşsiz özellikler ile elektronik malzemeler, piller, elektrotlar, ilaç taşıma sistemleri, hidrojen depolama, tekstil gibi çok çeşitli alanlarda kullanılabilmektedirler.

Katalitik kimyasal buhar birikimi (KKBB) yöntemi karbon nanotüp sentezinde ve özellikle seri üretimde yaygın olarak kullanılan bir yöntemdir. Uygun bir substrat üzerine doyurulmuş katalizör, katalitik kimyasal buhar birikimi yöntemi ile sentezlemede önemlidir. Katalitik kimyasal buhar depolama yöntemi ile karbon nanotüp sentezinde çeşitli katalizör ve substrat malzemeler kullanılmaktadır.

Bu çalışmada; demir (Fe), kobalt (Co), nikel (Ni), vanadyum (V) gibi metaller toz halindeki magnezyum oksit (MgO) substrat malzemesi ile doyurulmuş, elde edilen katalizörler ve karbon kaynağı olan asetilen (C_2H_2) ile KKBB yöntemi uygulanarak karbon nanotüpler sentezlenmiştir. Karbon nanotüp sentezi farklı koşullarda gerçekleştirilmiş: sentez süresi 30 ve 60 dakika, sentez sıcaklığı belirli katalizör substrat oranları için 500 ve 800°C olarak seçilmiştir. Metal katalizörlerin birbirleriyle olan etkileşimini incelemek amacıyla demir ve kobalt ikili katalizörü ile de karbon nanotüpler sentezlenmiştir. Sentezlenen karbon nanotüplerin karakterizasyonunda termogravimetrik analiz (TGA), Raman spektroskopisi, geçirimli elektron mikroskobu (TEM) gibi teknikler kullanılmıştır. Bu tekniklerle, farklı katalizörler kullanılarak sentezlenen karbon nanotüplerin karbon verimleri belirlenmiş ve karşılaştırılmıştır.

1. INTRODUCTION

In the last decade due demand of new generation of high technology materials, there is a tremendous interest in nanotechnology [1]. Due to their marvellous material properties nanomaterials differ from the isolated atom and the bulk phase. Nanotechnology aims production and improvement of smaller, cheaper, lighter, faster devices with more functionality, and less raw material and energy. Therefore, nanotechnology deals with materials having a size of 1-100 nano-meter (nm). The properties of the material change as the material size decreases. When the nanomaterials are considered, surface behaviour of the material dominates the behaviour of the overall material. Nanomaterials have unique mechanical, electrical, and optical properties. Therefore, they can be implicated to many fields such as electronics, chemicals, sensors, energy storage, and biotechnology.

The identification of the structure of fullerenes in 1985 by Kroto and his friends was a breakthrough in nanotechnology [2]. It was followed by the discovery of multi walled carbon nanotubes (MWCNT) in 1991 and single wall nanotubes in 1993 by lijima [3,4]. Thereafter the highly intensified research into the science of nanotechnology started due to superior mechanical strength, electronic properties, large surface area for adsorption of hydrogen, and high aspect ratio of CNTs [5,6,7,8]. They have many applications in different fields such as electronics, textile, electrodes, drug delivery systems, field emission applications, magnetic field applications, hydrogen adsorption.

CVD is an important method for CNT synthesis especially when mass production is concerned. There are different parameters (synthesis method, catalyst, substrate, carbon source, synthesis time) affecting the structure, morphology and the amount of the CNT synthesised. The catalyst plays an important role in growth of CNT. There are many studies in the literature about different catalysts such as iron, cobalt, nickel, vanadium, copper, titanium etc. and their binary combinations [5-8]. Regard to this, the purpose of this study is examine and compare the impact of different catalysts on CNT synthesis by CCVD method with changing parameters of temperature, time and weight ratio of the catalyst to the selected substrate material.

2. CARBON NANOTUBES

2.1   Carbon Structures

Carbon which is the basic element in living things can be found in the nature as well as being produced in the laboratory conditions. It can form compounds with different elements having changing type, number and strength of bonds. This diversity leads carbon to have isomers from zero dimension to three dimension.

The properties of carbon atom are a natural result of distribution of electrons around its nucleus. There are six electrons in a carbon atom, shared evenly by 1s, 2s and 2p orbitals. Since 2p orbital has two electrons carbon can make up to four bonds with other elements. Carbon can bind with sigma (σ) and pi (π) bond while forming a molecule. The final structure of the molecule depends on the hybridisation of the orbitals. A carbon atom with sp^1 hybridisation can make two σ and two π bonds while with sp^2 hybridisation can make three σ and three π bonds whereas with sp^3 hybridisation a carbon atom forms four σ bonds.

The number and nature of the bonds determine the geometry and properties of carbon allotropes, as shown in Figure 2.1 [9] . In nature carbon is mainly found as coal or natural graphite. However diamond is not found so commonly. Buckminsterfullerene (C_{60}), lonsdaleite, C_{450} fullerene, C_{70} fullerene, amorphous carbon, and CNT are other allotropes of carbon [10].

Graphite is made of atoms layered in a honeycomb structure with planar sp^2 hybridized carbon atoms. The carbon atoms in a graphite sheet are bonded with three electrons to each other which supplies a free movement for electrons from an unhybridized p orbital to another forming electrical conductivity of the graphite [9]. The geometry of the chemical bonds makes graphite a soft, slippery, opaque and electrically conductive material.

Diamond has a tetrahedral crystal structure where each hybridized carbon atom is bonded to four other atoms with sp^3 σ bonds. It exists in cubic and hexagonal form

[11]. Diamond is a wide gap semiconductor (5.47 eV) , hardest material in nature (Mohs hardness 10), has the highest thermal conductivity (~25 $W.cm^{-1}.K^{-1}$) known and the highest melting point (4500 K) due to its crystal structure . The sp^3 hybridization gives electrical insulation and optical transparency.

Amorphous carbon is a highly disoriented material with mainly sp^2 bonds and a low percentage of sp^3. It only has a short range order depending on the carbon bonding type and hydrogen content. Glassy carbon is another carbon material formed by degradation of polymers at temperature between 900 to 1000 ºC [12].

Buckminsterfullerenes have groups of molecules with spherical or cylindrical shape having atoms with all sp^2 hybridization. It was discovered by Kroto et. al. in 1985 as a result of laser ablation of graphite and named in honour of Buckminster Fuller for its resemblance to geodesic spheres developed by him[3]. C_{60} which is an icosahedral, like a soccer ball molecule with sixty carbon atoms bonded together with pentagons and hexagons was the first fullerene discovered. The stable form of the carbon clusters depend on the number of atoms. The most stable form of carbon clusters are: linear chains up to ten atoms ring for ten to thirty atoms, cage structures above forty atoms. C_{70}, C_{78} and C_{80} are other stable fullerenes.

Carbon nanofibers form an important group of graphite related carbon materials and are also very closely related to carbon nanotubes. Pitch fibre that is commercially available possess high bulk modulus and thermal conductivity whereas other commercial fiber so called polyacrylonitrile fiber is known with its high tensile strength [13]. The vapour grown as-synthesized carbon nanofibers have an onion skin and tree ring morphology. After heat treatment about 2500 ºC their shape resemble very much like carbon nanotubes.
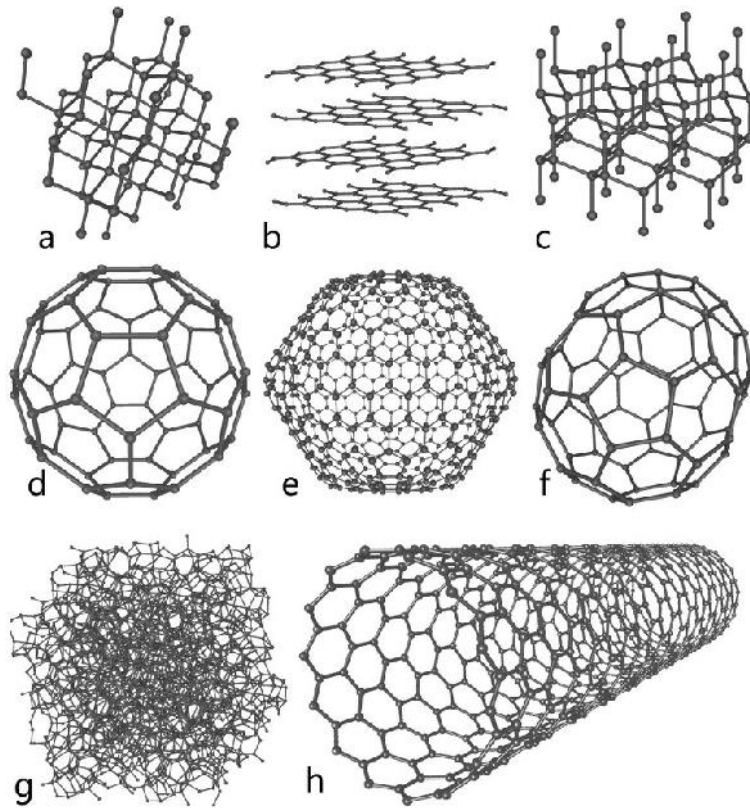
Figure 2.1 : Allotropes of carbon

The image is released by Michael Ströck under the GNU Free Documentation License: The structures of eight allotropes of carbon: a) Diamond b) Graphite c) Lonsdaleite d) C60 (Buckminsterfullerene) e) C540 Fullerene f) C70 Fullerene g) Amorphous carbon h) Single-walled carbon nanotube

2.2 Carbon Nanotubes

The discovery of fullerenes by Kroto and his team in 1985 is an important milestone in the path leading us to the CNTs [2]. In 1991 Lijima discovered multiwall carbon nanotubes (MWCNT), two years before Lijima and Bethune et al. discovered single wall carbon nanotubes (SWCNT) in separate researches [3,14]. Before the discovery of CNTs there have been studies on syntheses of carbon nanofibers which is very similar to CNT synthesis. In 1960 Bacon produced graphene scrolls in nanoscale and he suggested existence of CNTs before its discovery [15]. It is possible that scientist making research on carbon fibres might have also produced CNTs as syntheses of both materials require similar methods.

2.2.1 Crystal structure of carbon nanotubes

Carbon nanotubes can be classified as arm chair, zigzag and chiral according to their crystal structures. There are some basic terms to describe crystal structure of CNTs. Figure 2.2 shows one sheet of graphene that is rolled to form a single nanotube with chiral vector (C_h) and primitive translation vector (T) of the tube [16].
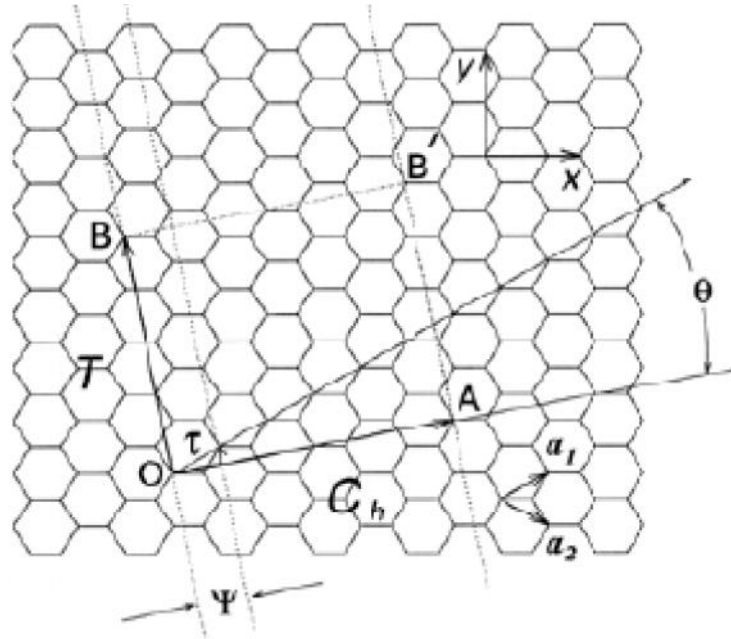
Figure 2.2 : Unit cell of a CNT

To express the circumference of a carbon nanotube chiral vector that is defined by two integers m and n and unit vectors of a graphene sheet is used:

$$c_h = n.a_1 + m.a_2 = (n+m) \tag{2.1}$$

In the figure the chiral vector connects two lattice points A and O having an angle of θ so called chiral angle with the zigzag direction of (n,0). An infinite strip perpendicular to chiral vector is cut through these two points. Diameter of the carbon nanotube and the chiral angle can be found depending on (n,m) values:

$$d_i = \frac{1}{\pi}(\sqrt{n^2 + m^2 + nm})a \tag{2.2}$$

$$\sin \theta = \frac{\sqrt{3}.m}{2\sqrt{n^2 + m^2 + n.m}}$$

When a graphene sheet rolled with a chiral angle of θ, a (n,m) carbon nanotube is formed. There are different types of carbon nanotubes depending on (n,m) values as shown in Figure 2.3 [16]. (n,0) nanotube with a chiral angle of 0° is called zigzag nanotube, (n,n) with a chiral angle of 30° is called armchair nanotube and if n is different from m and chiral angle is between 0° and 30° then it is called chiral nanotube. Different structural parameters of CNTs can be seen in Table 2.1 [16].
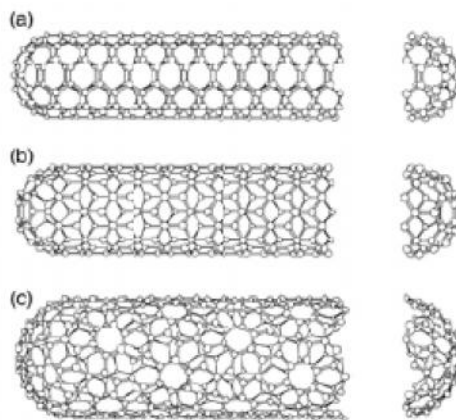
Figure 2.3 : a) armchair (n,n) b) zizag (n,0) c) chiral (n,m) nanotubes

Table 2.1: Structural parameters of CNTs

Symbol	Name	Formula	Value
a	length of unit vector	$a = \sqrt{3}a_{c-c} = 2.49\,Å$	$a_{c-c}=1.44$ Å
a_1,a_2	unit vectors	$\left(\dfrac{\sqrt{3}}{2},\dfrac{1}{2}\right)a, \left(\dfrac{\sqrt{3}}{2},-\dfrac{1}{2}\right)a$	x,y coordinate
b_1,b_2	reciprocal unit vectors		
C_h	chiral vector	$C_h = na_1 + ma_2 = (n+m)$	$, (0\le \lvert m \rvert \ge n)$
L	length of c_h	$L = \lvert C_h \rvert = a\sqrt{n^2 + m^2 + nm}$	x,y coordinate
d_t	diameter	$d_t = L/\pi$	
θ	chiral angle	$\sin\theta = \dfrac{\sqrt{3}m}{2\sqrt{n^2 + m^2 + nm}}$	$, (0\le \lvert \theta \rvert \ge \dfrac{\pi}{4})$
		$\cos\theta = \dfrac{2n + m}{2\sqrt{n^2 + m^2 + nm}}$	$\tan\theta = \dfrac{\sqrt{3}m}{2n + m}$
d	gcd(n,m)[b)]	$dR= \begin{cases} d \text{ if (n-m) is not multiple of 3} \\ 3d \text{ if (n-m) is multiple of 3d} \end{cases}$	
d_R	gcd(2n+m,2m+n)[b)]		
T	translational vector	$T = t_1 a_1 + t_2 a_2 = (t_1,t_2)$ $t_1 = \dfrac{2m + n}{d_R}, t_2 = -\dfrac{2n + m}{d_R}$	gcd(t_1,t_2)=1[b)]
T	length of **T**	$T = \lvert T \rvert = \dfrac{\sqrt{3}L}{d_R}$	
N	number of hexagons in the nanotube unit cell	$N = \dfrac{(m_2 + n_2 + nm)}{d_R}$	
R	symmetry vector	$R = pa_1 + qa_2 \equiv (p,q)$ $t_1 q - t_2 p = 1,$ $(0 < mp - nq \le N)$	gcd(t_1,t_2)=1[b)]
τ	pitch of **R**	$\left(\dfrac{\sqrt{3}}{2},\dfrac{1}{2}\right)a, \left(\dfrac{\sqrt{3}}{2},-\dfrac{1}{2}\right)a$	x,y coordinate
Ψ	rotation angle of **R**	$\psi = \dfrac{2\pi}{N}$	in radians
M	number of **T** in N**R**	N**R**=C_h+M**T**	

a)In this table n,m,t_1,t_2,p,q are integers and d, d_R, N and M are integer function of these integers
b) gcd(n,m)denotes the greatest common divisor of the two integers n and m

2.2.2 Types of carbon nanotubes

2.2.2.1 Single wall carbon nanotubes

Single wall carbon nanotubes (SWCNT) can be described as the fundamental structural unit of nanotube with one atom thick wall. As shown in Figure 2.4, the structure of a SWCNT is explained in one dimensional unit cell formed by rolling an infinite sheet of graphene having a diameter size distribution of 1-2 nm. [17]. However on zeolite substrate it could be managed to synthesise nanotubes with diameters of 0.4 nm [18]. SWCNTs are generally found in hexagonal crystal structure bundles which are bonded to each other by Van der Waals bonds and can have 100-500 SWCNTs [10, 16, 18, 19].
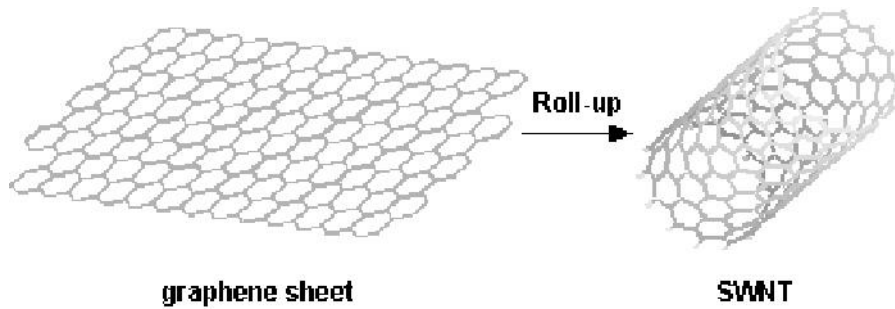
Figure 2.4 : SWCNT

When compared to multi wall carbon nanotubes SWCNTs have an elastic structure that allows them to be straight, bended. SWCNTs have zigzag and armchair structures. Figure 2.5 shows drawing and TEM image of SWCNTs [20].
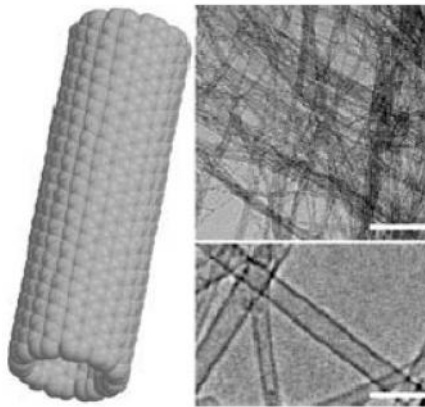
Figure 2.5 : a) drawing of SWCNT, b) 100nm scale TEM image of SWCNT, c) 5nm TEM image of SWCNT

9

2.2.2.2 Multi wall carbon nanotubes

Multiwall carbon nanotubes (MWCNTs) are formed of more than one SWCNTs placed one in other having a shape as shown in Figure 2.6 [21,22]. Lijima initially discovered the existence of MWCNTs with two to 20 layers [4]. MWCNTs have an inner diameter of 0.4-5 nm whereas the outer diameter is 15 nm [23]. The distance between the outer and the inner walls were calculated to be 0.339 nm and it is measured via x-ray diffraction and transmission electron microscope as 0.34-0.39 nm [19, 21, 24, 25]. As the measured distances are larger than the distances between the plates of graphite which is 0.334 nm, it is claimed that the walls are not crystallographically related [24]. Thus the walls of MWCNTs can rotate independently which is crucial for nano machines. Tangles and twists can be observed in MWCNTs as a result defects whereas SWCNTs have better structures. Furhtermore, the ends of MWCNTs may not be spherical all the time.
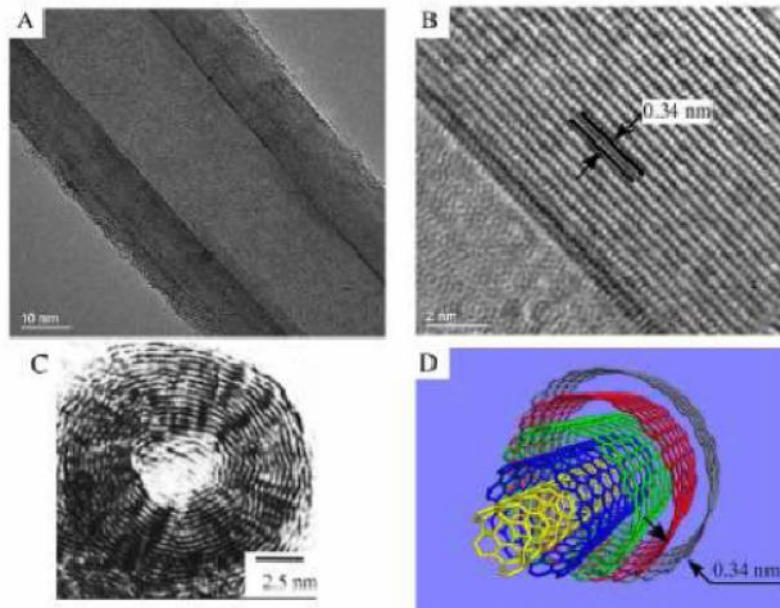
Figure 2.6 : MWCNT (A) Side view from TEM, (B) Side view from HRTEM, (C) Cross section from TEM, (D) Schematic structure of MWCNT

2.2.3 Properties of carbon nanotubes

As one class of nanostructured materials, carbon nanotubes (CNTs) have been receiving much attention due to their remarkable mechanical, optical, and unique electronic properties as well as the high thermal and chemical stability and excellent heat conduction [11].

2.2.3.1   Mechanical properties of carbon nanotubes

The remarkable mechanical properties of CNTs are closely related to carbon-carbon bonds. That is known to be the strongest in nature nanotube is structured with all σ bonding. Thus nanotube is regarded as fiber with the strength in its tube axis. Theoretical and experimental studies show elastic modulus and tensile strength of CNTs are changing in the range of 1000 and tens of GPa respectively [26]. It is known that CNTs have the highest elastic modulus among other materials including graphite [27]. In experimental studies Treacy et al. found the Young's modulus of MWCNT in a wide range of 0.4-4.15 TPa with an average of 1.8 TPa in a transmission electron microscope [6] Thus CNTs   can resist to any physical force applied to its walls.   Table 2.2 summarises the calculated Young's modulus and Tensile strength of CNTs [11].

Table 2.2: Mechanical properties of nanotubes

	Young's Modulus (GPa)	Tensile Strength (GPa)	Density (g/cm^3)
MWCNT	1200	~150	2.6
SWCNT	1054	75	1.3
SWCNT bundle	563	~150	1.3
Graphite (in-plane)	350	2.5	2.6
Steel	208	0.4	7.8

Various types of defect-free nanotubes are generally stronger than graphite. This is a result of increase in the axial component of σ bonding when graphite sheet is rolled to form SWCNT. Young's modulus is dependent on the tube diameter but it is independent of tube chirality. When the tube gets larger its Young's modulus is approaching to graphite but as the tube gets smaller it becomes mechanically stable. When different diameters of SWCNTs form a MWCNT, the Young's modulus will be higher than that of SWCNT as a result of Van der Waals force [11]. However, when SWCNTs form bundles, the Young's modulus will be smaller than a single SWCNT due to weak Van der Waals forces.

Elastic of CNTs is also remarkable. Majority of the hard materials fail with a strain of 1% as result of defects and dislocations. However, both theoretical and experimental studies concluded that CNTs can stand up to 15% tensile strain before fracture [28]. Thus, the tensile strength could be 150 GPa with a Young's modulus of 1TPa.   Salvetat et al. concluded that the elastic and shear modulus of a SWCNT are

1 TPa and 1GPa respectively [29]. As a result of their flexible structure CNTs can be bent repeatedly up to 90° without being broken or damaged.

2.2.3.2 Electrical properties of carbon nanotubes

Depending on the chirality, nanotubes can be either metallic or semiconductor even though they have the same diameter [17]. When a graphite sheet is rolled to form CNT not only the carbon atoms are ordered around the circular structure but also quantum mechanical wave functions of the electrons are ordered accordingly. The electrons are bounded in radial directions by the single layered graphite sheet. There exist periodical boundary conditions around the circle of the nanotube. If there are ten hexagons around nanotube then the eleventh hexagon fits to first hexagon. As a result of the quantum boundaries the electrons are effective only along the nanotube axis enabling the determination of the wave vectors. Thus small diameter nanotubes are either metallic or semiconductors.

According to their electrical properties nanotubes can be classified as large gap, tiny gap and zero gap nanotubes. Theoretical calculations show that electrical properties of nanotubes depend on geometric structure. Graphene is a zero gap semiconductor, according to the theory carbon nanotubes can be metals or semiconductors having different energy gaps depending on diameter and helicity of nanotubes. As the nanotube radius R increases the band gap of large gap and tiny gap nanotubes decrease with $1/R$ and $1/R^2$ dependence, respectively [30-31]. The electrical properties of SWCNTs depend on n and m values:

If n=m; formed armchair nanotube is metallic,

If n-m=3k; k $\in$ Z, k≠0 the nanotube is tiny-gap semiconductor which is metallic at room temperature

If n-m= 3k ± 1; k $\in$ Z, k≠0 the nanotube is large-gap semiconductor

Experimental studies performed by applying electrical field to nanotubes are proving the theoretical calculations. It was observed that SWCNT with a diameter of 0.4 nm became conductive at 20 K. In further experimental studies of electronic properties of nanotubes, it was observed that electrical conductivity is dependent on temperature in the range of 2-300 K [33].

In the measurements of SWCNTs, it was observed that each nanotube acts individually. Conductivity and the resistivity at 300 K is in the range of ~1.2×10^{-4}–5.1×10^{-6}. SWCNT bundles have metallic behaviour with a resistivity of 0.34×10^{-4} to 1.0×10^{-4} whereas copper has a resistivity of 1.7×10^{-6} ohmcm. Thus we can conclude that the electrical resistivity of CNTs is very close to copper's. Metallic nanotubes have remarkable conductivities. Although a CNT bundle can transport a current density of 1×10^9 A/cm^2 copper wires can transport 1×10^6 A/cm^2 which is thousand times less than CNTs' [32].

2.2.3.3 Thermal properties of carbon nanotubes

As well as their electrical and mechanical properties CNTs have a reputation for their thermal properties. Nanomaterials are affected by quantum properties. Low temperature, specific heat and the interaction of CNTs with each other are used to count phonons of CNT. Thermal properties of CNTs have been both theoretically and experimentally investigated. Theoretically thermal conductivity of CNTs is better than graphite. Experimentally, thermal conductivity of SWCNTs was measured to be 200W/mK whereas MWCNTs had an electrical conductivity of 300W/mK [34]. As result of its Fermi level current density, metallic SWCNT is a one dimensional metal. It has a linear electronic thermal capacity at low temperatures. Theoretically MWCNTs are expected to have lower thermal conductivity than graphite which has low thermal conductivity due to weak Van der Waals forces. MWCNTs have only Van der Waals forces between the nanotube layers. Thermal expansion of CNTs is expected to be better than graphite. The thermal conductivity is the ability of material to transport the heat from high temperature region to low temperature region as shown in Formula 2.4 where q is the change of heat in unit time per unit area, k is the thermal conductivity coefficient, and dT/dx is the thermal gradient along the material.

$$q = -k.\frac{dT}{dx}$$

(2.4)

Thermal conductivity of diamond is 1000-2600 W/mK and for graphite it is 120 W/mK at 100°C. Hone et al. calculated the thermal conductivity of an individual SWCNT as 1800-6000 W/mK at room temperature [35]. However in another

research, it was found to be 2980 W/mK and 6600 W/mK at room temperature [38,39]. Thermal conductivity of MWCNTs are found to be in the range of 1800 to 6000 W/mK.

2.2.3.4   Chemical properties of carbon nanotubes

Due to their small radius, large specific surfaces and σ-π hybridisation CNTs have strong sensitivity to chemical interactions. As a result of this fact they are attractive materials for chemical and biological applications [11]. However these properties challenges the characterisation of CNTs and determination of their properties.

Reactivity of CNTs are determined by direction of π orbitals and pyramidisation of the chemical bonds. Some bonds in CNTs are neither perpendicular nor parallel to the tube axis. Therefore π orbitals, which affect the reactivity of the CNT, cannot be properly directed. As the diameter of CNT decreases the reactivity of CNT increases.

As a result of the chemical stability and perfect structure of the CNTs the carrier mobility at high gate fields may not be affected by processing like in the conventional semiconductor channels. Nonetheless, low scattering, with the strong chemical bonding and extraordinary thermal conductivity, allows CNTs to withstand extremely high current densities up to ~109 A/ cm^2 [41].

2.2.4   Synthesis of carbon nanotubes

As CNTs have wide range of applications, the growth techniques which can sustain high purity, and more amount of CNT becomes crucial. CNT synthesis can be achieved by different methods such as:

- Arc discharge
- Laser ablation
- Chemical vapour deposition (CVD)

2.2.4.1   Arc discharge

In 1991 Lijima reported formation of carbon nanotubes with arc discharge method which was previously used for production of fullerenes [3]. The tubes were produced having diameters ranging from 4 to30 nm and having lengths up to 1μm [41].

In arc discharge method as shown in Figure 2.7 a direct current electric arc-discharge is produced in inert gas atmosphere by using two graphite electrodes [4, 42, 43]. The CNTs grow on the negative end of the carbon electrode which produces the direct current while Argon as inert gas passes through the system. In arc discharge method a power supply of low voltage (12 to 25 V) and high current (50 to 120 A) is used. Catalyst, Ar:He gas ratio, the distance between the anode and the cathode, the overall gas pressure are the other parameters affecting the quality and the properties(i.e. diameter, yield percent) of CNT synthesised by arc discharge method [44-46].
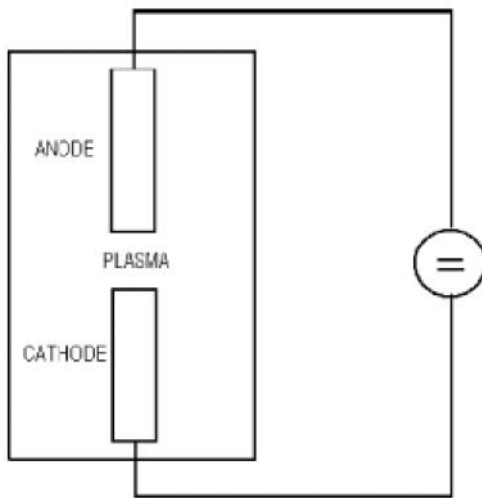
Figure 2.7 : Diagram of arc discharge method

In an arc discharge process CNTs are prepared with a power supply of low voltage (12 to 25 V) and high current (50 to 120 A). While the positive electrode is consumed in the arc discharge gas atmosphere (i.e. Ar, He) CNT bundles are formed on the negative electrode [47]. Length of MWCNTs produced by this method are generally around 1μm having a length to diameter ratio (aspect ratio) of 100 to 1000 [48]. As a result of high aspect ratio and small diameter of the produced MWCNTs they are classified as 1D carbon systems.

It has been reported that existence of catalyst (i.e. Fe, Co etc.) is required in the production of SWCNTs by arc discharge method [4,14,47,48]. Many catalyst compositions can produce MWCNTs but it is observed that Y and Ni mixture yield up to 90% with an average diameter of 1.2 to 1.4 nm [49].

2.2.4.2   Laser ablation

Laser ablation method is very similar to arc discharge method as it also uses a metal impregnated carbon source to produce SMCNT and MWCNT [50,51]. In this method Co to Ni atomic percent of 1.2% and 98.8% of graphite composite in an inert atmosphere around 500 Torr of He or Ar in a quartz tube furnace of 1200ºC [41]. With the treatment of pulsed or continuous laser light, the nano sized metal particles are formed in the vaporized graphite and these particles catalyse the growth of SWCNT and by products.   These products are condensed on the cold finger downstream of the source as shown in Figure 2.8 [41].   Smiley group in Rice University achieved the first large scale production of SWCNTs by laser ablation method in 1996 [48]. The production yield of weight was varying between 20 to 80% SWCNTs. The diameters of produced SWCNTs were between 1.0 to 1.6 nm.
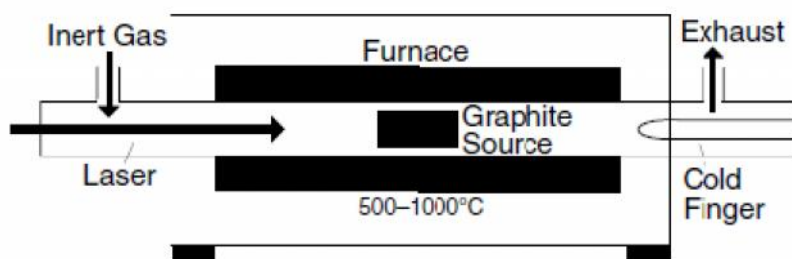
Figure 2.8 : Schematic view of laser ablation furnace

2.2.4.3   Chemical vapour deposition

Different from laser ablation and arc discharge methods, chemical vapour deposition (CVD) which is a thermal synthesis method depends on a thermal source to produce CNTs by breaking down the carbon source generally with existence of catalysis [41]. High pressure CO synthesis, flame synthesis, CVD and plasma enhanced chemical vapour deposition (PECVD) synthesis are methods using thermal source to produce CNTs.

CVD method is deposition of a hydrocarbon gas as carbon source (i.e. acetylene, methane etc.) on a metal catalyst (i.e. Fe, Co, Ni, Pd etc) at temperatures between 500 and 1200 ºC. CVD has been used for production of nanofibers for long time [53]. This method is preferred for CNT syntheses because of high purity and large scale production [41, 54, 55]. CVD which was first reported to produce MWCNTs by Endo et al., can synthesise both SWCNTs and MWCNTs. [46].   The main

challenges in CNT production is to maintain mass production and low cost. In this respect, the catalytic method is claimed to be best because of lower reaction temperatures and cost [56]. The amorphous carbon formed as by product during the thermal decomposition of hydrocarbons can be eliminated by purification.

CNT production by CVD can either be on a fixed or fluidized bed reactor. In fixed bed CVD method as shown in Figure 2.9, the furnace placed horizontal to the ground and the quartz tube is placed in it [26]. The substrate material (MgO, alumina, zeolite etc.) coated with a catalyst (Fe, Co, Ni, Ag, Ti, etc.) is placed in the quartz tube and fed by a carbon source (i.e. hydrocarbons). Generally an inert gas is used to maintain continuous gas flow. There are a number of parameters affecting the quality and amount of CNTs synthesised by CVD method:

- Temperature

- Type and amount of the catalyst material

- Type and amount of the substrate material

- Gas flow rate

- Duration of the synthesis

- Diameter of the reactor
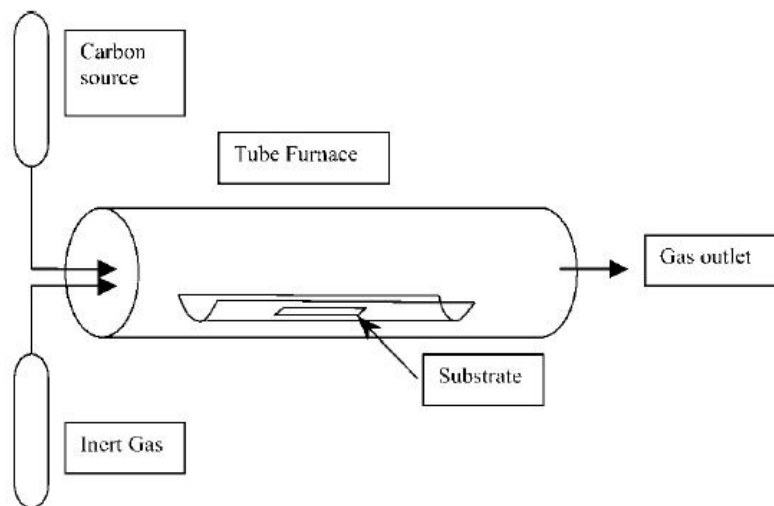
Figure 2.9 : Schematic view of fixed bed CVD reactor

In fluidised bed CVD method as the interaction area of the carbon source gases and the catalyst increases with fluidisation, large scale production becomes possible. As

shown in Figure 2.10 in this method the furnace is placed vertical to the ground and the quartz reactor is located in it. The substrate & catalyst couple is placed in the middle of the reactor in the hot zone of the furnace is placed in the hot zone of the furnace, and the gas flow through the reactor is maintained. As the carbon source gas flows through the reactor, it interacts with the catalyst and substrate and decomposes it for CNT synthesis.
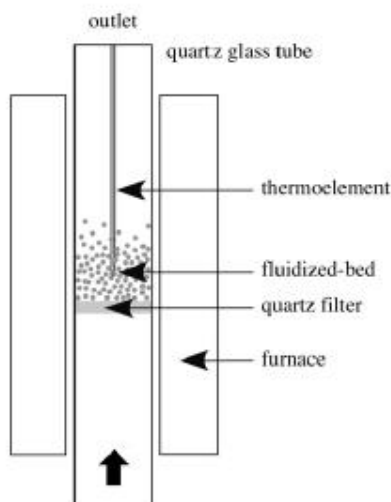
Figure 2.10 : Schematic view of fluidised bed CVD reactor

Plasma enhanced chemical vapour deposition (PECVD) method is required for some processes that cannot tolerate temperatures in thermal CVD. In CCVD method CNT is synthesis generally achieved above temperatures of 500°C. However, MWCNT, MWCNF production at 120 °C is possible by PECVD method [11]. Plasma can dissociate the hydrocarbon with reactive radicals. Therefore the hydrocarbon is generally fed to the system with another gas such as argon, hydrogen, ammonia [11] to dilute the hydrocarbon.

2.2.5 Purification of carbon nanotubes

As-synthesized CNTs prepared by different methods inevitably contain carbonaceous impurities and metal catalyst particles. The amount of the impurities commonly increases with the decrease of CNT diameter. Carbonaceous impurities typically include amorphous carbon, fullerenes, and carbon nanoparticles. Because the carbon source in arc discharge and laser ablation comes from the vaporization of graphite rods, some un-vaporized graphitic particles that have fallen from the graphite rods

often exist as impurity in the final product. In addition, graphitic polyhedrons with enclosed metal particles also coexist with CNTs synthesized by arc discharge and laser ablation as well as high temperature (>1000 °C) CVD. Fullerenes can be easily removed owing to their solubility in certain organic solvents. Amorphous carbon is also relatively easy to eliminate because of its high density defects, which allow it to be oxidized under gentle conditions. The most knotty problem is how to remove polyhedral carbons and graphitic particles that have a similar oxidation rate to CNTs, especially in SWCNTs. Metal impurities are usually residues from the transition metal catalysts. These metal particles are sometimes encapsulated by carbon layers making them impervious and unable to dissolve in acids. Another problem that needs to be overcome is that carbonaceous and metal impurities have very wide particle size distributions and different amounts of defects or curvature depending on synthesis conditions, which makes it rather difficult to develop a unified purification method to obtain reproducibly high-purity CNT materials. To fulfil the vast potential applications and to investigate the fundamental physical and chemical properties of CNTs, highly efficient purification of the as-prepared CNTs is, therefore, very important.

Purification methods of CNTs can be basically classified into three categories, namely chemical, physical, and a combination of both.

The chemical method purifies CNTs based on the idea of selective oxidation, wherein carbonaceous impurities are oxidized at a faster rate than CNTs, and the dissolution of metallic impurities by acids. This method can effectively remove amorphous carbon and metal particles except for those captured in polyhedral graphitic particles. However, the chemical method always influences and destroys the structure of CNTs due to the oxidation involved.

The physical method separates CNTs from impurities based on the differences in their physical size, aspect ratio, gravity, and magnetic properties, etc. In general, the physical method is used to remove graphitic sheets, carbon nanospheres (CNSs), aggregates or separate CNTs with different diameter/length ratios. In principle, this method does not require oxidation, and therefore prevents CNTs from severe damage. However, there are still some problems in physical techniques which need to be solved. One is that these methods are not very effective in removing impurities. Another is that they require CNT samples to be highly dispersible. Therefore, the as-

prepared sample is always first dispersed in solution by adding surfactants or treated by a chemical process to cut and/or add functional groups before purification. The third problem is the limited amount of sample that can be purified each time. Based on the above facts, physical methods are more suitable for use as an assistant step combined with chemical purification, except for the case where a small amount of CNTs with a particular structure or property are required.

The third kind of purification combines the merits of physical and chemical purification, and we denominate it as multi-step purification. This method can lead to high yield and high-quality CNT products. Owing to the diversity of the as-prepared CNT samples, such as CNT type, CNT morphology and structure, as well as impurity type and morphology, it needs a skilful combination of different purification techniques to obtain CNTs with desired purity. The key point is how to combine different methods according to one's requirement and the quality of the raw CNTs. Although considerable progress has been made, some merits of physico-chemical techniques have not been fully used and combined. For example, some physical methods capable of removing metal particles are rarely reported to be combined with gas oxidation. This combination may greatly improve gas phase purification yield owing to the early elimination of metal particles, which can catalyze the CNT oxidation [57, 58]

2.2.6 Characterization of carbon nanotubes

Characterization of nanostructures is a critical step for improvement of nanotechnology systems. Characterization is required for determining the basic properties and identification of nanoelements. The following methods are commonly used for characterization of nanomaterials.

2.2.6.1 Thermogravimetric analysis

Thermogravimetric analysis (TGA) is an analytical technique to determine a materials thermal stability by monitoring the change in mass as the specimen is heated [59, 60]. The measurement is carried out in air or inert atmosphere (i.e. Ar, He). The mass of sample is recorded as a function of time or temperature when the sample is heated/cooled with constantly increasing/decreasing temperature. Some TGA instruments can measure the change in temperature or heat flow, therefore the energy released or absorbed of a reaction can be measured. The mass change of

CNTs is result of oxidation of carbon in the air into carbondioxide and mass gain is due to oxidation of the metal catalyst into solid oxides [61, 62].

TGA instruments can be classified into as vertical and horizontal balance. Vertical balance instruments have a specimen pan hanging from the balance or located above the balance on a sample stem. Horizontal balance instruments generally have two pans (sample and reference) and can perform differential thermal analysis (DTA) and differential scanning calorimetry (DSC) measurements.

Generally TGA measurement is performed in air or inert gas atmosphere in which oxidation occurs with a linear temperature increase. The maximum temperature is selected to maintain stability in the specimen mass meaning that all chemical reactions are completed. Therefore we obtain two important numerical values; residual mass and the oxidation temperature. TGA measurement of as-synthesized CNTs generally gives one peak whereas purified CNTs may have more than one peak as a result of damaged CNTs and/or functional groups. The positions of the peaks are affected by the amount and the morphology of metal catalysts and other carbon based impurities. These peaks attribute to various components in CNTs such as amorphous carbon, nanotubes and graphitic materials.

TGA is commonly used in three different ways as isothermal, quasi-isothermal and dynamic thermogravimetry. In isothermal gravimetry, the mass of the specimen is recorded at constant temperature as a function of time. In quasi-isothermal thermogravimetry the specimen is heated up to a temperature to maintain constant mass with a series of temperature. In dynamic thermogravimetry which is generally called as TG the temperature of the specimen is increased linearly.

In a study of Alvarez et al. TGA is managed in an inert atmosphere with a temperature rate of 5-30°C/min up to 800-1000°C. CNT has stronger sp^3 bonds than sp^2 bonds. Regarding this fact it is expected to observe mass loss due to oxidation of SWCNT at 400-600°C, and MWCNT at 500-800°C [63]. As a result of TGA measurements, temperature versus mass change curve, the stability and chemical structure of the initial specimen, formed by-products and the resulting specimen can be determined.

Basic thermal decomposition of inorganic, organic and polymeric materials; corrosion of metals at different atmospheres and high temperatures; solid state

reactions, calcinations of minerals; distillation and evaporation of liquids; pyrolysis of wood and coal; humidity, volatile material and ash content can be determined by TGA measurements [64].

Oxidation temperature is a measure to determine the thermal stability of CNTs in air and depends on different parameters. Smaller diameter nanotubes oxidize at lower temperatures due to higher curvature strain. Defects in nanotube walls may also lower the thermal stability. Active metal particles in nanotube may catalyze the oxidation of carbon and therefore affect the thermal stability. Although these parameters affect the thermal stability, it is still a reliable method to determine the overall quality of the nanotubes. High purity and less defect results with higher oxidation temperature of the sample.

Lifting force affecting the pans, convection flows and turbulence in the furnace, fluctuations in the recording mechanism and pans, induction effects of the furnace, electrostatic effects, temperature measurement and calibration, any reactions between the pan and the specimen, and changes in the temperature are parameters causing errors in TGA measurements.

2.2.6.2 Raman spectroscopy

Raman scattering is one of the primary methods to determine fundamental properties of CNTs. It gives us information about the quality and the structure of the nanotube, phonon and the electron confinement [65]. Raman scattering is an interaction with phonons in a material. The incoming light interacting with an electron forms higher transition energy where the electron interacts with a phonon before making a transition back to its ground state. He/Ne, Ar^+ or Kr^+ ion lasers, CO_2 or N_2 based lasers are the most common heat source used for Raman measurements.

Raman is commonly used for qualitative measurements. Vibrations of $-C=C-$, $-C\equiv C-$, $-N=N-$, $-S-S-$, $-C-O-C-$ result with observation of very strong Raman bands. Therefore these bands having very low impact in infrared spectrum can very well be observed. As it is shown in Figure 2.11, the most prominent Raman active peaks in CNTs are low frequency, radial breathing beams (RBM) and the higher frequency of D, G and G' modes. While D, G and G' modes can also be observed in graphite, RBM is unique to CNTs and gives information about the diameter distribution of CNTs. Due to resonance behaviour of Raman, a number of laser lines

are required to determine the diameter distributions. The relative strength and width of D band makes a qualitative measurement how large a fraction of graphitic materials and nanotubes with defects exist. Table 2.3 shows the frequencies of these bands [66].

Table 2.3: Frequency values of the CNT peaks

Band	Frequency (nm^{-1})
G Band	37.1743
D Band	-7.6804
G' Band	140
RBM	50-300

The intensity of G band shows that there is sp^2 hybridization in the structure, whereas D band represents the defects in the material. G' is a secondary image of D band. As it can be observed from Figure 2.11, RBM peak is better observed with increasing wavelength. [66, 67] The diameter of SWCNT can be calculated from RBM peak with the following formula in which A=223 cm^{-1}/nm, B= 10 cm^{-1} and d is representing the diameter of the nanotube:

$$\omega(cm^{-1}) = A/d(nm) + B(cm^{-1})$$

(2.5)
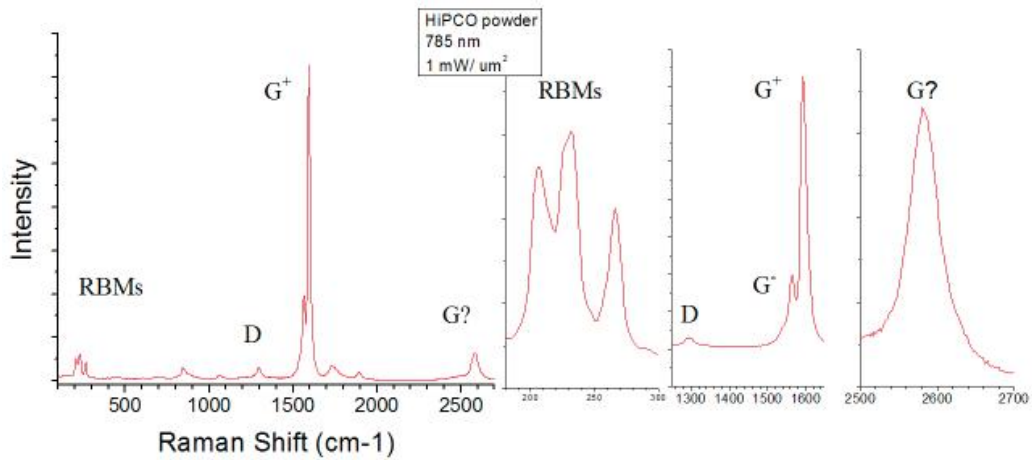
Figure 2.11 : Raman spectra of CNTs

The difference in the image of G band for SWCNT and MWCNT is important in Raman spectroscopy. There is an extra peak for SWCNTs and D band has low intensity whereas there is not an extra peak for MWCNT.

2.2.6.3 Transmission electron microscope

Microscopy based measurement can be applied to a wide range a materials with a broad distribution of particle size from nanometer size to milimeters. The type of the microscope is selected according to size of the powders to be investigated and the desired magnification and resolution. TEM enables the analysis of a material in a size range of 0.01 μm to 10 μm, retaining the necessary resolution to distinguish surface properties.

Resolution of TEM is limited to a minimum of 5 nm. The resolution and magnification of the instrument is set related to the sample to be analysed, the operational parameters and capacity of the instrument. The theoretical limit of resolving two discrete points with a distance d in between is expressed as in equation 2.6 where λ is the wavelength of the illumination source (expressed in μm) and NA is the numerical aperture:

$$d = \frac{0.61\lambda}{NA}$$
(2.6)

Sample preparation for TEM measurement requires high skill, effort and time. Depending on the size of the material to be analysed samples should be in form of replicas or thin films. Measurements with TEM are advantageous with depth of focus enables view of particles with different sizes in the same field of focus. That means there is no need to refocus for different size of particles.

2.2.7 Applications of carbon nanotubes

CNTs have a wide range of applications regarding to their remarkable material properties. The size and the morphology of CNTs affect the type of the application. If the diameter of the CNT is large, it is generally used in energy devices such as, fuel cells, lithium ion batteries and capacitors. Large fibers can also be used as thermal conductors and filler materials in composites. As the diameter decreases, CNT can be used as filler in three phase composites. The CNTs in the resin of the composites act as an interconnection between the fibers and enhance the electrical and thermal conductivity of the material. Nanotubes can also be used in field emitters, optical polarisers, hydrogen storage, and medical applications.

The exceptional mechanical properties lead us to two main applications: strengthening of fibers in high performance composites and replacing the carbon fibers, Kevlar and glass fibers as probes in scanning tunnelling microscopes (STM) and atomic force microscopy (AFM) [41]. One of the main problems in composite formation is to achieve good adhesion between the CNT and the matrix, which requires covalent coupling. In order to achieve this coupling, functional groups can be introduced to the walls forming sufficient number of connections to the walls without weakening the stability of the tubes.

CNTs with their polymer composites are used to increase the strength of automotive components. CNT composites can form semiconductor materials from insulators. It is expected CNTs may replace silicon in transistors of computer processors and rams [68]. They can also be used in chips with their ability to form Van der Waals bonds. Transport measurements on semiconducting nanotubes have shown that a nanotube connected to two metal electrodes has the characteristics of a field-effect transistor [42].

CNTs are also able to store energy with their porous, light structure and wide surface areas. There is a remarkable interest in especially hydrogen storage in CNTs. It is observed that CNTs have ability to store hydrogen up to 10% of their weight. This can be achieved either at high pressure or by electrochemical methods. In summary CNTs can be used in; composites, frequency selective surfaces, thermal barriers, nanosensors, nanodevices, hydrogen adsorption, magnetic field emitters, membranes, and biological and medical applications.

3. GROWTH OF CARBON NANOTUBES BY CVD

Growth of carbon nanotubes generally requires existence of a catalyst placed on high surface area materials of substrates. Practically catalyst particles serve as seeds for CNT growth. As mentioned above sections, there are a number of growth parameters affecting the CNT production by CVD method. Among these parameters we will be discussing the affect of the catalyst, and the substrate in this section.

3.1 Substrate

There are many researches previously conducted about substrate/ support materials. A single metal and mixture of metals supported on oxides, clays or zeolites have a great affect on CNT production by CCVD method [69, 70]. Metallic catalyst can be dispersed and stabilised by a number of oxides [71]. The interaction between the catalyst and the substrate material strongly affects the catalytic properties of the catalyst and substrate couple. In a research conducted by Zhu et al. Fe and Co salts are used as catalyst on mesoporous silica [72]. Catalyst/support ratio affecting the type of the CNT synthesised was deeply investigated. Although CVD method is promising for large scale synthesis; the productivity of the catalyst is limited for SWCNT. Hernadi et al. examined different catalyst supports such as silica gel, zeolite and alumina. It is suggested that only the catalysts on the external surfaces of porous support can form CNTs [73]. Ward et al. concluded that alumina film with iron catalyst was the best substrate as a result of the analysis of the effect of substrate on the growth of SWCNT on thin films [74]. The strength of the catalyst–support material and the type of support material may determine the conditions of metal free carbon nanotubes or carbon nanotubes filled with metal particles. The choice of the catalyst and support material may be a determining factor in the SWCNT synthesis [76, 77].

Separation of the support material from synthesised CNTs is an important parameter in selection. Therefore it is important to select an easily soluble substrate material

when CNTs are not soluble. For this reason, MgO is one of the most commonly used substrate material in CNT synthesis [75].

3.2   Catalysts

Majority of the CNT production methods require existence of catalyst. The type of the catalyst is important for the growth and morphology of the CNTs. Cobalt, iron, titanium, nickel, copper, zeolites and combinations of these metals and/or their oxides widely used catalyst materials in literature for multiwall or single wall CNT synthesis. [14, 33, 69-77]

There are some studies about the relationship between the CNT diameter and the catalyst size [79-81]. Li et al. produced SWCNT by using methane as the source gas with Ni catalyst having a particle size larger than 20 nm and they discovered that there is a linear relationship between the CNT diameter and the particle size of the catalyst. However it was claimed by Nerushev et al. that there is no relationship between the CNT structure produced by acetylene and the catalyst diameter. Colomer et al. achieved 70-80% SWCNT synthesis by MgO substrate and Co, Ni, Fe and Co&Fe catalysts [56].

In a study catalytic activities of Fe, Co and Fe&Co binary catalyst supported on alumina or silica are compared. The results of MWCNT were achieved at 700°C on hydrated alumina prepared from aluminium isopropoxide and containing a Fe and Co catalyst mixture [78]. In another study, the catalytic activity of Fe, Co, or Ni as the catalyst, and laser treated vanadium plates having high surface area as the catalyst support in the decomposition of acetylene at 720°C under CVD conditions studied [79]. Best quality CNTs were obtained over the iron catalyst with high density and small diameter of 10–15 nm.

In another study, Yokomichi et al. [80, 26] examined yield of nanotube of coatings of Al, Mg, Mn, Cu, Zn, Fe, Co, and Ni nitrate catalysts. They concluded that the yield of nanotube formation very well depends on catalyst metal and can be affected by changing tendency and size of the catalysts [80]. It is found that nanotube growth rate is dependent on the catalyst type in the order of Ni > Co > Fe [81]. However, iron catalyst resulted in the best crystalline structure of the nanotubes among the three catalysts [81].

In many of the results in the previous studies there is concern about MWCNT synthesis of Co catalyst rather than SWCNTs; also Ni catalysts lead to MWCNTs. It is observed that mixtures of transition metals (Fe&Ni, Fe&Co, Ni&Co) are often observed to be more efficient for CNT production than one metal alone [83,26]. Table 3.1 shows the highest carbon efficiencies are generally as a result of an optimum value of 5% metal to substrate [26].

Table 3.1: Carbon deposit by decomposition of acetylene on different catalysts

Catalyst	Catalyst (wt%)	Substrate	Carbon Source	Temp (°C)	Time (min)	Product	CNT diameter (nm)	Ref.
Fe	2.5	Graphite	Acetylene	700	>60	MWCNT	5-20	[53]
Co&V	2.5&2.5	Zeolite	Acetylene	600-700	30-60	MWCNT	3.5-12	[84]
Co&Fe	2.5&2.5	Y type zeolite	Acetylene	600-700	60	MWCNT	3.5-12	[84]
Fe&Co	2.6&2.6	$CaCO_3$	Acetylene	700	60	MWCNT	4.8-10	[85]
Ni&Cu&Al	2&1&1	-	Methane	750	11-220	MWCNT	60-90	[86]
Fe	24.5	Al_2O_3	Methane	1000	10	SWCNT	1-6	[87]
Fe&Co	2.5&2.5MgO	MgO	Methane	1000	10	SWCNT	0.8-2	[88]
Fe&Co	5	$CaCO_3$	Acetylene	720	30	MWCNT	-	[89]
Mo&Co	10&5	MgO	Methane	500-600	-	MWCNT	1.25	[90]
Mo&Co	10&5	MgO	Methane	700	-	MWCNT	10	[90]
Co	5	Aminophosphate	Acetylene	600-800	30-120	MWCNT	4-26	[75]
Ferrocene	9.6	Quartz	Toluene	550	60	MWCNT	10	[91]
Ferrocene	9.6	Quartz	Toluene	850	60	MWCNT	75	[91]
Ferrocene	9.6	Quartz	Toluene	940	60	MWCNT	<75	[91]
Fe&Mo	2.5-15	Al_2O_3 aerogel	Isopentane	450-800	0.5-40	SWCNT &MWCNT	0.9-2.7	[92]
Fe	-	SiO_2/Si	Acetyene	580-1000	30	MWCNT	<25	[93]
Ni	-	Ti&Sodalimeglass	Acetylene	850&550	10	-	10-20	[94]

3.2.1   Catalyst preparation

Although there are some studies reporting that CNT synthesis could be managed without catalysts, it is widely known that catalysts are required especially for CVD method. There are many methods to combine catalyst and substrate such as sol-gel, coreduction of precursors, impregnation and incubation, ion-exchange precipitation, ion-adsorption precipitation, reverse micelle, thermal decomposition, and physical deposition.

A porous precursor of the active component is impregnated with the precursor of a textural promoter in the heterogeneous sol−gel method. The textural promoter is needed to stabilize the active component structure and to prevent its sintering in the

course of post-treatments [95]. To get a catalyst precursor textural promoter is mixed with aqueous solution of precursor of the active component. The mixture is then gelated, and then dried to get rid of the excess water and solvent and at last calcinated [95]. In coreduction of precursor, nitrates of a catalyst and of a metal oxide support, are mixed with an organic compounds and water [96, 97]. The mixture is then heated to reduce the precursors to have mixed oxide particles. In the impregnation, incubation method a catalyst precursor is first dissolved in a solution and then contacted to a support with this solution. In this method, the whole precursor deposits onto or into the substrate. The solution is then evaporated and the catalyst is dried.

Ion-exchange–precipitation is formation of a solution of a catalyst precursor is also used and brought in contact with a zeolite support. The main point of this method is the anion exchange of the precursor with anion of the zeolite. Thermal decomposition id allowed by the calcinations and that forms a catalyst in an oxidized form. In ion adsorption and precipitation the support is put in a catalyst precursor solution. As a result of an acid base reaction, the catalyst precursor precipitates. An acid−base reaction takes place and then the sample is calcinated to have only the catalyst element in an oxidized form. In the reverse micelle method, a cationic surfactant is dissolved. Then metal salt is added to the solution followed by a reductor agent in order to reduce the oxidized metal to its neutral form. The colloidal solution formed is then placed on a substrate and dried at room temperature. In thermal decomposition of carbonyl complexes a metal is synthesised in the form of nanoclusters as a result of thermal decomposition of carbonyl complexes. When a metalorganic precursor is vaporized and then carried to the reactor zone by a gas it is metalorganic chemical vapour deposition which allows the precursor to decompose and to depose onto the substrate by heat. If the metal is evaporated in order to be deposited onto a substrate then it is called physical deposition. Depending on the heat treatment applied, the equilibrium shape is maintained.

3.3   Growth Mechanism

CNT growth by CVD method can be separated into two basic types as gas phase growth, and substrate growth depending on the location of the catalyst. In gas phase growth, the catalyst formation and the nanotube growth occurs in mid-air (tip

growth). In substrate growth (base growth), the catalyst is deposited on the substrate before the growth, as shown in Figure 3.1 [41].

Two mechanisms can be considered for both type of CNT growth. First one is surface carbon diffusion in which the metal particle remains a solid and the cracked carbon diffuses around the surface, and CNT nucleates on the side of the metal particle. The tube grows continuously as the carbon breaks down. Second mechanism is bulk carbon diffusion in which the carbon feedstock is "cracked" on the surface of the metal particle. The metal the carbon until it reaches saturation. From that point on a CNT with one or more walls grows from the outer surface. In this situation, the metal can either remain as a solid or become a liquid nano-droplet. In the 1960s this model was proposed to explain the formation of silicon and germanium whiskers and then used to explain formation of CNT by Saito et al [15, 16]. It is expected for a catalyst particle of unchanging size to continue CNT growth as soon as hydrocarbon gas is fed to the system.
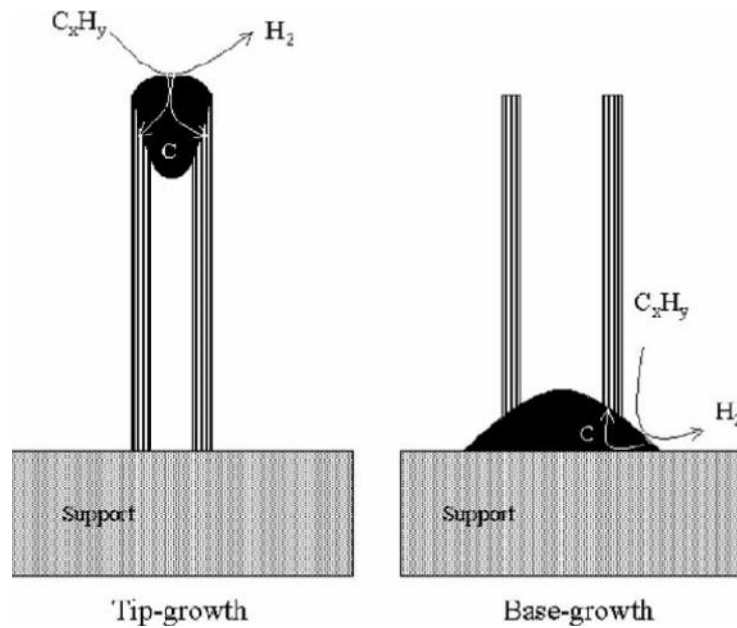
Figure 3.1 : Growth mechanism of CNTs

4. EXPERIMENTAL STUDIES

4.1   Catalyst Preparation

Metal catalysts of V, Ni, Fe, Co, were impregnated in MgO substrate. For Ni, Fe, Co catalysts nitrates of the metals ($(Ni(NO_3)_2.6H_2O)$, $(Fe(NO_3)_3.9H_2O)$, $(Co(NO_3)_2.6H_2O)$) were separately mixed with MgO substrate in ethanol solution by ultrasonic mixer with metal to MgO weight ratios of 1:100, 5:100 and 10:100. The amount of nitrates in the metal nitrate, MgO and ethanol solution was calculated according to the molecule ratios of metals in the compound. For V-MgO catalyst preparation V_2O_5 was mixed with MgO in ethanol solution with weight ratios of 5:100 and 10:100. As low quality products were observed with 5:100 and 10:100 weight ratios of V:MgO, 1:100 weight ratio was not experimented.

The metal nitrate, substrate and ethanol solution was mixed for 30 minutes in "Bandelin Sonoplus" ultrasonic mixer then kept in oven at 80 ºC for 18 hours. The dried catalyst-substrate mixture was than grinded to avoid any agglomeration that may affect the interaction between acetylene gas and the surface of mixture.

4.2   Binary Catalyst Preparation

In order to evaluate interaction between metal catalysts during CNT production binary catalysts of Fe and Co couple was chosen. Fe&Co:MgO weight ratio of 5:100 and 10:100 were chosen to be experimented. Fe&Co:MgO weight ratio catalyst of 5:100 was prepared by mixing 2.5:100 Fe:MgO and 2.5:100 Co:MgO. The amount of $Fe(NO_3).9H_2O$ and $Co(NO_3)_2.6H_2O$ to be in the metal nitrate, MgO and ethanol solution was calculated according to the molecule ratios in the compound. Accordingly for catalyst of 10:100 Fe&Co:MgO weight ratio, 5:100 weight ratios of Fe:MgO and Co:MgO were mixed homogeneously.

The binary catalyst solution was also mixed for 30 minutes in "Bandelin Sonoplus" ultrasonic mixer then kept in oven at 80 ºC for 18 hours. The dried catalyst-substrate

mixture was than grinded to avoid any agglomeration that may affect the interaction between acetylene and the surface of catalyst.

4.3   Carbon Nanotube Production

There was a fluidized bed system for CNT production with CCVD method in Material Production and Preparation Laboratory of Energy Institute in Istanbul Technical University. The system was composed of a "Protherm" furnace that can operate up to 1100 ℃ and a quartz reactor with a diameter of 2.5 cm and length of 94.5 cm. In the middle of the reactor is a nano porous silica disc allowing gas flow but not the produced CNTs. As fluidized bed system was used in production, the furnace was placed vertically and the quartz reactor is placed in it with the nano porous silica disc placed in the middle of hot region of the furnace. CNT production was held on the 5 to 10 cm length region around the quartz disc of the reactor on the quartz reactor. To fluidize the bed a certain flow rate of gas was necessary for a given substrate catalyst mixture. For this purpose argon was used as carrier and inert gas and acetylene was used as carbon source. The gas was fed to the system through the bottom of the reactor and it leaves the system from the top. Schematic view of CNT production is given in Figure 4.1[98].

high surface area MgO powder (A=100 $m^2 \cdot g^{-1}$)

impregnation in a $Fe(NO_3)_3$ ethanol solution

drying

heating (450-850 ℃)
⇒   formation of Fe_2O_3 cluster

pyrolysis of C_2H_2 in Ar atmosphere
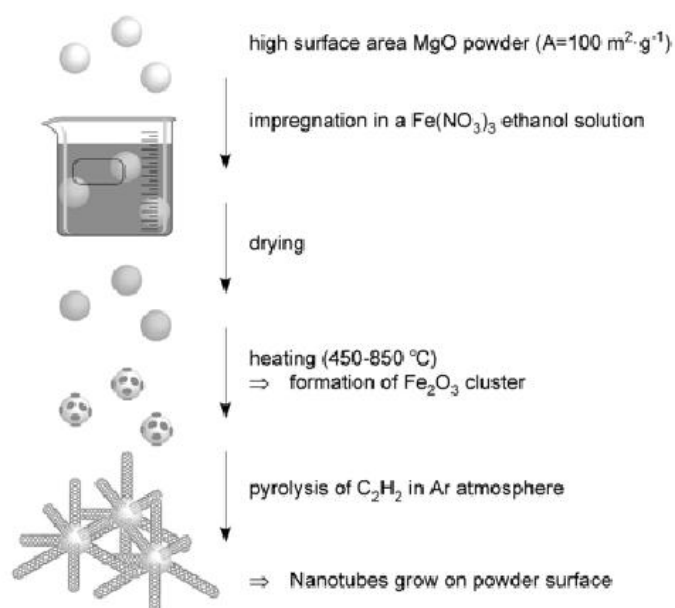
⇒   Nanotubes grow on powder surface

Figure 4.1 : The precursor powder preparation and CNT growth on powder grains

The catalyst and substrate mixture was placed homogeneously on the disc. For MWCNT and SWCNT production while heating the system to 500ºC and 800ºC respectively, 100 ml/min argon was fed to the system to maintain inert atmosphere and/or to make flow of other gases existing in the system. As the temperature reached 500ºC for MWCNT and 800ºC for SWCNT, acetylene flow started with a rate of 42 ml/min and the argon flow rate was increased to 368 ml/min to make acetylene flow easier. A vacuum pump was used to assist the gas flow during acetylene feeding. The reaction time was chosen as 30 and 60 minutes for MWCNT and 35 and 60 minutes for SWCNT production.

When the temperature of the furnace reached around 125ºC the iron in iron nitrate decomposes and forms Fe_2O_3. Then Fe_2O_3 and MgO form the substrate and catalyst combination. At around 360ºC cobalt nitrate and nickel nitrate decomposes and forms CoO and NiO, respectively. Then they form substrate and catalyst combination with MgO.

4.3.1 Characterization of carbon nanotubes

4.3.1.1 Thermogravimetric analysis

Thermogravimetric analysis (TGA) is necessary to characterize the total carbon loading and to determine the residual metallic catalyst. The amorphous carbon is completely oxidized at temperatures below 350°C and graphite burns above 750°C, the oxidation temperatures of the CNTs depend on the type of nanotube. The carbon yield of the as-synthesized CNTs were calculated depending on the mass loss of the analysed samples [66].

In this study, the TGA of synthesized CNTs were conducted by the TGA system of TA Q600 SDT in dry air atmosphere with an increase of 5°C/min between 25 and 800°C. The maximum operating temperature of the existing system is 1500°C. The thermal couple in the system is Pt-Rh alloy. The system is designed to work in various atmospheric conditions. The ultimate gas flow rate is 50 ml/min. It is possible to work under vacuum conditions up to 7 Pa and 0.05 Torr. The range of operating temperature increase is 0.1 to 100°C/min. The maximum amount of material to be analysed is 200 mg and the sensitivity of the system is 0.1 mg. TGA graphs of all synthesised CNTs are shown in Appendix A.2. The specifications of the

device are given in Table 4.1 and the TGA system used in analysis is shown in Figure 4.2.

Table 4.1: The specifications of the TGA system

Specification	Value
System design	Horizontal balance and furnace
Balance design	Dual beam (growth compensated
Sample capacity	200 mg (350 mg including sample holder)
Balance sensitivity	0.1μg
Furnace type	Bifilar wound
Temperature range	Ambient to 1773 K
Heating rate – Ambient to 1273 K	0.1 to 100 K/minute
Heating rate – Ambient to 1773 K	0.1 to 25 K/minute
Furnace cooling	Forced air 1773 to 50 K in < 30 minutes 1000 to 50 K in < 20 minutes
Thermocouples	Platinum/Platinum-Rhodium (type R)

Figure 4.2 : TGA system

4.3.1.2 Raman spectroscopy

The Raman spectroscopy measurements of the samples were analysed by Horiba Jobin YVON HR 800UV and with 632.88 nm of He-Ne laser light. In Figure 4.3 a picture of Raman spectra is seen.

Raman spectra of CNTs are quite interesting because of resonance phenomena and sensitivity to tube structure. That is, there is very strong excitation wavelength dependence of the spectra resulting from the electronic band structure. The features in the Raman spectra are diagnostic of the CNT type. Raman is a reliable diagnosis and a non destructive method to determine structure of CNT and requires a very little amount of sample preparation.

Figure 4.3 : Raman spectroscopy

4.3.1.3 Transmission electron microscope

20 kV Tecnai-G2 F-20 model of FEI was used for TEM measurements. The resolution of the device is ranging from 0.14 to 0.18 nm and the maximum thermal current is greater than 100 nA. There is 0.5 nA or larger current in 1 nm probe. The energy distribution is around 0.7 eV.

In order to have the TEM image the sample in a solution of 50% ethanol and 50% pure water was mixed with ultrasonic mixer. The formed homogeneous mixture

poured on copper grids and dried in oven at 45°C. Figure 4.4 shows a view of electron microscopes used for measurements.
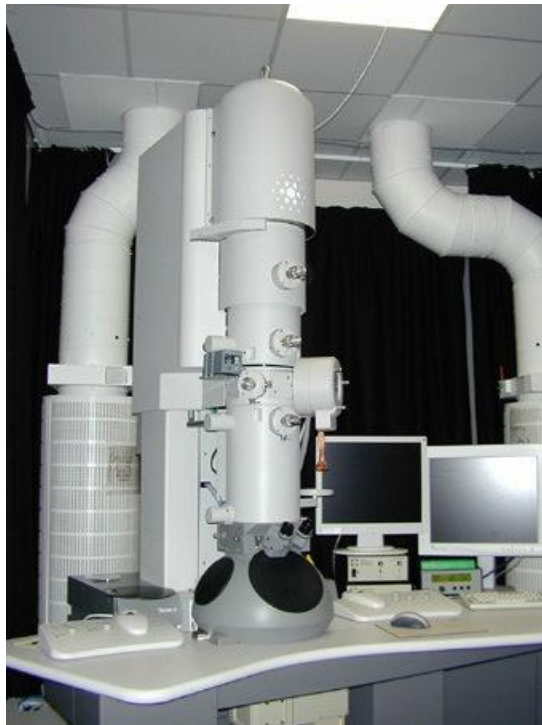

Figure 4.4 : Transmission electron microscope

5. RESULTS AND DISCUSSION

CNT production generally requires existence of a catalyst. The selection of a proper metallic catalyst may affect the morphology amount of the synthesised product, the quality of the product (i.e. electrical, physical, mechanical etc.). All these parameters in addition to economic factors should be taken into account to improve the efficiency of CNT production by catalyst. In this research the effects of time and weight percent of different catalysts (iron, nickel, cobalt, vanadium) to the substrate (magnesium-oxide) on production of CNTS in decomposition of acetylene were investigated. Thermogravimetric analysis (TGA), raman, and transmission electron microscope (TEM) measurements were used for characterization.

The carbon efficiencies of the as-synthesized CNTs were calculated according to TGA measurements shown in Appendix A.1. As different catalysts were examined during the experiments in order to eliminate any differences which may be caused due to moisture content of the as-synthesized samples, in the calculations the initial temperature was selected as 200ºC to have the dry weight percent and the final temperature was taken as 796ºC to have the same temperature value for all samples. The formula of carbon efficiency is:

$$Carbon\,efficiency(\%) = \frac{Weight\%(200°C) - Weight\%(796°C)}{Weight\%(200°C)} \times 100 \qquad (5.1)$$

5.1 CNT synthesis by Fe catalyst

There are many researches on iron as catalyst on different substrates for CNT synthesis in the literature [78,99]. $Fe(NO_3)_3).9H_2O$ that is selected as catalyst is mixed with MgO substrate and ethanol by ultrasonic mixer for 30 minutes and then dried in the oven for 18 hours. The formed catalyst is used for synthesis of CNT as a result of decomposition of acetylene by CCVD method. Fe catalyst with different weight ratios to MgO substrate (1:100, 5:100 and 10:100) is used for synthesis of MWCNT and SWCNT at 500 and 800ºC respectively. The reaction times were 30

and 60 minutes for 500ºC and 35 and 60 minutes for 800ºC. As a result of the experiments the effect of time, temperature and weight ratio of the Fe to MgO were analysed.

5.1.1   Effect of temperature

The effect of temperature is analysed for weight ratios of 1:100, 5:100 and 10:100 for two synthesis times. The selected synthesis temperatures were 500 and 800ºC Temperature is an important parameter in CNT synthesis as with temperature change the type of nanotubes. TEM images of these synthesized materials are given in Figure 5.1. It is evident that the structures synthesized by chemical vapour deposition method are CNTs. In Figure 5.1 (a), the diameter of the CNTs is nearly 10 nm and their appearance is darker in the picture. The CNTs in Figure 5.1 (b) have diameters between 1.5-5 nm and also are transparent. One possible explanation for the dark parts in both two figures is a result of the impurities within the structures. These observations lead to a conclusion such that in the temperature of 500°C MWCNTs were grown and at the temperature of 800°C SWCNTs were synthesized.

(a)   (b)
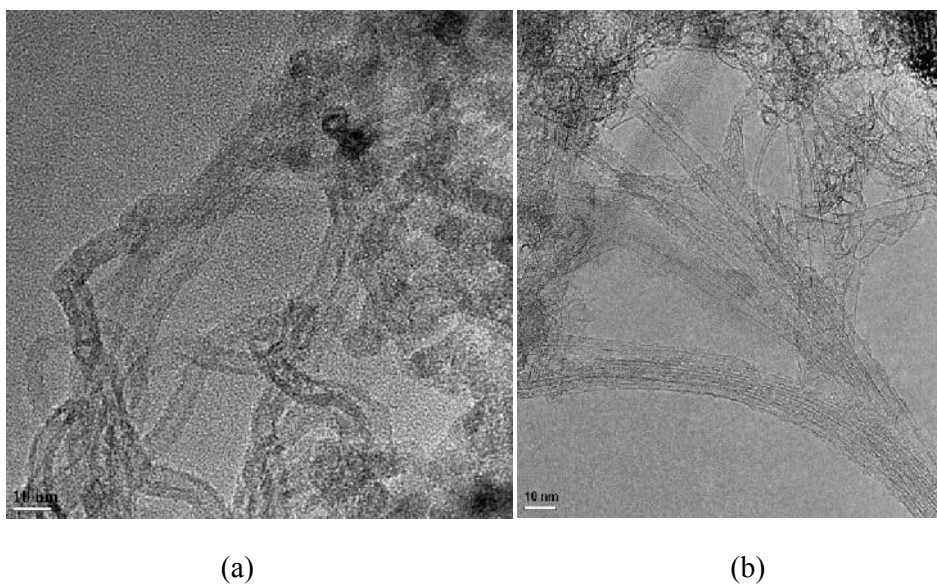
Figure 5.1 : TEM images of CNTs synthesized at (a) 500°C (b) 800°C

The change of the nanotube type as a function of temperature is also clearly seen in the Raman spectra. Raman spectroscopy is a powerful technique for the characterization of the structure of carbon nanotubes. Figure 5.2 shows Raman spectrum for carbon deposits excited by 633 nm laser. The spectra of MWCNT and

that of SWCNT show a clear difference at the G band (around 1580 cm^{-1}). The intensity of the G band for SWCNT, which is synthesized at 800°C, is considerably higher than MWCNT, which is synthesized at 500°C. Furthermore, at 500°C, the D-band (around 1350 cm^{-1}) is more intense than the G-band. At the temperature of 800°C, the intensity of the G-band becomes higher. The absolute intensities of the bands are increased at 800°C compared to 500°C. The ratio between the D band and the G band and the radial breathing mode (RBM) and its relation with diameter distribution are very important factors in the way that allows us to distinguish between the three variants of nanotubes with one single analysis, which is a probe of the high performance of Raman spectrometer. As seen from Figure 5.2, the spectrum in RBM band which is a characteristic of SWCNT is observed in the two samples. The reason of this spectrum which is observed at MWCNTs is that the innermost tube diameter is below 2 nm and this result is consistent with other studies found in literature [100]. If nanotube diameter is greater than 2 nm, RBM spectrum becomes difficult to be observed.
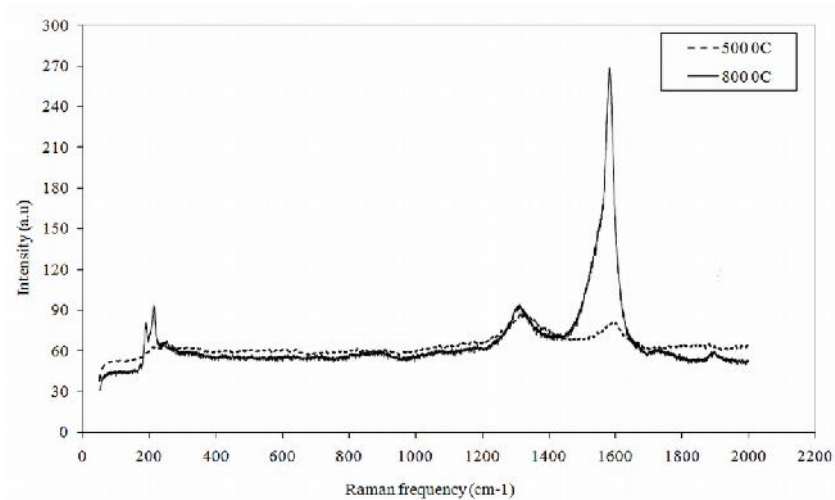
Figure 5.2 : Raman spectra of CNTs

It is determined that peaks seen on RBM bands have different intensity and appearance of CNTs synthesized at 500 and 800°C. While RBM peak of sample synthesized at 800°C is higher and narrow shape, peak of sample synthesized at 500°C have more wide and scattered shape and it is stated that intensity of this peak is much low. Moreover, it is seen that peak of sample synthesized at 500°C shifted upwards to peak of sample synthesized at 800°C. This shift is explained nearly 5% in the literature [101]. At Raman spectra, the intensity ratio of D and G band (I_D/I_G)

express the quality of CNTs. The higher ratio explains the higher amorphous carbon content and defect formation. As seen from Figure 5.2, the I_D/I_G ratio of MWCNT is much higher than that of SWCNT and amorphous carbon content and defect formation is much higher. This observation was consistent with that of Mauron, who reported that with existence of 5% Fe catalyst MWCNT synthesis is observed in a temperature range of 500-650 ºC and SWCNT synthesis is observed in temperature range of 650-850 ºC [98].

In Figure 5.3 the effect of temperature on carbon efficiency for synthesis of 30 minutes (for MWCNT) and 35 minutes (for SWCNT) is shown. It is seen that there is a tremendous increase in carbon efficiency (from 9.74 to 18.76%) of 1:100 Fe to MgO weight ratio with temperature whereas there exists a decrease in efficiency of 5:100 (from 57.52 to 41.63%) and a drastic decrease in the efficiency of 10:100 (from 54.75 to 19.53%) Fe to MgO weight ratios. With this result it can be said that with the increase in Fe weight ratio there becomes a decrease in the carbon efficiency. In summary the order the carbon efficiency of given temperature of 500ºC for 30 and 35 minutes is 5:100≈10:100>1:100, whereas for 800ºC it is 5:100>1:100=10:100.
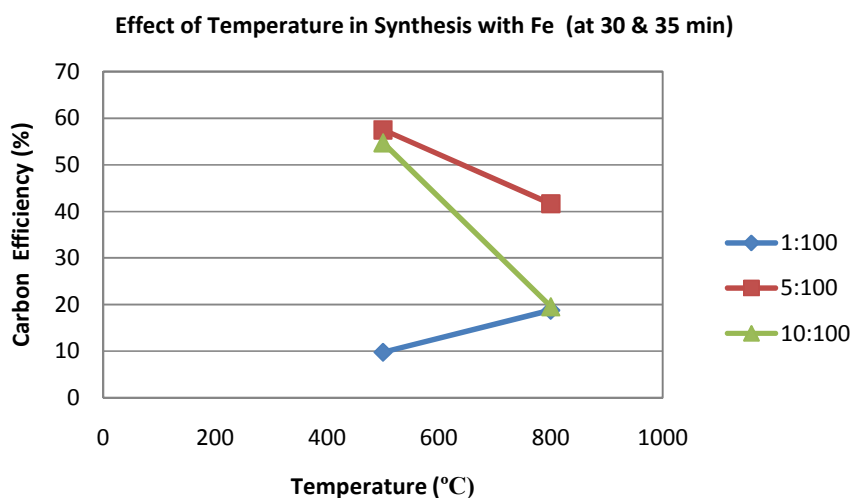

Figure 5.3 : Temperature vs. carbon efficiency graph of Fe for 30&35min

When we consider CNT synthesis for 60 minutes at 500 and 800ºC as shown in Figure 5.4, it is seen that there is also a tremendous incerase (from 9.97 to 51.02%) for 1:100 Fe to MgO ratio for 60 minutes synthesis. There is a slight increase in

effiency (from 53.3 to 54.2%) of 5:100 weight ratio with increasing temperature. 10:100 Fe to MgO weight ratio again shows a drastic decrease in efficiency (from 70.61 to 23.75%) with the incerasing temperature which may be related to insufficient contact of acetylene to catalsyt due to low fluidization. In summary the order the carbon efficiency of given temperature of 500ºC for 60 minutes is 10:100>5:100>1:100, whereas for 800ºC it is 5:100≈1:100>10:100.
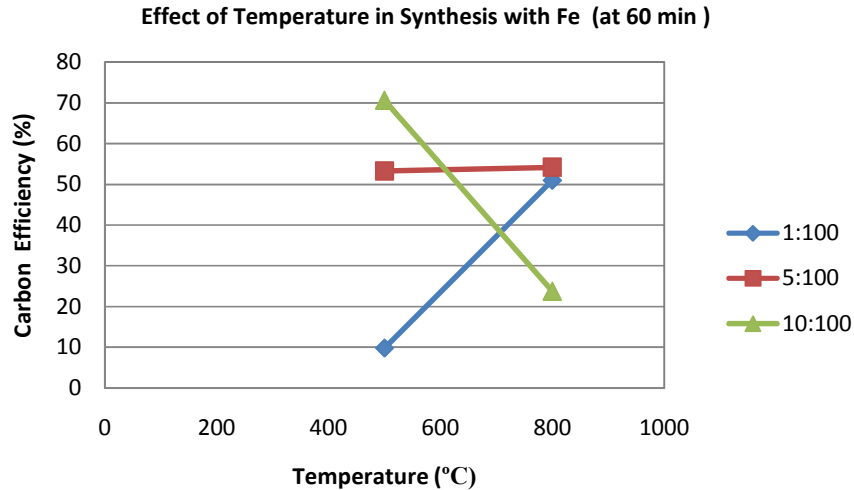

Effect of Temperature in Synthesis with Fe (at 60 min)

Figure 5.4 : Temperature vs. carbon efficiency graph of Fe for 60 min

5.1.2 Effect of time

The effect of time is analysed for SWCNT and MWCNT synthesis at 800ºC and 500ºC respectively. It is observed that for MWCNT synthesis at 500ºC in low Fe to MgO ratio (1:100) there is no change in the carbon efficiency (9.74 to 9.79%) with respect to synthesis time (30 and 60 minutes) as shown in Figure 5.5. With Fe to MgO ratio of 5:100 there is a slight decrease in the carbon efficiency (57.52 to 53.3%) as the synthesis time increases whereas, with weight ratio of 10:100 there is a remarkable rise (54.75 to 70.61%) as a result of time increase. In summary the order the carbon efficiency of given weight ratios for 30 minutes is 5:100≈10:100>1:100, and for 60 minutes is 10:100>5:100>1:100.
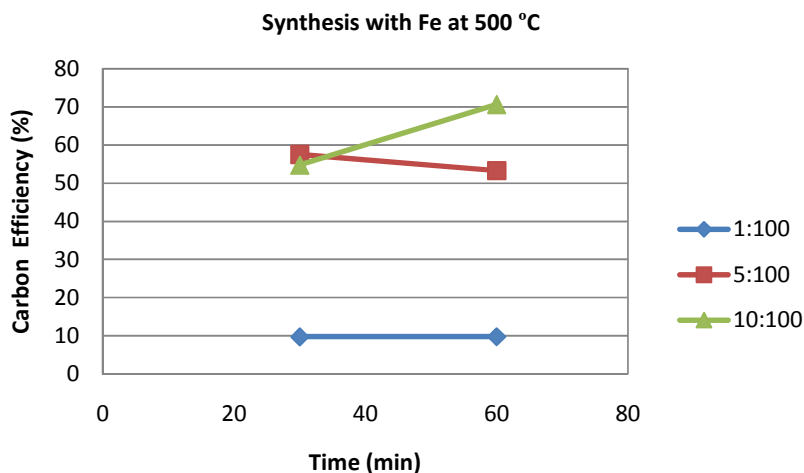
Figure 5.5 : Time vs. carbon efficiency graph of Fe at 500ºC

It is observed for SWCNT synthesis at 800ºC for 35 minutes Fe to MgO ratio of 1:100 and 10:100 have the same percentage of carbon efficiency (18.76 and 19.53% respectively) whereas 5:100 weight ratio of Fe has twice as much carbon efficiency (41.63%) than the others. When the synthesis time is increased to 60 minutes it is observed that there is a tremendous rise in the efficiency (51.02%) of 1:100 weight ratio.
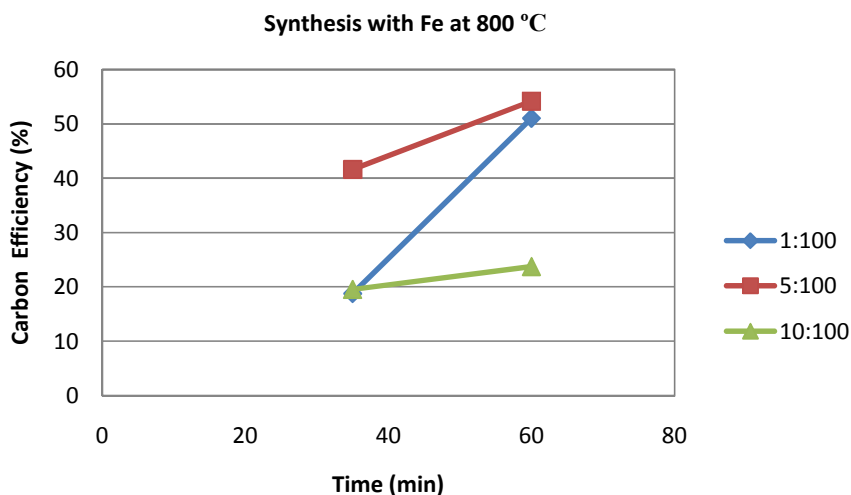

Figure 5.6 : Time vs. carbon efficiency graph of Fe 800ºC

For 60 minutes synthesis time of 10:100 Fe to MgO ratio has the lowest carbon efficiency (23.75%). In summary the order the carbon efficiency of given weight ratios for 35 minutes is 5:100>1:100=10:100, and for 60 minutes is

5:100≈1:100>10:100. When SWCNT synthesis at 800ºC is considered as shown in Figure 5.6 it is seen that the carbon efficiency of the catalysts show different behaviour with changing temperature.

5.1.3 Effect of weight ratio

The effect of weight ratio is analysed for SWCNT and MWCNT synthesis at 800ºC and 500ºC respectively. As it is shown in Figure 5.7 at 500ºC for a synthesis time of 30 minutes there is a considerable increase in the carbon efficiency from 1:100 (9.74%) to 5:100 Fe to MgO weight ratio (57.52%) whereas 10:100 has lower carbon efficiency (54.74%) than 5:100 weight ratio.   When synthesis time is 60 minutes the carbon efficiency increases with increasing weight ratio (9.79, 53.3 and 70.61% respectively). In summary at 500ºC the order of the carbon efficiency of given weight ratios for 30 minutes is 5:100≈10:100>1:100 whereas for 60 minutes it is 10:100>5:100>1:100.

Figure 5.7 : Weight ratio vs. carbon efficiency graph of Fe at 500ºC

As it can be seen in Figure 5.8, at 800ºC the effect of weight ratio to carbon efiiciency shows identical behaviour for both 35 minutes and 60 minutes of synthesis times. It can be obsserved from the graph that for a synthesis time of 35 minutes, the carbon efficiency increases from 1:100 (18.76%) weight ratio to 5:100 (41.63%) and makes a climax at this point. Then decreases to almost the same efficiency value with 1:100 when the weight ratio is increased to 10:100 (19.53%). Whereas it is seen that for a synthesis time of 60 minutes there is an increase of approximately 10% in the

carbon efficiency with an increase of 5:100 weight ratio. However weight ratio reaching 10:100 results with a drastic decrease in the carbon efficiency. In summary at 800ºC the order of the carbon efficiency of given weight ratios for 35 minutes is 5:100>10:100=1:100 whereas for 60 minutes it is 1:100≈5:100>10:100.
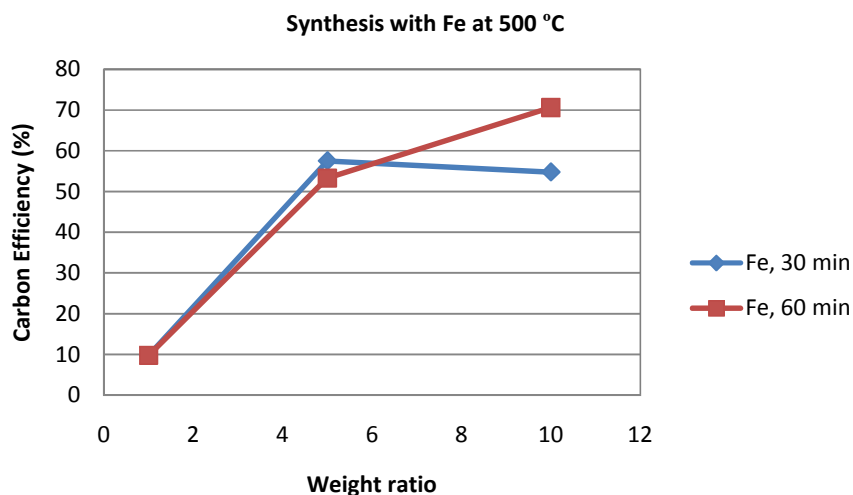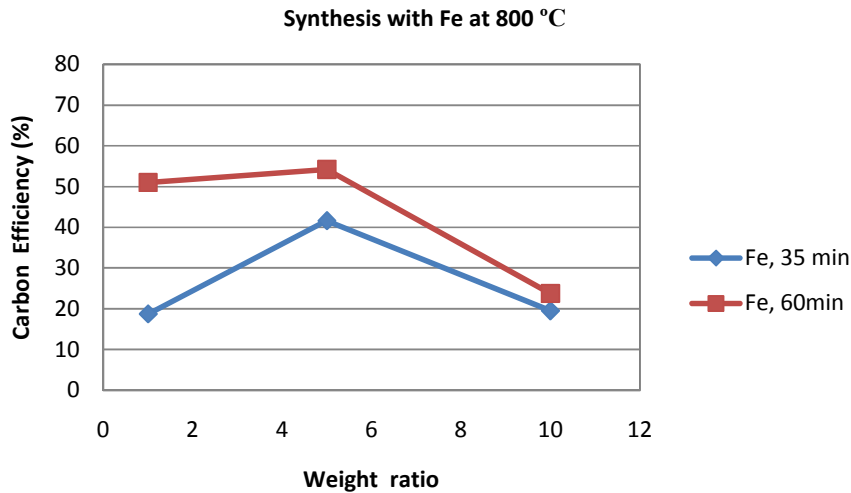

Figure 5.8 : Weight ratio vs. carbon efficiency graph of Fe at 800ºC

5.1.4 Statistical results

In this thesis, a statistical design technique was also applied by use of a two level factorial design matrix to interpret the CNTs synthesis with Fe catalyst experimental results [102]. A major advantage of the statistical model over the analytical ones is that they do not use rough approximations and allow for a greater number of factors. In two level factorial design experiments, process variables were selected as synthesis temperature (T) (500 and 800°C), synthesis time (t) (30 and 60 min) and Fe:MgO weight ratio (R) (5 and 10). The carbon efficiency of as-synthesized CNTs was selected as the objective function.

The number of trials required for this purpose is given by the following equation [102]:

$$N = 2^n \tag{5.2}$$

where, N and n are the numbers of trials and variables, respectively.

Since the number of variables in the present case are three, the number of experiments required is 8, excluding replicates. If a_k represents the variables, then

$$a_{k,b} = (a_{k,\max} + a_{k,\min})/2 \tag{5.3}$$

where; $a_{k,b}$ = *base level*

$a_{k,\max}$ = *upper level*

$a_{k,\min}$ = *lower level*

It is customary to convert the a_k coordinates to a new dimensionless system of coordinates as follows:

$$X_k = (a_k - a_{k,b})/\Delta a_k \tag{5.4}$$

where,

$$\Delta a_k = (a_{k,\max} - a_{k,\min})/2 \tag{5.5}$$

and x_k stands for coded factors. Thus the upper level of x_k becomes +1 and lower level -1 in the coded form. At the base level, the value of x_k becomes zero.

The actual and coded values of the variables of experiments are shown in Table 5.1. The design matrix and results of experiments are listed in Table 5.2. The regression equation developed to predict the carbon efficiency of the synthesized sample and optimize the process conditions using a multi-factor linear model as follows:

$$Y = A_0 + A_1X_1 + A_2X_2 + A_3X_3 + A_4X_1X_2 + A_5X_1X_3 + A_6X_2X_3 + A_7X_1X_2X_3 \tag{5.6}$$

The variance test of the parameters for the sample showed that one of the variables is not statistically significant. Therefore, its respective terms can be rejected in the following proposed model:

$$Y = 109.41 - 74.63X_1 + 57.75X_2 - 58.95X_3 - 70.89X_1X_2 - 61.03X_2X_3 + 63.14X_1X_3 \tag{5.7}$$

The correlation coefficient of Eq. 5.7 was determined as 0.89. The relationship between the coded values (X_k) and actual values can be given as follows:

$$X_1 = (T - 650)/37.5 \tag{5.8}$$

$$X_2 = (R - 7.5)/2.5 \tag{5.9}$$

$$X_3 = (t - 45)/15 \tag{5.10}$$

Table 5.1: Actual and coded values of the variables

Level	Upper Level	Lower Level	Base Level
a_1 (T) Synthesis Temperature (°C)	500	800	650
X_1	+1	-1	0
a_2 (R) Fe:MgO weight ratio	10	5	7.5
X_2 Coded	+1	-1	0
a_3 (t) Synthesis time (min)	30	60	45
X_3 Coded	+1	-1	0

Table 5.2: Design matrix and results of Fe catalyst experiments

Trial No	X_1	X_2	X_3	Y
1	-1	-1	-1	57.52
2	-1	-1	1	53.30
3	-1	1	-1	54.75
4	-1	1	1	70.61
5	1	-1	-1	41.63
6	1	-1	1	54.2
7	1	1	-1	19.53
8	1	1	-1	23.75

The regression equation clearly show that since the coefficient of synthesis temperature is the highest among all the coefficients, the effect of this parameter on the carbon efficiency of the CNT sample is the strongest. Nevertheless, the carbon efficiency of the CNT was affected negatively by this variable. Synthesis time and Fe:MgO weight ratio are also effective parameters on the carbon efficiency. Increasing the Fe:MgO weight ratio effectively enhance the carbon efficiency. However, carbon efficiency decreases with increasing synthesis time. It may also concluded from the regression model that the interactional effects such as (synthesis temperature x Fe:MgO weight ratio) $(X_1.X_2)$, (Fe:MgO weight ratio x synthesis time) (X_2X_3) and (synthesis temperature x synthesis time) $(X_1.X_3)$ influence the carbon efficiency of the CNTs positively and negatively respectively, at 89 % confidence

level. In other words, if one of the variables is changed with respect to another one, it will have a considerable effect on the carbon efficiency.

5.2 CNT synthesis by Co catalyst

Cobalt is considered to be one of the best resulting catalysts in CNT synthesis in the previous researches [69, 103, 104]. $Co(NO_3)_2).6H_2O$ that is selected as catalyst is mixed with MgO substrate and ethanol by ultrasonic mixer for 30 minutes and then dried in the oven for 18 hours. The formed catalyst is used for synthesis of CNT as a result of decomposition of acetylene by CCVD method. Co catalyst with different weight ratios to MgO substrate (1:100, 5:100 and 10:100) is used for synthesis of MWCNT and SWCNT at 500ºC and 800ºC respectively. The reaction times were 30 minutes and 60 minutes. As a result of the experiments the effect of time, temperature and weight ratio of the Co to MgO were analysed.

5.2.1 Effect of temperature

In Figure 5.9 the effect of temperature on carbon efficiency of Co catalyst for synthesis of 30 minutes (for MWCNT) and 35 minutes (for SWCNT) is shown. It is seen that there is a tremendous decrease in carbon efficiencies with increase in temperatures. For 5:100 weight ratio of Co to MgO the carbon efficiency decreases from 53.14 to 17.38% and it decreases from 68.05 to 24.21% for 10:100 weight ratio with increase of temperature from 500 to 800ºC. In summary the order the carbon efficiency of given temperature of 500ºC for 30 and 35 minutes is 10:100>5:100>1:100, and for 800ºC it is 10:100>5:100.

When CNT synthesis for 60 minutes at 500ºC and 800ºC is considered as shown in Figure 5.10, it is seen that there is also a decerase in carbon efficiency of Co catalyst with increase in temperature. For 5:100 weight ratio of Co to MgO, the carbon efficiency decresaes from it decreases from 54.69 to 43.69% and it decreaes from 68.94 to 53.77% for 10:100 weight ratio with increase of temperature from 500 to 800ºC. In summary the order the carbon efficiency of given temperature of 500ºC and 800 ºC for 60 minutes is 10:100>5:100.
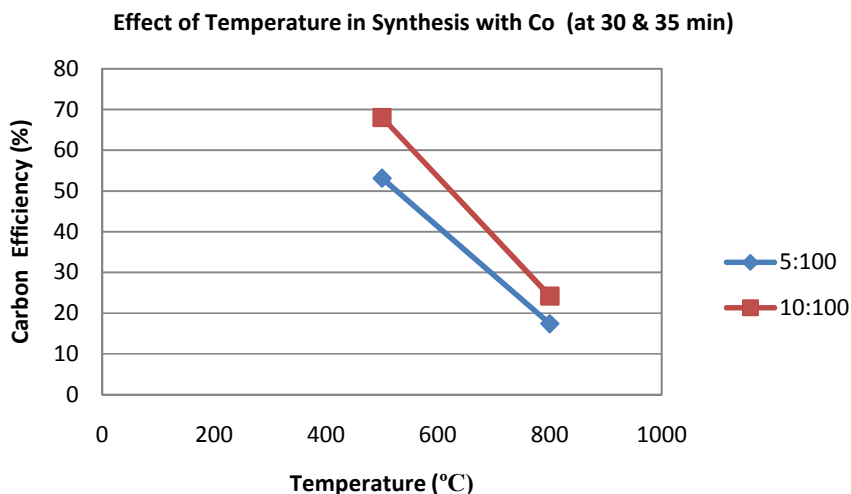
Figure 5.9 : Temperature vs. carbon efficiency graph of Co for 30&35 min
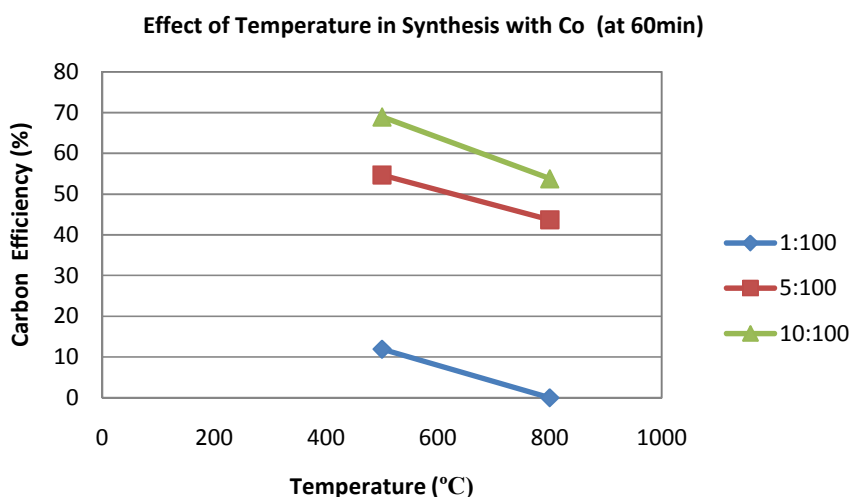

Figure 5.10 : Temperature vs. carbon efficiency graph of Co for 60 min

5.2.2 Effect of time for Co catalyst

The effect of time is analysed for MWCNT synthesised with Co catalyst at 500 and 800ºC. It is observed at 500ºC that for all Co to MgO ratios there is a slight change in the carbon efficiency with respect to the synthesis time. As it can be seen Figure 5.11 there is a slight change in the carbon efficiency with respect to synthesis time (30 and 60 minutes) with all weight ratios. When the carbon efficiencies of three weight ratios are compared it is seen that 1:100 has the lowest carbon efficiency (10.51 and 11.95%), it is followed by 5:100 (53.14 and 54.69%) and 10:100 has the highest carbon efficiency (68.15 and 68.94%) at both synthesis times (30 and 60 min

respectively). As-synthesized CNTs with a cobalt weight ratio of 10:100 have very considerable carbon efficiency reaching 70%. It shows when cobalt is used as catalyst synthesis time does not affect the carbon efficiency. In summary at 500 ºC the order of the carbon efficiency of given weight ratios for 30 and 60 minutes is 10:100>5:100>1:100.
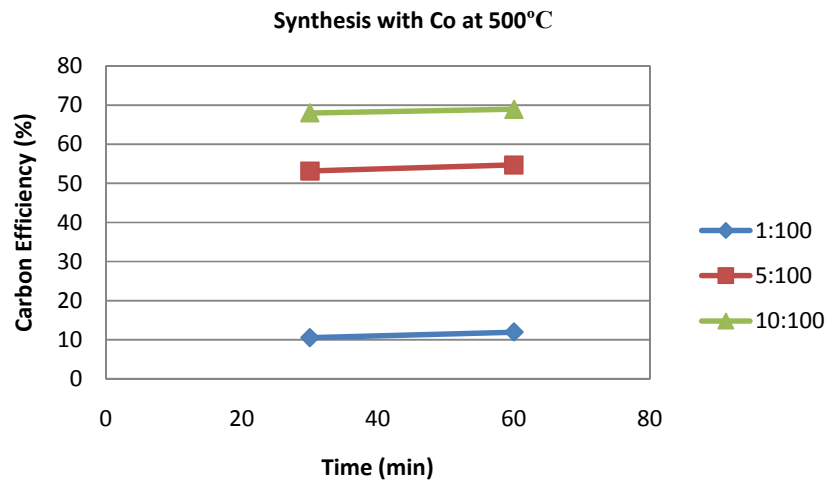
Synthesis with Co at 500ºC

Figure 5.11 : Time vs. carbon efficiency graph of Co at 500ºC
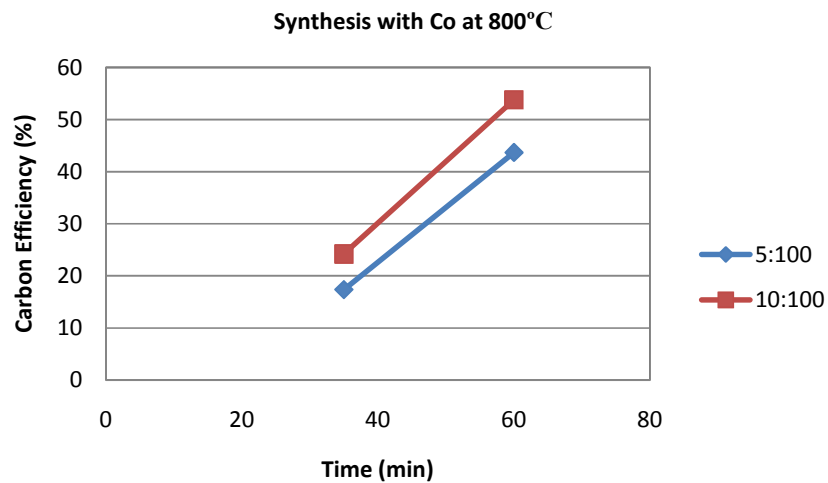
Synthesis with Co at 800ºC

Figure 5.12 : Time vs. carbon efficiency graph of Co at 800ºC

As 1:100 weight ratio had very low carbon efficiency for MWCNT synthesis, we ignored it for SWCNT synthesis. It is observed that at 800 ºC for 5:100 and 10:100 weight ratios of Co to MgO there is a remarkable increase in the carbon efficiency with respect to the synthesis time. As it can be seen Figure 5.12 with increase of time

from 30 to 60 minutes the carbon efficiency of 5:100 weight ratio increases from 17.38 to 43.69%. and for 10:100 weight ratio increases from 24.21 to 53.77%. As-synthesized SWCNTs with a cobalt catalyst do not have very high carbon efficiencies. In summary at 800 ºC the order of the carbon efficiency of given weight ratios for 30 and 60 minutes is 10:100>5:100.

5.2.3 Effect of weight ratio

The effect of weight ratio is analysed for MWCNT synthesised with Co catalyst at 500 ºC. As it can be seen in Figure 5.13 that the carbon efficiency increases with increasing weight ratio. The blue and red lines representing synthesis times of 30 and 60 minutes respectively show the same behaviour. Cobalt has carbon efficiency changing from 10% to 70% as a result of increasing weight percentages with synthesis times having almost no effect on the efficiency. In summary at 500 ºC the order of the carbon efficiency of given weight ratios is 10:100>5:100>1:100.
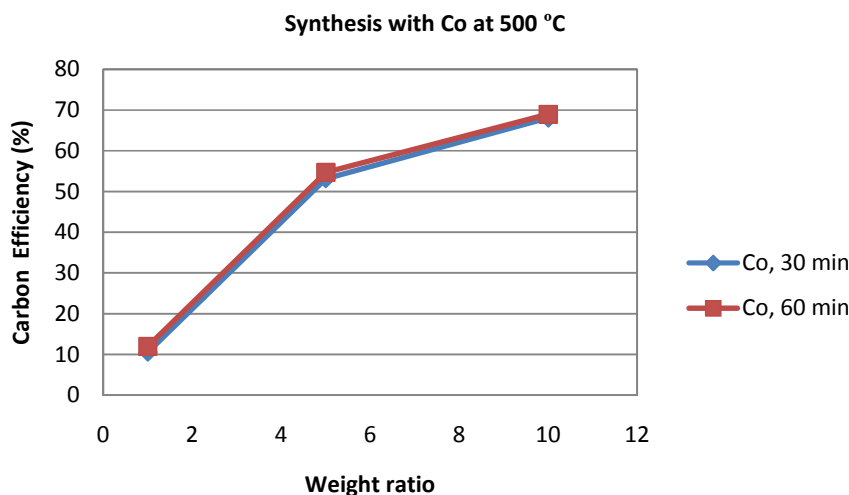

Figure 5.13 : Weight ratio vs. carbon efficiency graph of Co at 500ºC

The effect of weight ratio is also analysed for SWCNT synthesised with Co catalyst at 800 ºC. As it is also seen in Figure 5.14 that the carbon efficiency increases with increasing weight ratio. The blue and red lines representing synthesis times of 35 and 60 minutes respectively show the same behaviour. Cobalt has carbon efficiency increasing from 17.38 to 24.21% for 35 minutes and 43.69 to 53.77 for 60 minutes of synthesis time. In summary at 800 ºC the order of the carbon efficiency of given weight ratios is 10:100>5:100.
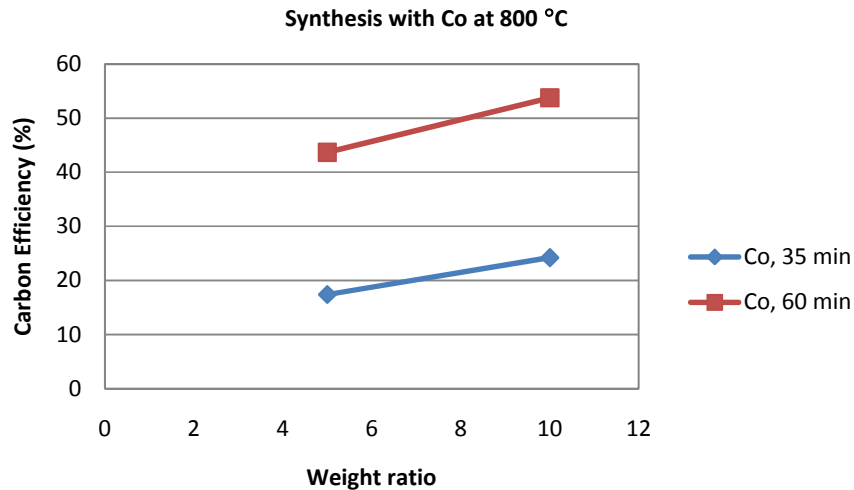
Figure 5.14 : Weight ratio vs. carbon efficiency graph of Co at 800ºC

5.2.4   Statistical results

Table 5.3 summarizes interpretation of the results for Co catalyst achieved by use of the statistical design technique which is described in detail in Chapter 5.1.4 Experimental tests were performed using a 2^3 factorial design by considering the temperature, time and siliceous Co:MgO weight ratio as variables. The data given in Table 5.3 show the design matrix and results of experiments.

Table 5.3: Design matrix and results of Co catalyst experiments

Trial No	X_1	X_2	X_3	Y
1	-1	-1	-1	53.14
2	-1	-1	1	54.69
3	-1	1	-1	68.05
4	-1	1	1	68.94
5	1	-1	-1	17.38
6	1	-1	1	43.69
7	1	1	-1	24.21
8	1	1	1	53.77

The regression equation developed to predict the carbon efficiency of the synthesized sample and optimize the process conditions using a multi-factor linear model as follows:

$$Y = 47.98 - 13.22X_1 + 5.76X_2 + 7.29X_3 - 1.53X_1X_2 + 6.68X_1X_3 \qquad \textbf{(5.11)}$$

The correlation coefficient of Eq. 5.11 was determined as 0.99. The relationship between the coded values (X_k) and actual values can be given as follows where T is synthesis temperature, R is Co:MgO weight ratio and t is synthesis time:

$$X_1 = (T - 650)/37.5 \qquad \textbf{(5.12)}$$

$$X_2 = (R - 7.5)/2.5 \qquad \textbf{(5.13)}$$

$$X_3 = (t - 45)/15 \qquad \textbf{(5.14)}$$

The regression equation clearly show that since the coefficient of synthesis temperature is the highest among all the coefficients, the effect of this parameter on the carbon efficiency of the CNT sample is the strongest. Nevertheless, the carbon efficiency of the CNT was affected negatively by this variable. Synthesis time and Co:MgO weight ratio are also effective parameters on the carbon efficiency. Increasing the Co:MgO weight ratio effectively enhance the carbon efficiency. Carbon efficiency also increases with increasing synthesis time. It may also concluded from the regression model that the interactional effects such as (synthesis time x Co:MgO weight ratio) (X1.X2), and (synthesis temperature x synthesis time) (X1.X3) influence the carbon efficiency of the CNTs positively and negatively respectively, at 99 % confidence level. In other words, if one of the variables is changed with respect to another one, it will have a considerable effect on the carbon efficiency.

5.3   CNT synthesis by Ni catalyst

Nickel is another most commonly used transition metal catalyst in CNT synthesis. Ni based catalyst are generally used to produce MWCNTs. There are variety of Ni and substrate combinations which resulted with different quality of CNTs [105-116]. $(Ni(NO_3)_2).6H_2O$ that is selected as catalyst is mixed with MgO substrate and ethanol by ultrasonic mixer for 30 minutes and then dried in the oven for 18 hours. The formed catalyst is used for synthesis of CNT as a result of decomposition of acetylene by CCVD method. Co catalyst with different weight ratios to MgO substrate (1:100, 5:100 and 10:100) is used for synthesis of MWCNT and SWCNT at 500ºC and 800ºC respectively. The reaction times were 30 and 60 minutes. As a

result of the experiments the effect of time, temperature and weight ratio of the Ni to MgO were analysed.

5.3.1 Effect of temperature

In Figure 5.15 the effect of temperature on carbon efficiency of Ni catalyst for synthesis of 30 minutes (for MWCNT) and 35 minutes (for SWCNT) is shown. It is seen that there is an increase in carbon efficiencies with increase in temperature. For 5:100 weight ratio of Ni to MgO carbon efficiency increases from 18.54 to 36.83% and it increase from 26.37 to 34.27% and for 10:100 weight ratio with increase of temperature from 500 to 800ºC. In summary the order the carbon efficiency of given temperature of 500ºC for 30 and 35 minutes is 10:100>5:100, whereas for 800ºC it is 5:100>10:100.
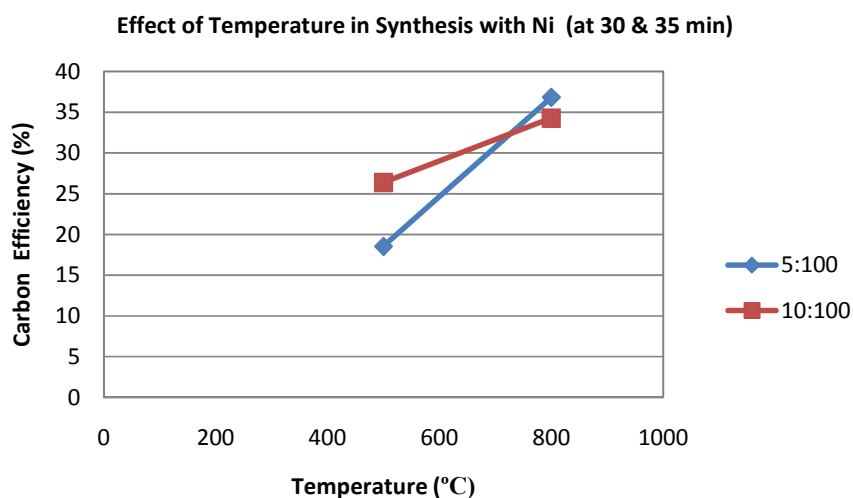

Figure 5.15 : Temperature vs. carbon efficiency graph of Ni for 30&35 min

In Figure 5.16 the effect of temperature on carbon efficiency of Ni catalyst for synthesis of 60 minutes for MWCNT and SWCNT is shown. It is seen that there is an increase in carbon efficiencies with increase in temperatures. With these experimental parameters both weight ratios have almost the same carbon efficiencies. For 5:100 weight ratio of Ni to MgO carbon efficiency increases from 19.37 to 51.82% and it increase from 23.2 to 48.74% for 10:100 weight ratio with increase of temperature from 500 to 800ºC. In summary the order the carbon efficiency of given temperature of 500ºC is 10:100>5:100, whereas for 800ºC it is 5:100>10:100 for 60 minutes of synthesis time.
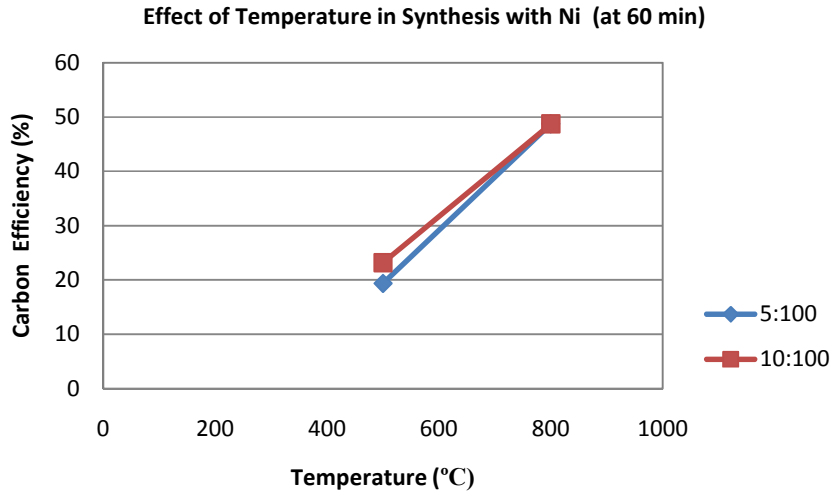
Figure 5.16 : Temperature vs. carbon efficiency graph of Ni for 60 min

5.3.2 Effect of time

The effect of time is analysed for MWCNT synthesized with Ni catalyst at 500 and 800 ºC. It is seen from Figure 5.17 that with increasing synthesis time the carbon efficiency of 1:100 (12.34 to 14.21%) and 5:100 (18.54 to 19.37%) Ni to MgO weight ratios slightly increases. However 10:100 weight ratio of Ni:MgO slightly decreases (26.37 to 23.2%). In summary at 500 ºC the order of the carbon efficiency of given weight ratios is 10:100>5:100>1:100.

It is seen from Figure 5.18 that at 800 ºC with increasing synthesis time the carbon efficiency of both 5:100 (36.83 to 51.82%) and 10:100 (34.27 to 48.74%) Ni to MgO weight ratios show the similar increasing behaviour. It was seen from Figure 5.17 at 500 ºC there was almost no change in the carbon efficiency with respect to time. However, at 800 ºC with increasing time of synthesis there is an increase in the carbon efficiency of Ni catalyst. In summary at 800 ºC the order of the carbon efficiency of given weight ratios is 5:100>10:100 for both 30 and 60 minutes of synthesis time.
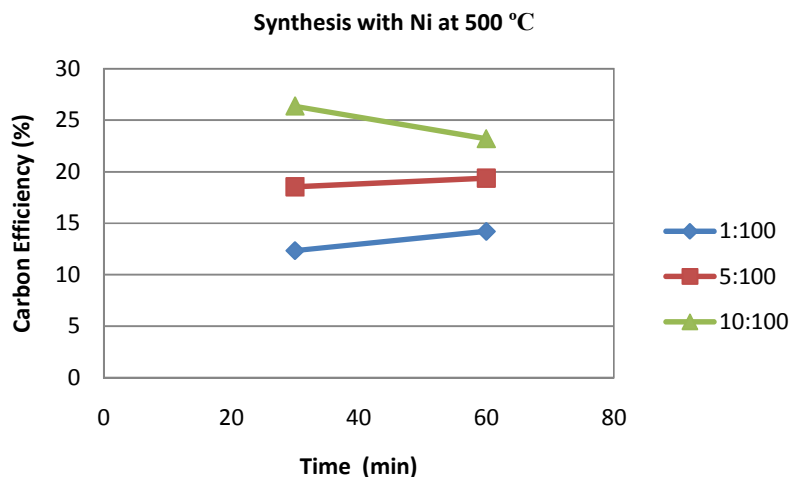
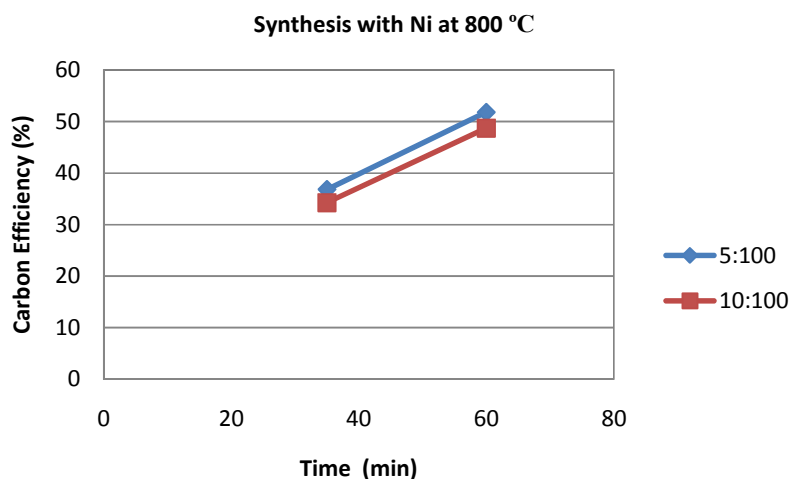**Figure 5.17 :** Time vs. carbon efficiency graph of Ni at 500ºC

Figure 5.18 : Time vs. carbon efficiency graph of Ni at 800ºC

5.3.3 Effect of weight ratio

The effect of weight ratio is analysed for both MWCNT and SWCNT synthesised with Ni catalyst at 500 and 800ºC respectively. It is seen from Figure 5.19 that at 500ºC the carbon efficiency of Ni shows a linear increase with increasing weight ratio. The maximum efficiency of Ni is found only about 26%. However, in some studies it is suggested that Ni and its alloys or compounds have high catalytic activity as a result of different catalyst preparation methods [107]. The difference in carbon efficiency of synthesis times for 30 and 60 minutes is negligible. In summary at 500ºC the order of the carbon efficiency of given weight ratios is 10:100>5:100>1:100.

Figure 5.20 that at 800ºC the carbon efficiency of Ni shows a linear increase with increasing weight ratio. As it is seen from the graph that Ni catalyst shows higher carbon efficiency at 800 ºC than it does at 500ºC. Ni catalyst has higher carbon efficiency at 60 minutes than 30 minutes at 800ºC for both 5:100 and 10:100 weight ratios.
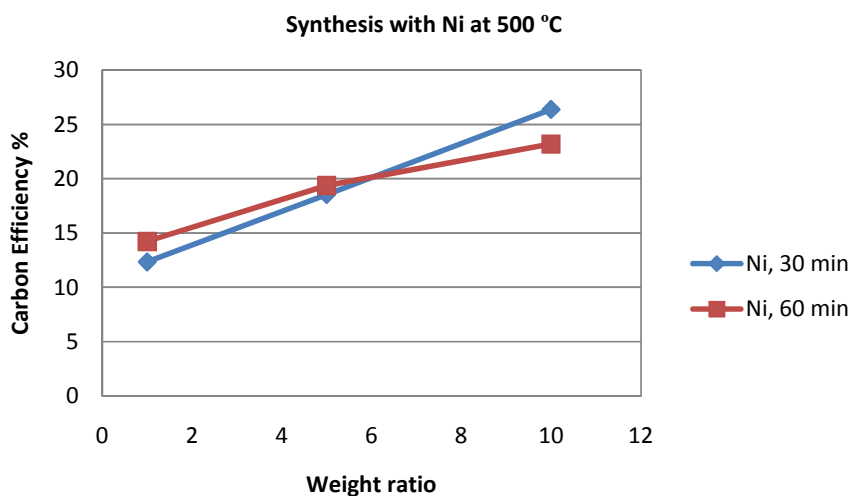

Figure 5.19 : Weight ratio vs. carbon efficiency graph of Ni at 500ºC
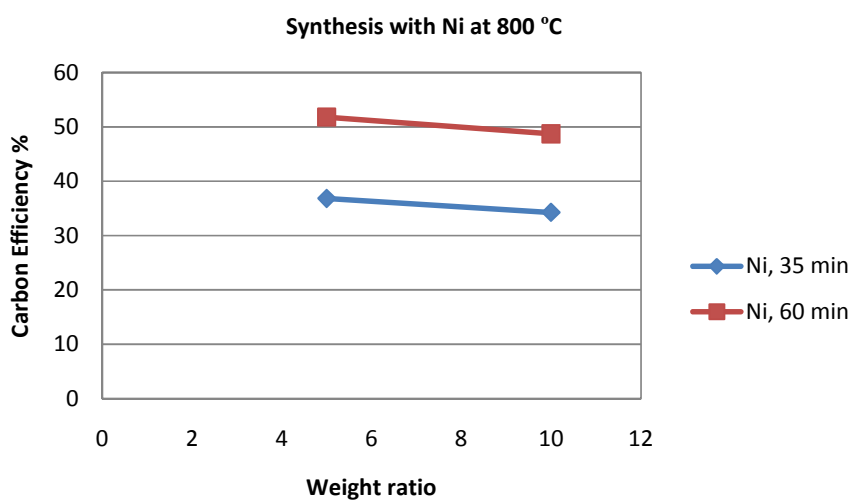

Figure 5.20 : Weight ratio vs. carbon efficiency graph of Ni at 800ºC

5.3.4   Statistical Results

Table 5.4 summarizes interpretation of the results for Ni catalyst achieved by use of the statistical design technique which is described in detail in Chapter 5.1.4 Experimental tests were performed using a 2^3 factorial design by considering the

temperature, time and siliceous Ni:MgO weight ratio as variables. The data given in Table 5.4 show the design matrix and results of experiments.

Table 5.4: Design matrix and results of Ni catalyst experiments

Trial No	X_1	X_2	X_3	Y
1	-1	-1	-1	18.54
2	-1	-1	1	19.37
3	-1	1	-1	26.37
4	-1	1	1	23.20
5	1	-1	-1	36.83
6	1	-1	1	51.82
7	1	1	-1	34.27
8	1	1	1	48.74

The regression equation developed to predict the carbon efficiency of the synthesized sample and optimize the process conditions using a multi-factor linear model as follows:

$$Y = 32.39 + 10.52X_1 + 0.75X_2 + 3.39X_3 - 2.16X_1X_2 + 3.98X_1X_3 \qquad \textbf{(5.15)}$$

The correlation coefficient of Eq. 5.15 was determined as 0.99. The relationship between the coded values (Xk) and actual values can be given as follows where T is synthesis temperature, R is Ni:MgO weight ratio and t is synthesis time:

$$X_1 = (T - 650)/37.5 \qquad \textbf{(5.16)}$$

$$X_2 = (R - 7.5)/2.5 \qquad \textbf{(5.17)}$$

$$X_3 = (t - 45)/15 \qquad \textbf{(5.18)}$$

The regression equation clearly show that since the coefficient of synthesis temperature is the highest among all the coefficients, the effect of this parameter on the carbon efficiency of the CNT sample is the strongest. Nevertheless, the carbon efficiency of the CNT was affected positively by this variable. Synthesis time and Ni:MgO weight ratio are also effective parameters on the carbon efficiency. Increasing the Ni:MgO weight ratio effectively enhance the carbon efficiency. Carbon efficiency also increases with increasing synthesis time. It may also concluded from the regression model that the interactional effects such as (synthesis

time x Ni:MgO weight ratio) (X1.X2), and (synthesis temperature x synthesis time) (X1.X3) influence the carbon efficiency of the CNTs positively and negatively respectively, at 99 % confidence level. In other words, if one of the variables is changed with respect to another one, it will have a considerable effect on the carbon efficiency.

5.4   CNT synthesis by V catalyst

Vanadium catalyst is not very commonly used in CNT synthesis due to its high price and low efficiency. There are some studies in which V is pre-treated to overcome low efficiency. In a research conducted by Seo et al. V catalyst is used in CNT synthesis after a laser treatment to increase the surface are and therefore the interaction of the vanadium with the carbon source [99]. In this research V_2O_5 that is selected as catalyst is mixed with MgO substrate and ethanol by ultrasonic mixer for 30 minutes and then dried in the oven for 18 hours.   The formed catalyst is used for synthesis of CNT as a result of decomposition of acetylene by CCVD method. V catalyst with different weight ratios to MgO substrate (5:100 and 10:100) is used for synthesis of MWCNT at 500 ºC.   The reaction times were 30 minutes and 60 minutes. Also SWCNT was synthesised at 800ºC with 5:100 weight ratio of V with a synthesis time of 60 minutes. As a result of the experiments the effect of time, temperature and weight ratio of the V to MgO were analysed.

5.4.1   Effect of temperature

In Figure 5.21 the effect of temperature on carbon efficiency of V catalyst for synthesis of 60 minutes for both MWCNT and SWCNT for 5:100 weight ratio of V:MgO is shown. It is seen that there is an increase in carbon efficiency of V catalyst with increase in temperature. For 5:100 weight ratio of V to MgO carbon efficiency increases from 11.46 to 34.83%.
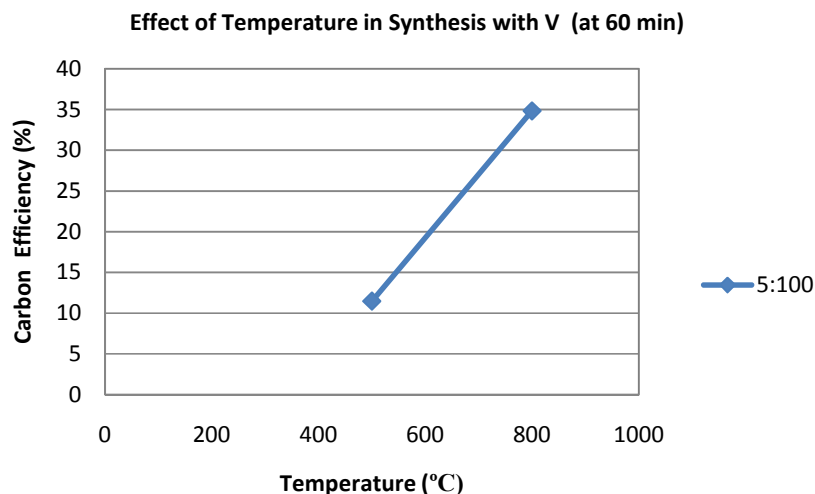
Figure 5.21 : Temperature vs. carbon efficiency graph of V for 60 min

5.4.2 Effect of time

The effect of time is analysed for MWCNT synthesized with V catalyst at 500 ºC. As it is shown in Figure 5.22, 5:100 (9.78 to 11.46 %) and 10:100 (8.3 to 9.88%) weight ratios of V:MgO have low carbon efficiency with synthesis times of 30 and 60 minutes respectively. Regarding to this results 1:100 weight ratio of V was not experimented. For both of the weight ratios there is a slight increase with increasing synthesis time. As it is also shown in Figure 5.22 synthesis time does not affect the carbon efficiency of vanadium catalyst for MWCNT. In summary at 500 ºC the order of the carbon efficiency of given weight ratios is 5:100≈10:100.
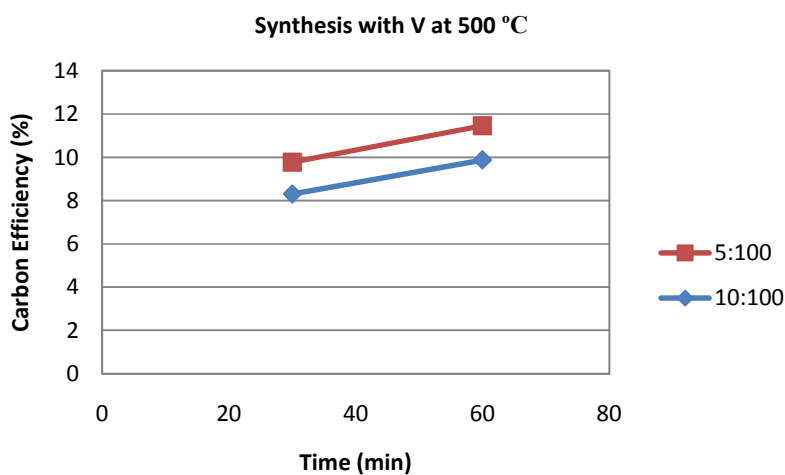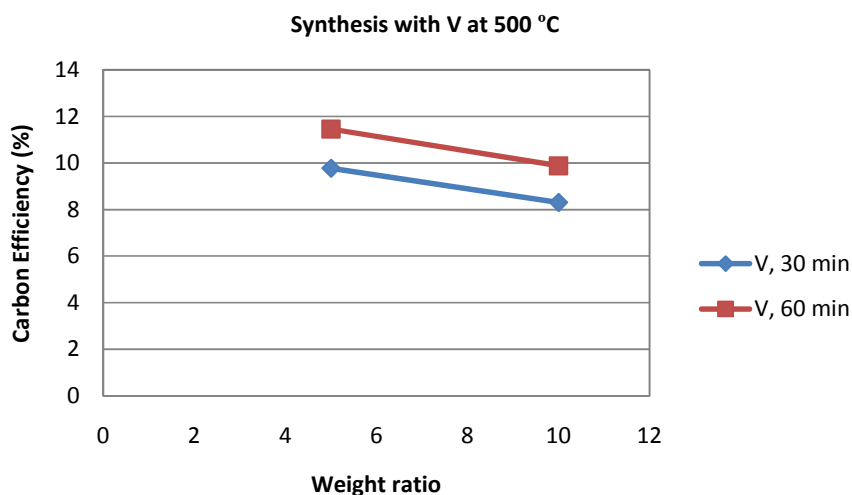

Figure 5.22 : Time vs. carbon efficiency graph of V at 500 ºC

5.4.3 Effect of weight ratio

The effect of weight ratio is analysed for MWCNT synthesized with V catalyst at 500 °C. As it is seen from Figure 5.23 that when weight ratio of V increases from weight ratio of 5:100 to 10:100 there becomes a slight decrease in the carbon efficiency. It is also observed that the change in weight ratio does not affect the carbon efficiency of vanadium catalyst. In summary at 500°C the order of the carbon efficiency of given weight ratios is 5:100≈10:100.

Figure 5.23 : Weight ratio vs. carbon efficiency graph of V at 500 ºC

5.5 CNT synthesis by Fe&Co binary catalyst

Fe and Co are most commonly used catalysts in the literature [69, 98,117]. In this study, Co and Fe were found to be the most efficient catalysts whereas V and Ni were the least efficient catalysts. Therefore Co&Fe were selected as binary catalyst and the carbon efficiency on CNT synthesis was investigated. The experiments of Fe & Co binary catalyst were carried out with weight ratios of 5:100 and 10:100 to MgO since higher carbon efficiency than 1:100 weight ratio was observed with 5:100 and 10:100 weight ratios. While preparing the binary catalyst with ratio of 5:100, Fe to MgO weight ratio of 2.5:100 is added to Co amount satisfying Co to MgO weight ratio of 2.5:100 and then mixed with MgO substrate and ethanol by ultrasonic mixer for 30 minutes. Afterwards the mixture was dried in the oven for 18 hours. The prepared catalyst is used for CNT synthesis by CCVD method with decomposition of acetylene. The reaction times were 30 minutes and 60 minutes for MWCNT and

SWCNT synthesis at 500 and 800ºC respectively. As a result of the experiments the effect of time, temperature and weight ratio of the Fe & Co to MgO were analysed.

5.5.1 Effect of temperature

In Figure 5.24 the effect of temperature on carbon efficiency of Fe&Co catalyst for synthesis of 30 minutes (for MWCNT) and 35 minutes (for SWCNT) is shown. It can be observed from the graph that the carbon efficiency of Fe&Co binary catalyst shows a mixture of Fe and Co catalysts. For 5:100 weight ratio of Fe&Co to MgO the carbon efficiency increases from 45.32 to 50.77% whereas it decreases from 80.61 to 43.97% for 10:100 weight ratio with increase of temperature from 500 to 800ºC. In summary the order the carbon efficiency of given temperature of 500ºC for 30 and 35 minutes is 10:100>5:100, whereas for 800ºC it is 5:100>10:100.

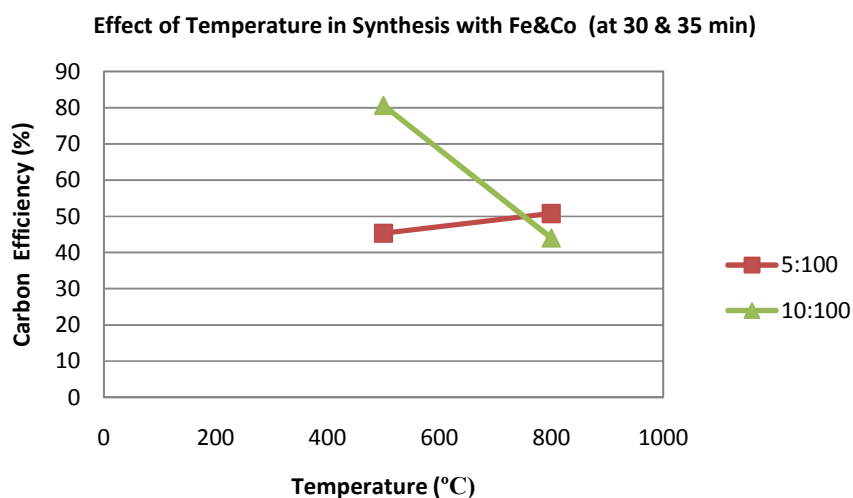**Effect of Temperature in Synthesis with Fe&Co (at 30 & 35 min)**

Figure 5.24 : Temperature vs. carbon efficiency graph of Fe&Co for 30&35 min

Figure 5.25 the effect of temperature on carbon efficiency of Fe&Co catalyst for synthesis of 60 minutes for MWCNT and SWCNT is shown. It can be observed from the graph that the carbon efficiency of Fe&Co binary catalyst also shows a mixture of Fe and Co catalysts for 60 minutes of synthesis time. For 5:100 weight ratio of Fe&Co to MgO the carbon efficiency increases from 47.22 to 52.21% whereas it decreases from 81.45 to 54.3% for 10:100 weight ratio with increase of temperature from 500 to 800ºC. In summary the order the carbon efficiency of given temperature of 500ºC for 30 and 35 minutes is 10:100>5:100, whereas for 800ºC it is 5:100≈10:100.
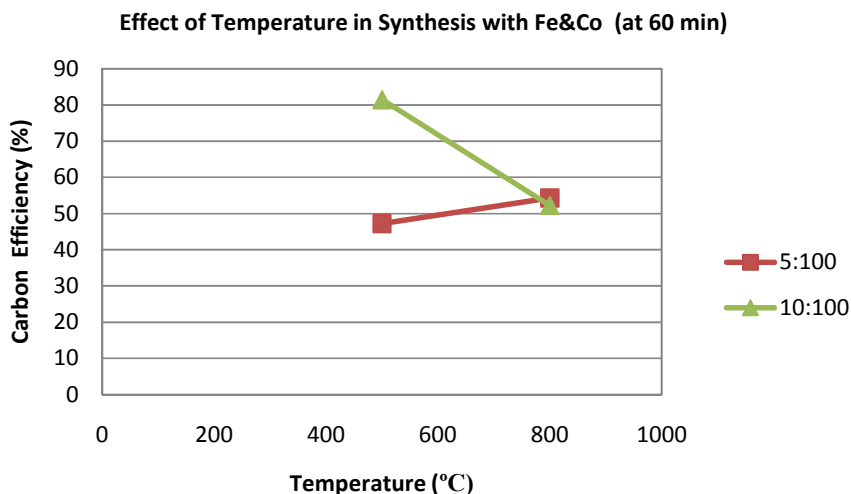
Figure 5.25 : Temperature vs. carbon efficiency graph of Fe&Co for 60 min

5.5.2   Effect of time

The effect of time is analysed for MWCNT synthesized with binary Fe & Co catalyst at 500 ºC. As it is seen from Figure 5.26 the Fe & Co binary catalyst has extremely high carbon efficiency. Weight ratio of 5:100 for 30 minutes has carbon efficiency of approximately 45% and 10:100 has carbon efficiency of 80%. With synthesis time increasing from 30 minutes to 60 minutes does not make a considerable change in the carbon efficiency. Therefore we can suggest that the increasing synthesis time does not make a substantial gain in the carbon efficiency. In summary at 500ºC the order of the carbon efficiency of given weight ratios is 10:100>5:100.
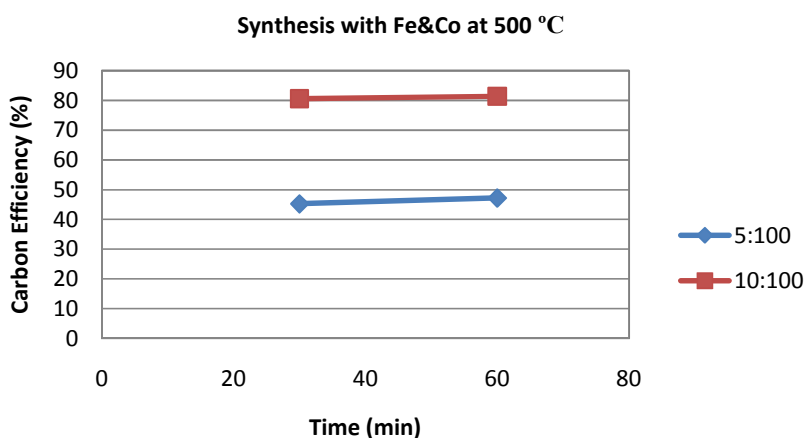

Figure 5.26 : Time vs. efficiency graph of Fe&Co catalyst at 500 ºC

It can be seen from Figure 5.27 that the Fe & Co binary catalyst has high carbon efficiency at 800 ºC as well. Weight ratio of 5:100 for 30 minutes has carbon efficiency of approximately 35.50% and 10:100 has carbon efficiency of 35.44%. With synthesis time increasing from 30 minutes to 60 minutes increases the carbon efficiency. Therefore it can be suggested that the increasing synthesis time affects the carbon efficiency in positive manner. In summary at 800ºC the order of the carbon efficiency of given weight ratios is 5:100>10:100 for 35 and 60 minutes of synthesis time.
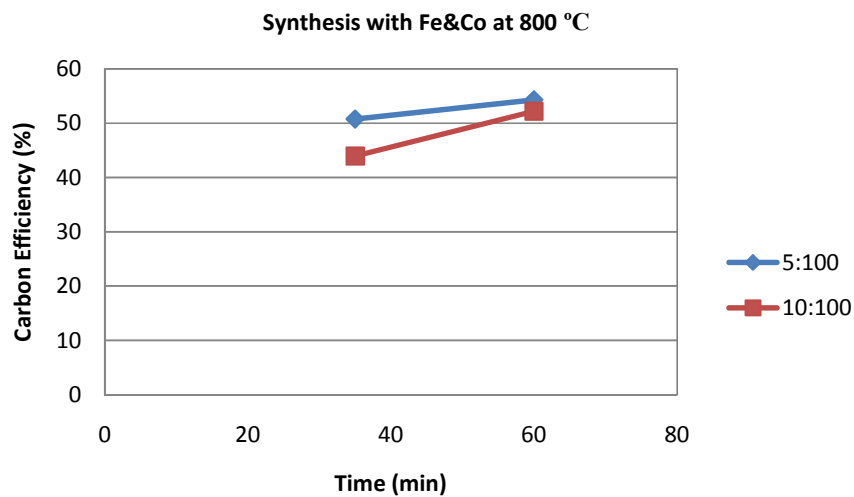
Figure 5.27 : Time vs. efficiency graph of Fe&Co catalyst at 800 ºC

5.5.3 Effect of weight ratio

The effect of weight ratio is analysed for MWCNT synthesized with binary Fe & Co catalyst at 500 ºC. As it is shown in Figure 5.28 with weight ratio increasing from 5:100 to 10:100, carbon efficiency increases from 45% to 81%. The increase in the carbon efficiency with increasing weight ratio is 44.44%. In summary at 500ºC the order of the carbon efficiency of given weight ratios is 10:100>5:100.
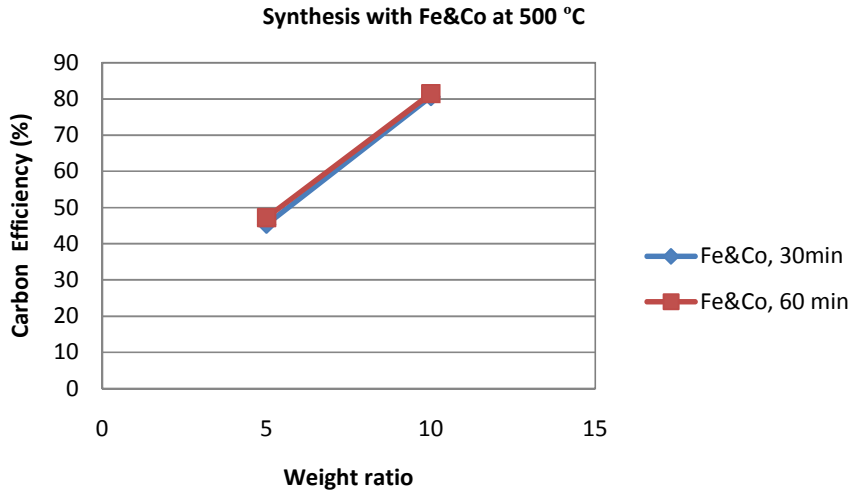
Figure 5.28 : Weight ratio vs. carbon efficiency graph of Fe&Co at 500 ºC

The effect of weight ratio is also analysed for SWCNT synthesized with binary Fe & Co catalyst at 800 ºC. As it is shown in Figure 5.29 with weight ratio increasing from 5:100 to 10:100, carbon efficiency decreases from 50.77% to 43.97% for 35 minutes of synthesis time and it decreases from 54.3 to 52.1% with increase of weight ratio from 5:100 to 10:100 for 60 minutes of synthesis time at 800ºC. In summary at 800ºC the order of the carbon efficiency of given weight ratios is 10:100>5:100.
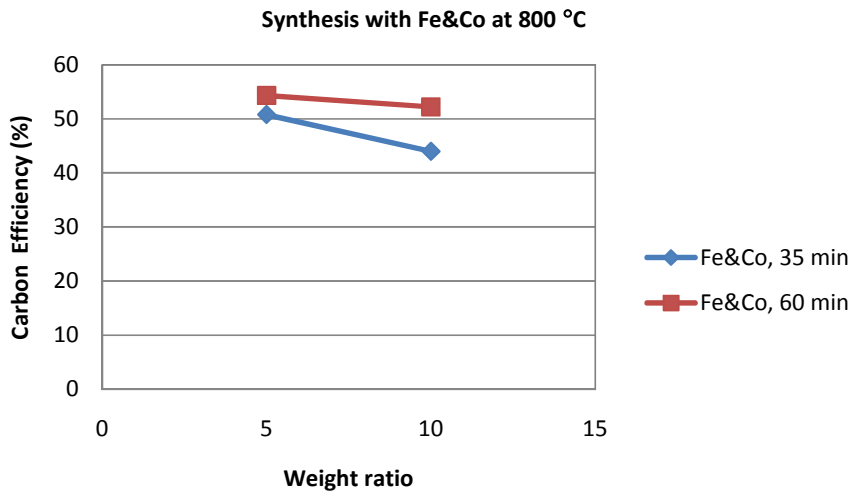

Figure 5.29 : Weight ratio vs. carbon efficiency graph of Fe&Co at 500 ºC

5.5.4 Statistical results

Table 5.5 summarizes interpretation of the results for Fe&Co binary catalyst achieved by use of the statistical design technique which is described in detail in

Chapter 5.1.4 Experimental tests were performed using a 2^3 factorial design by considering the temperature, time and siliceous Fe&Co:MgO weight ratio as variables. The data given in Table 5.5 show the design matrix and results of experiments.

The regression equation developed to predict the carbon efficiency of the synthesized sample and optimize the process conditions using a multi-factor linear model as follows:

$$Y = 56.98 - 6.67X_1 + 7.58X_2 + 1.81X_3 - 9.80X_1X_2 + 1.13X_1X_3 + 0.72X_1X_2X_3 \qquad \textbf{(5.19)}$$

The correlation coefficient of Eq. 5.19 was determined as 0.99. The relationship between the coded values (X_k) and actual values can be given as follows where T is synthesis temperature, R is Fe&Co:MgO weight ratio and t is synthesis time:

$$X_1 = (T - 650)/37.5 \qquad \textbf{(5.20)}$$

$$X_2 = (R - 7.5)/2.5 \qquad \textbf{(5.21)}$$

$$X_3 = (t - 45)/15 \qquad \textbf{(5.22)}$$

The regression equation clearly show that since the coefficient of synthesis temperature is the highest among all the coefficients, the effect of this parameter on the carbon efficiency of the CNT sample is the strongest. Nevertheless, the carbon efficiency of the CNT was affected negatively by this variable. Synthesis time and Fe&Co:MgO weight ratio are also effective parameters on the carbon efficiency. Increasing the Fe&Co:MgO weight ratio effectively enhance the carbon efficiency. Carbon efficiency also increases with increasing synthesis time. It may also concluded from the regression model that the interactional effects such as (synthesis time x Fe&Co:MgO weight ratio) ($X_1.X_2$), (synthesis temperature x synthesis time) ($X_1.X_3$), and (synthesis temperature x Fe&Co:MgO weight ratio x synthesis time) ($X_1.X_2.X_3$) influence the carbon efficiency of the CNTs positively and negatively respectively, at 99 % confidence level. In other words, if one of the variables is changed with respect to another one, it will have a considerable effect on the carbon efficiency.

Table 5.5: Design matrix and results of Fe&Co catalyst experiments

Trial No	X_1	X_2	X_3	Y
1	-1	-1	-1	45.32
2	-1	-1	1	47.22
3	-1	1	-1	80.61
4	-1	1	1	81.45
5	1	-1	-1	50.77
6	1	-1	1	54.30
7	1	1	-1	43.97
8	1	1	1	52.21

5.6 Comparison of different catalysts

The carbon efficiency of each catalyst was examined separately in previous sections. Furthermore, the comparison of carbon efficiencies of all examined catalysts is discussed in this section. The effect of weight ratio on carbon efficiency for CNT synthesis at 500°C for 30 and 60 minutes is given in Figure 5.30 and 5.31. Weight ratio of 1:100 is experimented with only Fe, Co and Ni catalysts. It can be observed that the carbon efficiencies of these three metals were found close to 10% for 1:100 weight ratio for synthesis times of both 30 and 60 minutes. The catalysts have different carbon efficiencies for 5:100 weight ratio. For this weight ratio with synthesis time of 30 minutes Fe has the highest carbon efficiency whereas V has the lowest carbon efficiency. The order of carbon efficiencies for weight ratio of 5:100 with 30 minutes of synthesis time is Fe>Co>Fe&Co>Ni>V. When the synthesis time is increased to 60 minutes, Fe and Co have the highest efficiency but the order of the efficiencies of the other catalysts does not change.
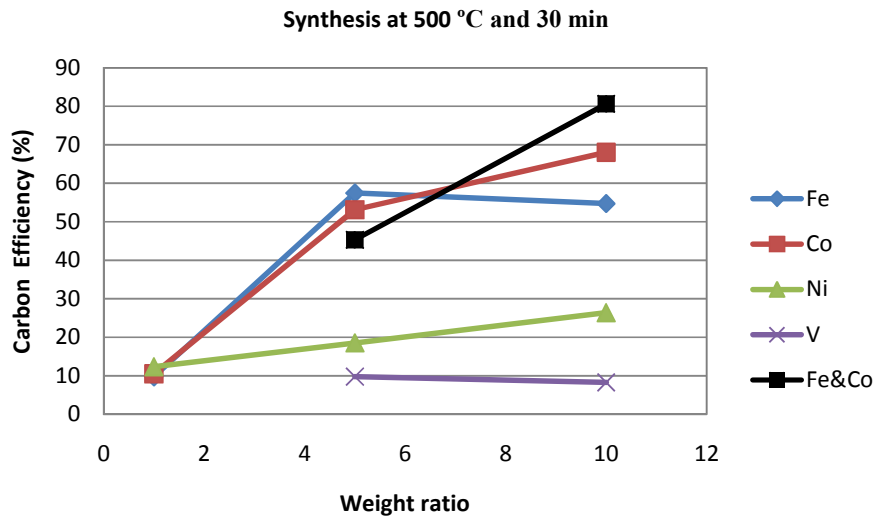
Figure 5.30 : Weight ratio vs. carbon efficiency graph at 500 ºC and 30 min
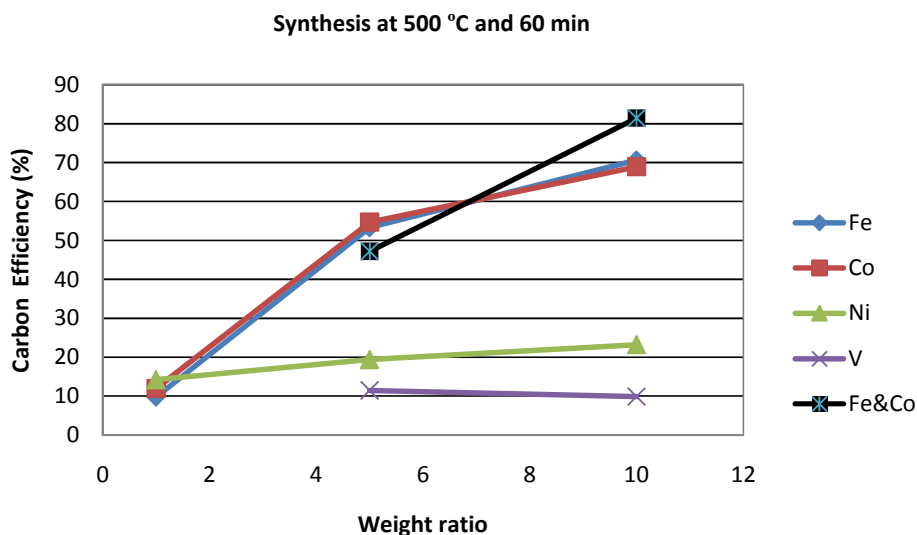

Figure 5.31 : Weight ratio vs. carbon efficiency graph at 500 ºC and 60 min

As it can be seen from the graphs the catalysts also have changing carbon efficiencies for 10:100 weight ratio. For this weight ratio with synthesis time of 60 minutes Fe&Co binary catalyst has the highest carbon efficiency whereas V has the lowest carbon efficiency. The order of carbon efficiencies for weight ratio of 10:100 with synthesis time of 30 minutes were in the order of Fe&Co>Co>Fe>Ni>V. It is suggested that increasing synthesis time increases the carbon efficiency of Fe catalyst whereas there is not a difference in efficiency of Co catalyst. In summary, the order

of the efficiencies for 10:100 weight ratio with synthesis time of 60 minutes is Fe&Co>Co≈Fe>Ni>V.

The effect of weight ratio on carbon efficiency for CNT synthesis at 800°C for 35 and 60 minutes is given in Figure 5.32 and 5.33. Weight ratio of 1:100 is experimented with only Fe catalysts. It can be observed from Figure 5.32 that for 35 minutes of synthesis time for 5:100 weight ratio Fe&Co binary catalyst has the highest carbon efficiency whereas Co has the lowest carbon efficiency. The order of carbon efficiencies for weight ratio of 5:100 with 35 minutes of synthesis time at 800°C is Fe&Co>Fe>Ni>Co. When the synthesis time is increased to 60 minutes, Fe and Fe&Co have the highest efficiency with almost the same carbon efficiencies and the efficiencies of Ni and Co also increase with increasing synthesis time.
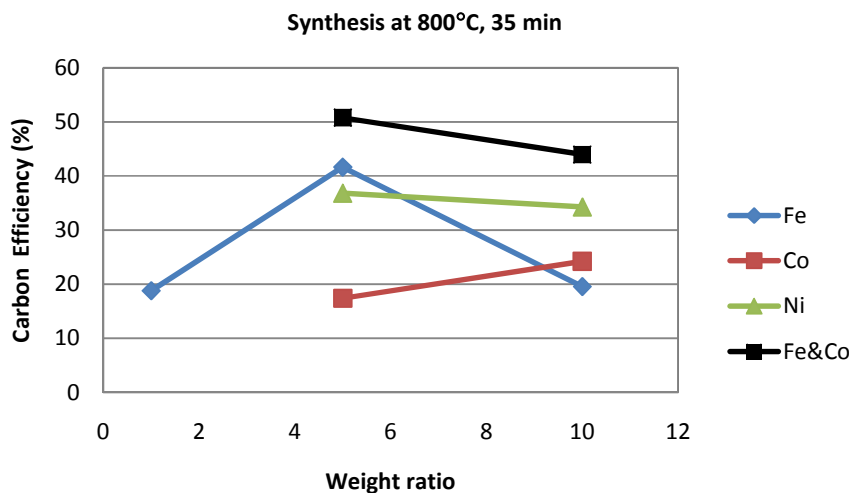
Figure 5.32: Weight ratio vs. carbon efficiency graph at 800 ºC and 35 min

For 10:100 weight ratio with synthesis time of 30 minutes Fe&Co binary catalyst has the highest carbon efficiency whereas Fe has the lowest carbon efficiency. The order of carbon efficiencies for weight ratio of 10:100 with synthesis time of 30 minutes were in the order of Fe&Co>Ni>Co>Fe. All of the catalysts have an increase in the carbon eeficiency. In summary, the order of the efficiencies for 10:100 weight ratio at 800 ºC with synthesis time of 60 minutes is Co>Fe&Co>Ni>Fe.
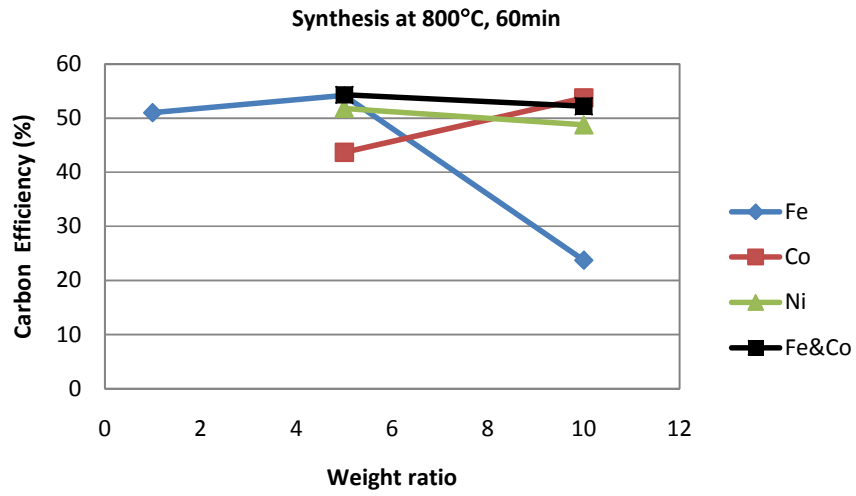
Figure 5.33 : Weight ratio vs. carbon efficiency graph at 800 ºC and 60 min

6.   CONCLUSIONS AND RECOMMENDATIONS

In this study, CNT synthesis with different catalysts by using CCVD method was performed. The effect of temperature (500 and 800°C), time (30 and 60 minutes), and weight ratio of catalyst (Fe, Co, Ni, V) to MgO (1:100, 5:100, and 10:100) on carbon efficiency was investigated. Furthermore, binary catalyst of Fe&Co for weight ratios of 5:100 and 10:100 with synthesis times of 30 and 60 minutes at 500°C was examined. The carbon efficiencies of synthesized CNTs with all catalysts were determined and compared.

6.1   Concluding Remarks

1. Fe was found to be one of the most efficient catalysts in CNT synthesis.

2. It is observed that with the change of the synthesis temperature for Fe catalyst the type of the synthesised CNTs were changed. In the temperature of 500°C MWCNTs were grown and at the temperature of 800°C SWCNTs were synthesized.

3. As a result of TEM images the diameter of MWCNTs were nearly 10 nm and their appearance was darker whereas diameters of SWCNTs were between 1.5-5 nm and also were transparent.

4. The spectra of MWCNT and that of SWCNT show a clear difference at the G band (around 1580 cm^{-1}). The intensity of the G band for SWCNT is considerably higher than MWCNT. The spectrum in RBM band which is a characteristic of SWCNT was observed in the two samples. The I_D/I_G ratio of MWNT was much higher than that of SWNT and amorphous carbon content and defect formation was much higher.

5. There was a tremendous increase in carbon efficiency of 1:100 weight ratio with temperature whereas a drastic decrease in efficiency of 5:100 and 10:100 weight ratios was observed for synthesis time of 30 minutes. In summary the

order the carbon efficiency of 500 ºC for 30 minutes is 5:100≈10:100>1:100, whereas for 800 ºC it is 5:100>1:100=10:100.

6. There was also a tremendous increase in carbon efficiency of 1:100 weight ratio with temperature and slightly increase in efficiency of 5:100 whereas a drastic decrease 10:100 weight ratios was observed for synthesis time of 60 minutes. In summary the order the carbon efficiency of 500 ºC for 60 minutes is 10:100>5:100>1:100, whereas for 800 ºC it is 5:100≈1:100>10:100.

7. A statistical design technique was applied by use of a two level factorial design matrix to interpret the CNTs synthesis with Fe catalyst experimental results. Multi-linear mathematical model developed to predict the carbon efficiency of CNTs was found to be successful with correlation coefficient of 0.89.

8. Co was also found to be one of the most efficient catalysts in MWCNT synthesis.

9. It was observed that for all Co to MgO ratios there was a slight change in the carbon efficiency with respect to the synthesis time. At 500 ºC the order of the carbon efficiency of given weight ratios for 30 and 60 minutes is 10:100>5:100>1:100 and for 800ºC it is 10:100>5:100.

10. A statistical design technique was also applied by use of a two level factorial design matrix to interpret the CNTs synthesis with Co catalyst experimental results. Multi-linear mathematical model developed to predict the carbon efficiency of CNTs was found to be successful with correlation coefficient of 0.99.

11. Ni was found to be one of the least efficient catalysts in MWCNT synthesis.

12. With increasing synthesis time for Ni catalyst the carbon efficiency of 1:100 and 5:100 weight ratios slightly increases. However the carbon efficiency of 10:100 weight ratio slightly decreases. At 500 ºC the order of the carbon efficiency of given weight ratios was 10:100>5:100>1:100. The difference in carbon efficiency of synthesis times for 30 and 60 minutes was negligible. For 800ºC the carbon efficiency is 5:100>10:100 and it increases with increasing synthesis time.

13. A statistical design technique was applied by use of a two level factorial design matrix to interpret the CNTs synthesis with Ni catalyst experimental results. Multi-linear mathematical model developed to predict the carbon efficiency of CNTs was found to be successful with correlation coefficient of 0.99.

14. V was found to be the lowest efficient catalyst in CNT synthesis.

15. For the weight ratios of 5:100 and 10:100 there was a slight increase with increasing synthesis time. At 500ºC the order of the carbon efficiency of given weight ratios is 5:100≈10:100. It was also observed that the change in weight ratio does not affect the carbon efficiency of vanadium catalyst. However with increase in synthesis temperature from 500 to 800 ºC for 5:100 weight ratio of V:MgO there is a considerable increase in the carbon efficiency.

16. Co and Fe were found to be the most efficient catalysts whereas V and Ni were the least efficient catalysts for CNT. Therefore Co&Fe were selected as binary catalyst and the carbon efficiency on CNT synthesis was investigated.

17. The Fe&Co binary catalyst had extremely high carbon efficiency. Weight ratio of 5:100 for 30 minutes had carbon efficiency of approximately 45% and 10:100 had carbon efficiency of 80%. At 500ºC with synthesis time increasing from 30 minutes to 60 minutes did not make a considerable change in the carbon efficiency. With increase in temperature from 500 to 800 ºC the carbon efficiency of 5:100 increases whereas 10:100 weight ratio of Fe&Co catalyst decreases drastically.

18. With weight ratio increasing from 5:100 to 10:100, carbon efficiency Fe&Co binary catalyst increased from 45% to 81% at 500 ºC.

19. A statistical design technique was also applied by use of a two level factorial design matrix to interpret the CNTs synthesis with Fe&Co binary catalyst experimental results. Multi-linear mathematical model developed to predict the carbon efficiency of CNTs was found to be successful with correlation coefficient of 0.99.

20. The carbon efficiencies of all examined catalysts were compared.

21. For 5:100 weight ratio with synthesis time of 30 minutes at 500°C Fe has the highest carbon efficiency whereas V has the lowest carbon efficiency. The order of carbon efficiencies for this ratio was Fe>Co>Fe&Co>Ni>V. When the synthesis time was increased to 60 minutes, Fe and Co have the highest efficiency but the order of the efficiencies of the other catalysts did not change.

22. The order of carbon efficiencies for weight ratio of 5:100 with 35 minutes of synthesis time at 800°C is Fe&Co>Fe>Ni>Co. When the synthesis time is increased to 60 minutes, Fe and Fe&Co have the highest efficiency with almost the same carbon efficiencies and the efficiencies of Ni and Co also increase with increasing synthesis time.

23. For 10:100 weight ratio with synthesis time of 30 minutes Fe&Co binary catalyst has the highest carbon efficiency whereas V has the lowest carbon efficiency. The order of carbon efficiencies for this ratio was Fe&Co>Co>Fe>Ni>V. It is suggested that increasing synthesis time increases the carbon efficiency of Fe catalyst whereas there is not a difference in efficiency of Co catalyst. The order of the efficiencies for 10:100 weight ratio with synthesis time of 60 minutes was Fe&Co>Co≈Fe>Ni>V.

24. At 800 ºC the order of carbon efficiencies for weight ratio of 10:100 with synthesis time of 30 minutes were in the order of Fe&Co>Ni>Co>Fe. All of the catalysts have an increase in the carbon efficiency. In summary, the order of the efficiencies for 10:100 weight ratio at 800 ºC with synthesis time of 60 minutes is Co>Fe&Co>Ni>Fe.

6.2   Recommendations

The carbon efficiencies of the CNTs for various metal catalysts used in this study shows differences from the previously conducted researches in the literature. These differences are mainly due to catalyst preparation method, and the substrate material used. In the further studies:

- The different catalyst preparation methods (insipient wetness impregnation, ion-exchange, sol-gel technique and organometallic grafting)   except the method applied in this thesis can be conducted in the future.

- The different substrate materials (silica, alumina, zeolite, nickel plates, quartz, conductive glass) other than MgO can be examined in the future.

- The different catalysts (Al, Mg, Mn, Cu, Zn, Mo, Au etc.) can be used in the CNT synthesis by CCVD method.

- The different hydrocarbon source (methane, ethylene, propane etc.) can be used in the CNT synthesis by the CCVD method.

- In CNT synthesis by CCVD method, the catalyst decomposition can be conducted in the reductant gas atmosphere to improve the carbon efficiency of the metal catalyst.

REFERENCES

[1] Pileni, M.P., 2002: Nanostructured materials, Selected synthesis methods, properties and applications, edited by Knauth, P., Schoonman, J.,Kluwer Academic Publishers, pp 1-22.

[2] Kroto, H. W., Heath, J. R., O'Brien, S. C., Curl, R. F., and Smalley, R. E., 1985: C-60- Buckminsterfullerene, *Nature,* Vol. 318, p. 162.

[3] Iijima, S., 1991: Helical microtubules of graphitic carbon, *Nature,* Vol. **354**, pp. 56–58.

[4] Iijima, S. and Ichihashi, T., 1993: Single-shell carbon nanotubes of 1-nm diameter. *Nature,*Vol **363**, pp. 603–615.

[5] Zettl, A., Saito, S., 2008: Carbon Nanotubes: Quantum cylinders of graphene, Elsevier, Oxford

[6] Treacy, M. M. J., Ebbesen, T. W., and Gibson, J. M., 1996: Exceptionally high Young's modulus observed for individual carbon nanotubes, *Nature*, Vol. **381**, Issue 6584, p 678.

[7] Nakayama, Y., Akita, S., and Shimada, Y., 1995: Thermally activated electrical conduction in carbon nanotubes, *Japanese Journal of Applied Physics*, Vol. **34**, pp L10-12.

[8] Dillon, A.C., Jones, K.M., Bekkedahl, T.A., Kiang, C.H., Bethune, D.S., and Haben, M.J., 1997: Storage of hydrogen in single walled carbon nanotubes, *Nature* Vol**. 386**, Issue 6623, p. 377.

[9] Kam, N. W. S. , O'Connell, M., Wisdom, J. A., and Dai., H., 2005: Carbon nanotubes as multifunctional biological transporters and near-infrared agents for selective cancer cell destruction, *Proceedings of the National Academy of Sciences of the USA*, Vol. **102**, 11600.

[10] Dresselhaus, M.S., Dresselhaus, G., and Eklund, P. C., 1996: Science of Fullerenes and Carbon Nanotubes, Academic Press, Florida.

[11] Meyyappan, M., 2005: Carbon nanotubes science and applications, pp. 1-24, CRC Press, Florida.

[12] Ebbesen, T.W., 1997: Carbon nanotubes, Chapter 1, CRC Press, Florida.

[13] Dresselhaus, M. S., Dresselhaus, G., Sugihara, K., Spain, I. L., and Goldberg, H. A., 1998: Graphite Fibers and Filaments. *Materials Science*, Vol. 5, Springer Verlag, New York

[14] Bethune, D.S., Kiang, C.H., de Vries, M.S., Gorman, G., Savoy, R., Vazquez, J., and Beyers, R., 1993: Cobalt-catalysed growth of carbon nanotubes with single-atomic-layer walls. *Nature* **363**, pp. 605–607.

[15] Bacon, R., 1960: Growth, structure, and properties of graphite whiskers, *Journal of Applied Physics*, Vol. **31,** p 283

[16] Saito R., Dresselhaus G., and Dresselhaus M.S., 1998: Physical properties of carbon nanotubes. Imperial College Press , London.

[17] Dresselhaus, M.S., Dresselhaus, G., and Avouris, P., 2001: Carbon nanotubes: Synthesis, structure, properties and applications, Springer, London.

[18] Terrones M., 2003: science and technology of the twenty-first century: synthesis, properties, and applications of carbon nanotubes, *Annual Review of Materials Research*, Vol. **33**, pp. 419-501

[19] Andrews R. (2001) Carbon Nanotubes: Synthesis, Properties, and Applications,

Critical Review of Solid State Materials Science; Vol 26, Issue 3, pp. 145-249

[20] Hata, K., Futaba, D. N.,Mizuno, K., Namai, T., Yumura, and M. Lijima, S., 2004: Water-assisted highly efficient synthesis of impurity-free single-walled carbon nanotubes. *Science,* Vol. **306,** pp. 1362–1364.

[**21] Kiselev, N.A. and Zakharov, D.N., 2001:** Electron Microscopy of Carbon Nanotubes, *Crystallography Reports***,** Vol. **46,** No. 4, pp. 577-585.

[22] Miki-Yoshida M., Elechiguerra, J.L., Antúnez-Flores, W., Aguilar-Elguezabal, A., and José-Yacamán, M. 2004: Atomic Resolution of Multi-Walled Carbon Nanotubes., *Microscopy and Microanalysis*, **Vol**. 10(Suppl. 02), pp 370-371

 [23] Qin, L.C., Zhao X.L., Hirahara, K., Miyamoto, Y., Ando, Y., and Lijima, S., 2000: The smallest carbon nanotube, *Nature*, Vol. 408, p. 50.

[24] Sun, X., Kiang, C. H., Endo, M., and Takeuchi, K., ,1996: Stacking characteristics of graphene shells in carbon nanotubes, *Physical Review B: Condensed Matter*, Volume **54**, Issue 18/PT2, p. R12629.

[25] **Kuchibhatla, S. V. N. T., Karakoti, A. S., Bera, D., and Seal, S.** ,2007: One dimensional nanostructured materials, *Progress in Materials Science*, Vol. **52**, Issue 5, pp. 699-913

[26] **Oncel, Ç., and Yurum, Y.,** 2006: Carbon nanotube synthesis via catalytic CVD method: A review on the effect of reaction parameters. *Fullerenes, nanotubes and carbon nanostructure*s, Vol. **14**, pp. 17-37.

[27] **Wong, E.W., Sheehan, P.E., and Lieber, C.E.,** 1997: Nanobeam mechanics: elasticity, strength, and toughness of nanorods and nanotubes. *Science*, Vol. **277**, p. 1971.

[28] Han, J., and Jaffe, R.,1998: Energetic and geometries of carbon nanoconic tips, *Journal of Chemical Physics*., Vol. **108**, p. 2817-2824.

[29] Salvetat, J. P., Briggs, G. A., Bonard, J. M., Basca, R. R., Kulik, A. J., Stockli, T., Burnham, N. A., Forro, 1999: Elastic and shear moduli of single walled carbon nanotube ropes, *Physical Review Letters,* Vol. **82**, p. 944.

[30] **Chico, L., Crespi, V. H., Benedict, L . X., Louie, S. G., Cohen, M. L.,** 1996: Pure carbon nanoscale devices: Nanotube heterojunctions, *Physical Review Letters*, Vol. **76**, pp. 971–974.

[31] **Saito, R., Fujita M.,, Dresselhaus, G., Dresselhaus, M. S.**, 1992: Electronic structure of chiral graphene tubules, *Applied Physics Letters*, Vol. **60**, pp.2204–2206.

[32] **Mintmire, J.W., Dunlap, B. I., White, C. T.,** 1992: Are fullerene tubules metallic? *Physical Review Letters,* Vol. **68**, pp. 631–634.

[33] **Liew, K.M., Wong, C.H., Tan, M.J.,** 2005: Buckling properties of carbon nanotube bundles, *Applied Physics Letters*, Vol. **87**, 041901.

[34] **Hone, J.**, 2004: Carbon nanotubes: Thermal properties*, Dekker Encyclopedia of Nanoscience and Nanotechnology*, DOI: 10.1081/E-ENN 120009128, Columbia University, NewYork.

[35] **Hone, J., Whitney, M., Zettl, A.,** 1999: Thremal conductivity of single walled carbon nanotubes, *Synthetic metals,* Vol. **103**, pp. 2498-2499.

[38] **Cao, A., Xu, C., Liang, J., Wu, D., Wei., B.,** 2001: X ray diffraction characterization on the alignment degree of carbon nanotubes, *Chemical Physics Letters*, Vol. **344**, pp. 13- 17.

[39] **Berber, S., Kwon, Y. K., Tomanek, D.,** 2000: Unusually high thermal conductivity of carbon nanotubes, *Physics Review Letter*, Vol. **84**, pp. 4613-4616.

[41] **O'Connel, M.J.,** 2006: Carbon nanotubes: Properties and Applications, Taylor & Francis., Florida.

[42] **Popov, V. N.,** 2004: Carbon nanotubes: properties and applications. *Materials Science and Engineering R*, **43**, 61-102

[43] **Wang, M., Zhao, X. L., Ohkohchi, M., Ando, Y.,** 1996: Carbon nanotubes grown on the surface of cathode deposit by arc discharge, *Fullerene Science and Technology*, Vol. **4**, pp. 1027-1039.

[44] **Farhat, S., de La Chapelle, M. L., Loiseau, A., Scott, C. D., Lefrant, S., Journet, C., and Bernier, P.**, 2001: Diameter control of single-walled carbon nanotubes using argon-helium mixture gases. *Journal of Chemical Physics*, Vol. **115**, pp. 6752–6759.

[45] **Waldorff, E.I., Waas, A.M., Friedmann, P.P., and Keidar, M.**, 2004: Characterization of carbon nanotubes produced by arc discharge: effect of the background pressure. *Journal of Applied Physics,* Vol. **95**, pp. 2749–2754.

[46] **Journet, C., Maser, W. K., Bernier, P., Loiseau, A., dela Chapelle, M. L., Lefrant, S., Deniard, P., Lee, R., and Fischer, J. E.,** 1997: Large-scale production of single-walled carbon nanotubes by the electric-arc technique. *Nature*, Vol. **388**, pp. 756–758.

[47] **T. W. Ebbesen**, 1994: Carbon nanotubes- review. *Annual Review of Materials Science*, Vol. **24**, pp. 235-264.

[48] **Burchell, T. D.,** 1999: Carbon materials for advanced technologies, Pergamon, Oak Ridge

[49] **Endo, M., Takeuchi, K., Igarashi, S., Kobori, K., Shiraishi, M., and Kroto, H.W.,** 1993: The production and structure of pyrolytic carbon nanotubes (PCNTs). *Journal of the Physics and Chemistry of Solids* Vol. **54**, pp. 1841–1848.

[50] **Guo, T., Nikolaev, P., Thess, A, Colbert, D.T. , Smalley, R.E.,** 1995: Catalytic growth of single walled nanotubes by laser vaporisation, *Chemical Physics Letters*, Vol. **243**, p. 49.

[51] **Kataura,H., Kimura, A., Ohtsuka, Y., Suzuki, Sh., Maniwa, Y., Hanyu, T., Achiba, Y.,** 1998: Formation of thin single wall carbon nanotubes by laser vaporisaiton of Rh/Rd graphite composite rod, *Japanese Journal of Applied Physics Part 2-Lett.*, Vol. **37**, L616-L618.

[53] **Yacaman, M. J., Yoshida, M., Rendon, L., Santiesteban, J. G.,** 1993: Catalytic growth of carbon microtubules with fullerene structure, *Applied Physics Letters*, Vol. **62**, p 657

[54] **Mukhopadhyay, K., Koshio, K., Tanaka, N., and Shinohara, H.,** 1998: A simple and novel way to synthesize aligned nanotube bundles at low temperature, *Japanese Journal of Applied Physics*, Vol. **37**: L1257.

[55] **Maruyama, S., Kojima, R., Miyauchi, Y., Chiashi, S., and Kohno, M.,** 2002: Low-temperature synthesis of high-purity single-walled carbon nanotubes from alcohol, *Chemical Physics Letters*, Vol. **360**, p. 229.

[56] **Colomer, J. F., Piedigrosso, P., Willems, I., Journet, C., Bernier, P., Van Tendeloo G., Fonseca, A., and Nagy, J. B.,** 1998: Purification of catalytically produced MWCNTs, *Journal of The Chemical Society, Faraday Transactions*, Vol. **94**, pp. 3753-3358.

[57] **Chiang, I. W., Brinson, B. E., Smalley, R. E., Margrave, J. L., and Hauge, R. H.,** 2001: Purification and characterization of single-wall carbon nanotubes, *Journal of Physical Chemistry B*, Vol. **105**, Issue 6, pp. 1157–61;

[58] **Hou, P. X., Liu, C., and Cheng, H. M.,** 2008: Purification of carbon nanotubes. *Carbon*, Vol. **46**, p. 25.

[59] **Zhou, O., Shimoda, H., Gao, B., Oh, S. J., Fleming, L., and Yue, G. Z. ,** 2002: Materials science of carbon nanotubes: fabrication, integration, and properties of macroscopic structures of carbon nanotubes, *Accounts of Chemical Research*, Vol. **35**, pp. 1045-53

[60] **Mamedov, A. A., Kotov, N. A., Prato, M., Guldi, D. M., Wicksted, J. P., and Hirsch, A.,** 2002: Molecular design of strong single-wall carbon nanotube/polyelectrolyte, multilayer composites, *Nature Materials*, Vol. **1**, p. 257.

[61] **Giles J.,** 2004: Growing nanotech trade hit by questions over quality, *Nature*, Vol. **432**, p.791

[62] **Itkis ME, Perea DE, Niyogi S, Love J, Tang J et al.,** 2004: Optimization of the Ni-Y catalyst composition in bulk electric arc synthesis of single walled carbon nanotubes by use of near infrared spectroscopy, *Journal of Physical Chemistry B*, Vol. **108**, pp. 12770-12775

[63] **Yu L. T., Petit, J., Josefowics, M., Belorgey, G., and Buvet, R.**, 1965: Conductivity of emeraldine acid sulphate for continuous current, *C. R. Acad. Sci.* Paris, Ser. C, 260, 5026-5029.

[64] **Alvarez, W. E., Kitiyanan, B., Borgna, A., and Resasco, D. E.,** 2001: Synergism of Co and Mo in the catalytic production of single wall carbon nanotubes by decomposition of CO, *Carbon,* Vol. **39**, pp. 547-558

[65] **Thomsen, C., Reich, S. , and Maultzsch, J., 2008:** Raman Scattering in Carbon Nanotubes: Basic Concepts and Physical Properties. *Wiley-VCH Verlag GmbH*, Weinheim, Germany, Chapter 7.

[66] **Freiman, S., Hooker, S., Migler, K., and Arepalli, A.,** 2008: Measurement issues in single wall carbon nanotubes, NIST, Washington.

[67] **Baskaran, D., Mays J. V., Bratcher, M.S.,** 2005: Polymer adsorption in the grafting reactions of hydroxyl terminal polymers with multi-walled nanotubes, *Polymer*, Vol. **46**, pp. 5050-5057.

[68] **Marchetti, M., Frezza, F., Regi, M., Mazza, F., Carnà, E**. 'Development and characterization of nanostructured frequency selective surfaces (FSS)', *Proceeding 46th IACAS – Israel Annual Conference on Aerospace Structures*, 1–2 March 2006

[69] **Willems, I., Konya, Z., Colomer, J. F., Tendelo, G. V., Nagaraju, N., Fonseca, A., and Nagy J. B.,** 2001: Control of the outer diameter of thin carbon nanotubes synthesized by catalytic decomposition of hydrocarbons. *Chemical Physics Letters*, Vol. **317**, pp. 71-76.

[70] **Thaib, A., Martin, G.A., Pinheiro, P., Schouler, M.C., and Gadelle, P.,** 1999: Formation of carbon nanotubes from the carbon monoxide disproportionation reaction over Co/Al_2O_3 and Co/SiO_2 catalysts, *Catalysis Letters*, Vol. **63**, p. 135

[71] **Alvin, S.,** 1987: Catalyst Supports and Supported Catalysts Theoretical and Applied Concepts; Butterworths: London.

[72] **Zhu, J., Yudasaka, M., and Iijima, S.,** 2003: A catalytic chemical vapour deposition synthesis of double-walled carbon nanotubes over metal catalysts supported on a mesoporous material, *Chemical Physics Letters*, Vol. **380**, p. 496.

[73] **Su, M., Zheng, B., and Liu, J**., 2000: A scalable CVD method for the synthesis of single-walled carbon nanotubes with high catalyst produtivity, *Chemical Physics Letters*, Vol. **322**, p. 321.

[73] **Hernadi, K., Konya, Z., Siska, A., Kiss, J., Oszko, A., Nagy, J.B., and Kiricsi, I.,** 2002: On the role of catalyst, catalyst support and their interaction in synthesis of carbon nanotubes by CCVD, *Materials Chemistry and Physics*, Vol. **77**, p. 536.

[74] **Ward, J.W., Wei, B.Q., and Ajayan, P.M.** (2003) Substrate effects on the growth of carbon nanotubes by thermal decomposition of methane. *Chemical Physics Letters*, Vol. **376**, p. 717.

[75] **Sinha, A.K., Hwang, D.W., and Hwang, L.-P.,** 2000: A novel approach to bulk synthesis of carbon nanotubes filled with metal by a catalytic

chemical vapour deposition method, *Chemical Physics Letters*, Vol. **332**, p. 455.

[76] **Colomer, J.-F., Bister, G., Willems, I., Konya, Z., Fonseca, A., Van Tendeloo, G., and Nagy, J.B.,** 1999: Synthesis of single-wall carbon nanotubes by catalytic decompositions of hydrocarbons, *Chemical Communications*, Issue 14, p 1343.

[77] **Flahaut, E., Govindaraj, A., Peigney, A., Laurent, Ch., Rousset, A., and Rao, C.N.R.,** 1999: Synthesis of single-walled carbon nanotubes using binary (Fe, Co, Ni) alloy nanoparticles prepared in situ by the reduction of oxide solid solutions. *Chemical Physics Letters*, Vol. **300**, p. 236.

[78] **Nagaraju, N., Fonseca, A., Konya, Z., and Nagy, J.B.,** 2002: Alumina and silica supported metal catalysts for the production of carbon nanotubes. *Journal of Molecular Catalysis A: Chemical*, Vol. **181**, p. 57.

[79] **Li, Y., Kim, W., Zhang, Y., Rolandi, M., Wang, D., and Dai, H.,** 2001: Growth of Single-Walled Carbon Nanotubes from Discrete Catalytic Nanoparticles of Various Sizes, *Journal of Physical Chemistry B*, **105**, pp. 11424-11431

[80] **Dai, H., Rinzler, A. G., Nikolaev, P., Thess, A., Colbert, D. T., and Smalley, R. E.,** 1996: Single-wall nanotubes produced by metal-catalyzed disproportionation of carbon monoxide, *Chemical Physics Letters*, **260**, p. 471.

[81] **Li, Y. L., Kinloch, I. A., Shaffer, M. S. P., Geng, J., Johnson, B., Windle, A. H.,** 2004: Synthesis of single-walled carbon nanotubes by a fluidized-bed method, *Chemical Physics Letters*, **384**, pp. 98-102

[82] **Nerushev, O. A., Morjan, R. E., Ostrovskii, D. I., Sveningsson, M., Jonsson, M., Rohmund, F., and Campbell, E. E. B.,** 2002: The temperature dependence of Fe-catalysed growth of carbon nanotubes on silicon substrates, Physica B, 323,p. 51

[83] **Dupuis A. C.,** 2005: The catalyst in the CCVD of nano tubes-a review. *Progress in Materials Science*, Vol. **50**, pp. 929-961.

[84] **Mukhopadhyay, K., Koshio, A., Sugai, T., Tanaka, N., Shinohara, H., Konya, Z., and Nagy, J. B.**, 1999: Bulk production of quasi-aligned carbon nanotube bundles by the catalytic chemical vapour deposition (CCVD) method, *Chemical Physics Letter*, **303**, p.117.

[85] **Kathyayini, H., Nagaraju, N., Fonseca, A., and Nagy, J. B.,** 2004: Catalytic activity of Fe, Co. and Fe/Co supported on Ca and Mg oxides, hydroxides and carbonates in the synthesis of carbon nanotubes, *Journal of Molecular Catalysis A,* **223**, p. 129.

[86] **Zhao, N., He, C., Jiang, Z., Li, J., and Li, Y., 2006:** Fabrication and growth mechanism of carbon nanotubes by catalytic chemical vapor deposition, *Material Letters,* **60**, p.159.

[87] Kong, J., Cassell, A. M., and Dai, H., 1998: Chemical vapor deposition of methane for single-walled carbon nanotubes, *Chemical Physics Letters*, **292**, p. 567.

[88] J.F., Colomer, C., Stephan, S., Lefrant, G., Van Tendeloo, I., Willems, Z., Konya, A., Fonseca, C., Laurent, and J.B., Nagy, 2000: Large-scale synthesis of single-wall carbon nanotubes by catalytic chemical vapor deposition (CCVD) method*., Chemical Physics Letters*, **317** , pp. 83-89.

[89] Couteau, E., Hernadi, K., Seo, J. W., Thien-Nga, L., Miko, C., Gaal, R., and Forro, L., 2003: CVD synthesis of high-purity multiwalled carbon nanotubes using CaCO3 catalyst support for large-scale production, *Chemical Physics Letters*, **378**, p. 9.

[90] Tang, S., Zhong, Z., Xiong, Z., Sun, L., Liu, L., Lin, J., Shen, Z.X., and Tan, K.L., 2001: Controlled growth of single-walled carbon nanotubes by catalytic decomposition of CH4 over Mo/Co/MgO catalysts*, Chemical Physics Letters,* **350**, pp. 19-26

[91] Singh, C., Shaffer, M.S.P., and Windle, A.H., 2003: Production of controlled architectures of aligned carbon nanotubes by an injection chemical vapor deposition method, *Carbon*, **41** , p. 359.

[92] Su, M., Zheng, B., and Liu, J., 2000: A scalable CVD method for the synthesis of single-walled carbon nanotubes with high catalyst productivity, *Chemical Physics Letters*, pp. 322-321.

[93] Klinke, C., Bonard, J. M., and Kern, K., 2001: Comparative study of the catalytic growth of patterned carbon nanotube films. *Surface Science*, Vol. **492**, pp. 195–201.

[94] Lee, C.J., Park, J., Han, S., and Ihm, J., 2001: Growth and field emission of carbon nanotubes on sodalime glass at 5508C using thermal chemical vapour deposition, *Chemical Physics Letters*, pp. 337-398.

[95] Ermakova, M.A., Ermakov, D. Y., Chuvilin, A. L., Kuvshinov, G. G., 2001: Decomposition of methane over iron catalysts at the range of moderate temperatures: the influence of structure of the catalytic systems and the reaction conditions on the yield of carbon and morphology of carbon filaments, *Journal of Catalayst*s, Vol. **201**, pp. 183–197.

[96] Chen, P., Zhang, H. B., Lin, G. D., Hong, Q., Tsai, K. R., 1997: Growth of carbon nanotubes by catalytic decomposition of CH4 or CO on a Ni–MgO catalyst, *Carbon*, Vol. **35**, p. 1495.

[97] Bacsa, R. R., Laurent, C., Peigney, A., Bacsa, W. S., Vaugien, T., Rousset, A., 2000: High specific surface area carbon nanotubes from catalytic chemical vapour deposition process, *Chemical Physics Letters*, Vol. **323**, pp. 566–571.

[98] Mauron, P., 2003: Growth mechanism and structure of carbon nanotubes, Dissertation, Hansdruckerei Universitat Freiburg.

[99] Seo, J.W., Hernadi, K., Miko, C., and Forro, L., 2004: Behaviour of transition metals catalysts over laser-treated vanadium support surfaces in the decomposition of acetylene, *Applied Catalysis A: General*, Vol. **260**, p. 87.

[100] Curran, S., Carroll, D.L., Ajayan, P.M., Redlich, P., Roth, S., Rühle, M., Blau, W., 1998: Picking Needles from the Nanotube-haystack. *Advanced Materials*, Vol. **10,** Issue 14, p. 1091.

[101] Athalin, H., Lefrant, S., 2005: A correlated method for quantifying mixed and dispersed carbon nanotubes: analysis of the Raman band intensities and evidence of wavenumber shift. *Journal of Raman Spectroscopy*, Vol. **36**, pg. 40.

[102] Montgomery, D.C., 1991: *Design and Analysis of Experiments*, Third Edition, pp. 278-288

[103] Melechko, A. V., Merkulov, V. I., McKnight, T. E., Guillorn, M. A., Lowndes, D. H., and Simpson, M. L., 2005: Vertically aligned carbon nanofibers and related structures: Controlled synthesis and directed assembly. *Journal of Applied. Physics.*, Vol. **97**, Issue 4, pp. 041301-041340.

[104] Awasthi, K., Srivastava, A., and Srivastava, O. N., 2005: Synthesis of Carbon Nanotubes. *Journal of Nanoscience and Nanotechnology*, Vol. **5**, Issue 10, pp. 1616-1636.

[105] Ivanov, V., Nagy, J. B., Lambin, P., Lucas, A., Zhang, X. F., Bernaerts, D., Tendeloo, G. V., Amelinckx, S., and Landuyt, J. V, 1994: The study of carbon nanotubules produced by catalytic method. *Chemical Physics Letter*, Vol. **223**, Issue 4, pp. 329–335.

[106] Yudasaka, M., Kikuchi, R., Matsui, T., Yoshimas, O., and Yoshimu, S. 1995: Specific conditions for Ni catalyzed carbon nanotube growth by chemical vapor deposition, *Applied Physics Letters*, Vol. **67**, Issue 17, p. 2477.

[107] Teo, K. B. K, Chhowalla, M., Amaratunga, G. A. J., Milne, W. I., Hasko, D. G., Pirio, G, P. Legagneux, F. Wyczisk, and D. Pribat, 2001: Uniform patterned growth of carbon nanotubes without surface carbon. *Applied Physics Letter*, Vol. **79**, pp.1534-1536.

[108] Ren, Z. F., Huang, Z. P., Xu, J. W., Wang, J. H., Bush, P., and Siegal, M. P., 1998: Synthesis of large arrays of well aligned carbon nanotubes on glass. *Science*, Vol. **282**, pp. 1105–1107.

[109] Choi, Y. C., Shin Y. M., Lee, Y. H., Lee, B. S., Park, G. S., and Choi, W. B. ,et al., 2000: Controlling the diameter, growth rate, and density of vertically aligned carbon nanotubes synthesized by microwave plasma-enhanced chemical vapor deposition. *Applied Physics Letters*, Vol. **76**, pp. 2367-2369.

[110] Huang, Z. P., Xu, J. W., Ren, Z. F., Wang, J. H., Siegal, M. P., and Provencio, P. N., 1998: Growth of highly oriented carbon nanotubes by plasma-enhanced hot filament chemical vapor deposition. Applied Physics Letter, Vol.**73,** pp. 3845-3847.

[111] Jiao, J., and Seraphin, S., 2000: Single-walled tubes and encapsulated nanoparticles: comparison of structural properties of carbon nanoclusters prepared by three different methods. *Journal of Physical Chemical Solids*, Vol. **61**, pp. 1055–1067.

[112] Kukovitsky, E. F., L'vov, S. G., Sainov, N. A., Shustov, V. A., Chernozatonskii, L. A., 2002: Correlation between metal catalyst particle size and carbon nanotube growth. *Chemical Physical Letters*, Vol. **355**, pp.497–503.

[113] Nolan, P. E., Lynch, D. C., and Cutler A. H.., 1998: Carbon deposition and hydrocarbon formation on group VIII metal catalysts. *Journal of Phys. Chem. B, Vol.* **102**, pp. 4165–4175.

[114] Siegal, M. P., Overmyer, D. L., and Provencio, P. P., 2002: Precise control of multiwall carbon nanotube diameters using thermal chemical vapor deposition. Applied Phys Lett, Vol. **80**, pp.2171.

[115] Wright, A. C., Xiong, Y., Maung, N., Eichho rn SJ,Young RJ., 2003: The influence of the substrate on the growth of carbon nanotubes from nickel clusters—an investigation using STM,FE-SEM,TEM and Raman spectroscopy. *Materials Science & Engineering C*, Vol. 23, pp. 279–283.

[116] Yudasaka, M., Kikuchi, R., Ohki, Y., Ota, E., Yoshimura, S., 1997: Behavior of Ni in carbon nanotubenucleation. *Applied Physics Letters*, Vol. **70**, pp. 1817-1818.

[117] Esconjauregui, S., Whelan, C. M., and Maex, C., 2009: The reasons why metals catalyze the nucleation and growth of carbon nanotubes and other carbon nanostructures. *Carbon*, Vol. **47**, Issue 3, pp. 659-669.

APPENDICES

APPENDIX A.1 : Experimental Data of All Catalysts
APPENDIX A.2 : TG And DTG Curves of As-synthesized CNTs

APPENDIX A.1

Table A.1: Experimental data of all catalysts

Catalyst	x:100	T(C)	min	weight % (200ºC)	weight% (796ºC)	%efficiency
Co	1	500	30	98.75	88.24	10.51
Co	1	500	60	98.79	86.84	11.95
Co	5	500	30	99.54	46.4	53.14
Co	5	500	60	99.43	44.74	54.69
Co	10	500	30	99.41	31.36	68.05
Co	10	500	60	99.38	30.44	68.94
Co	1	800	35	0	0	0
Co	1	800	60	0	0	0
Co	5	800	35	99.21	81.83	17.38
Co	5	800	60	100.8	57.11	43.69
Co	10	800	35	98.56	74.35	24.21
Co	10	800	60	99.48	45.71	53.77
Fe	1	500	30	98.58	88.84	9.74
Fe	1	500	60	100	90.21	9.79
Fe	5	500	30	98.37	40.85	57.52
Fe	5	500	60	98.5	45.2	53.3
Fe	10	500	30	97.78	43.03	54.75
Fe	10	500	60	99.56	28.95	70.61
Fe	1	800	35	99.04	80.28	18.76
Fe	1	800	60	99.57	48.55	51.02
Fe	5	800	35	99.21	57.58	41.63
Fe	5	800	60	99.47	45.27	54.2
Fe	10	800	35	99.47	79.94	19.53
Fe	10	800	60	99.1	75.35	23.75
Fe+Co	1	500	30	0	0	0
Fe+Co	1	500	60	0	0	0
Fe+Co	5	500	30	98.52	53.2	45.32
Fe+Co	5	500	60	98.99	51.77	47.22
Fe+Co	10	500	30	99.5	18.89	80.61
Fe+Co	10	500	60	99.37	17.92	81.45
Fe+Co	1	800	35	0	0	0
Fe+Co	1	800	60	0	0	0
Fe+Co	5	800	35	99.83	49.06	50.77
Fe+Co	5	800	60	100.4	46.1	54.3
Fe+Co	10	800	35	99.94	55.97	43.97
Fe+Co	10	800	60	99.45	47.24	52.21
Ni	1	500	30	98.71	86.37	12.34
Ni	1	500	60	98.55	84.34	14.21
Ni	5	500	30	98.78	80.24	18.54
Ni	5	500	60	98.09	78.72	19.37

| Catalyst	x:100	T(C)	min	weight % (200ºC)	weight% (796ºC)	%efficiency
Ni	10	500	30	98.48	72.11	26.37
Ni	10	500	60	98.48	75.28	23.2
Ni	5	800	35	99.39	62.56	36.83
Ni	5	800	60	100.2	48.38	51.82
Ni	10	800	35	99.46	65.19	34.27
Ni	10	800	60	99.86	51.12	48.74
V	1	500	30	0	0	0
V	1	500	60	0	0	0
V	5	500	30	98.44	88.66	9.78
V	5	500	60	98.49	87.03	11.46
V	10	500	30	98.34	90.04	8.3
V	10	500	60	99.27	89.39	9.88
V	5	800	60	99.82	64.99	34.83
*x: the weight of the catalsyt						
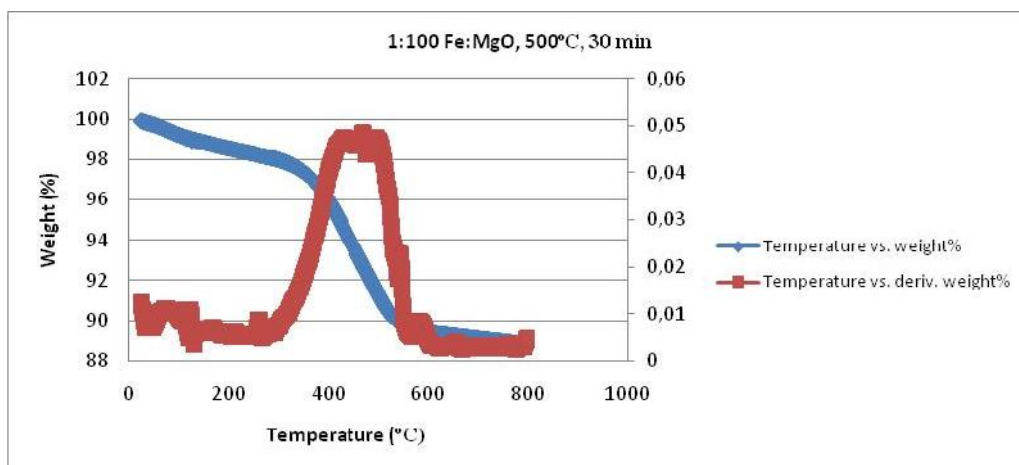
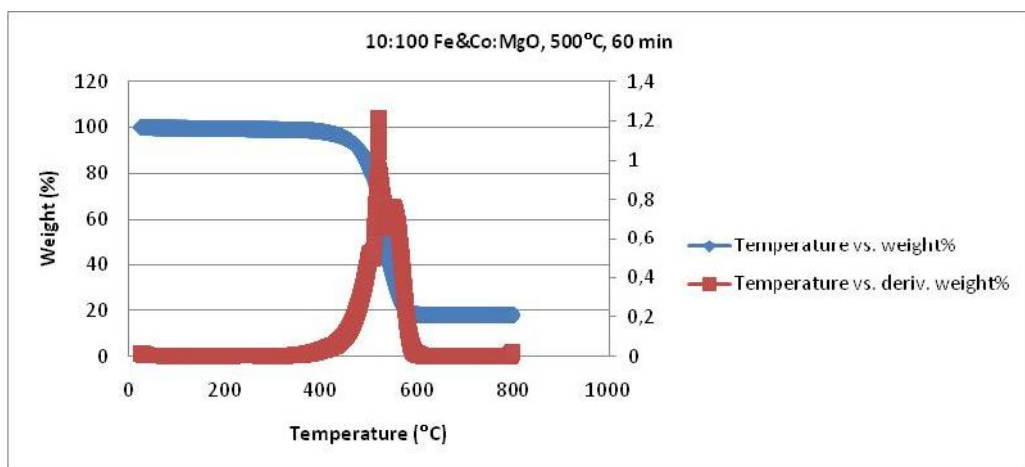**Figure A.1:**TG,DTG curves of CNT synt. at 1:100 Fe:MgO,500°C,30 min
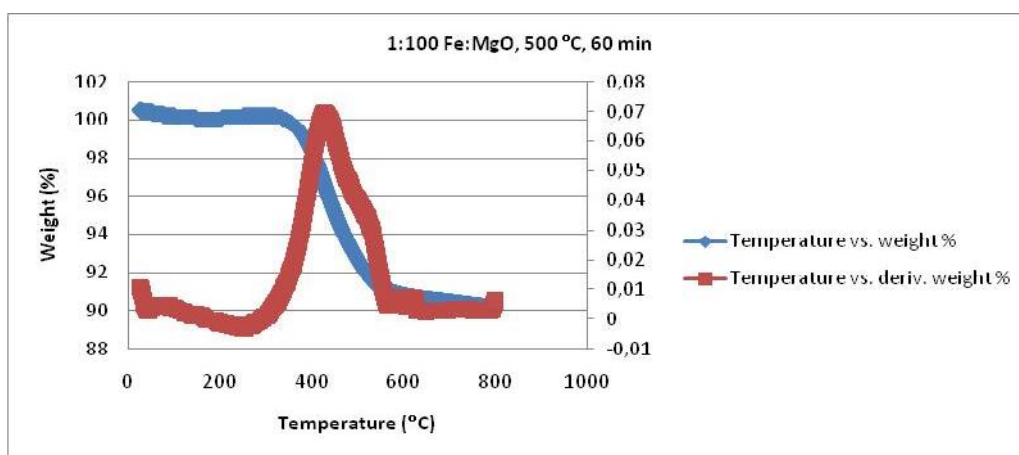
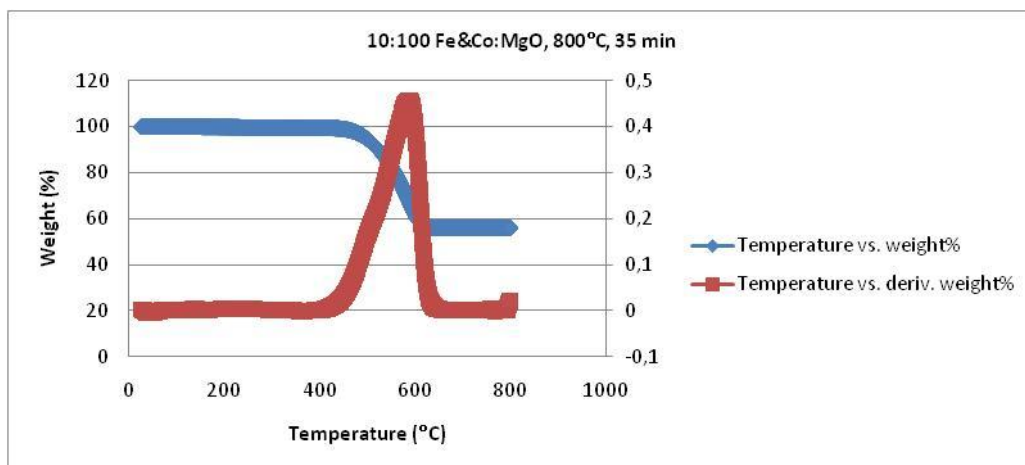**Figure A.2:**TG,DTG curves of CNT synt. at 1:100 Fe:MgO,500°C,60 min
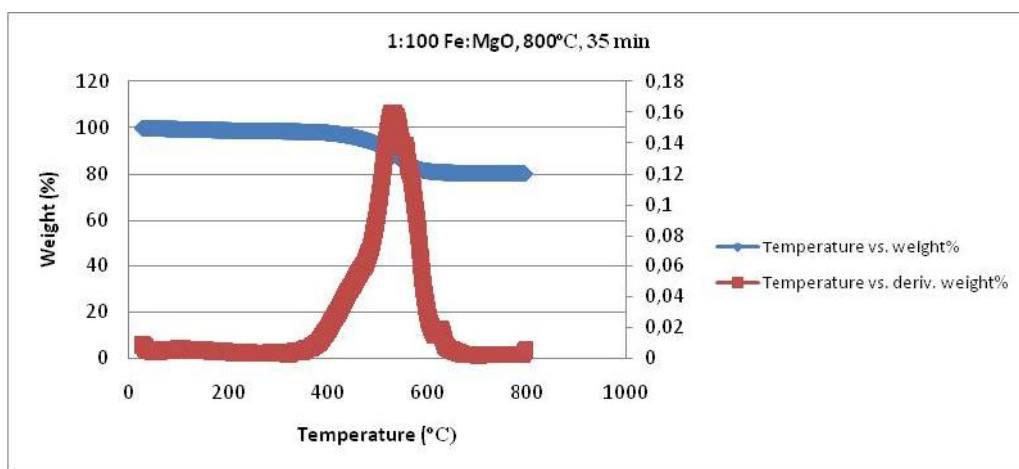
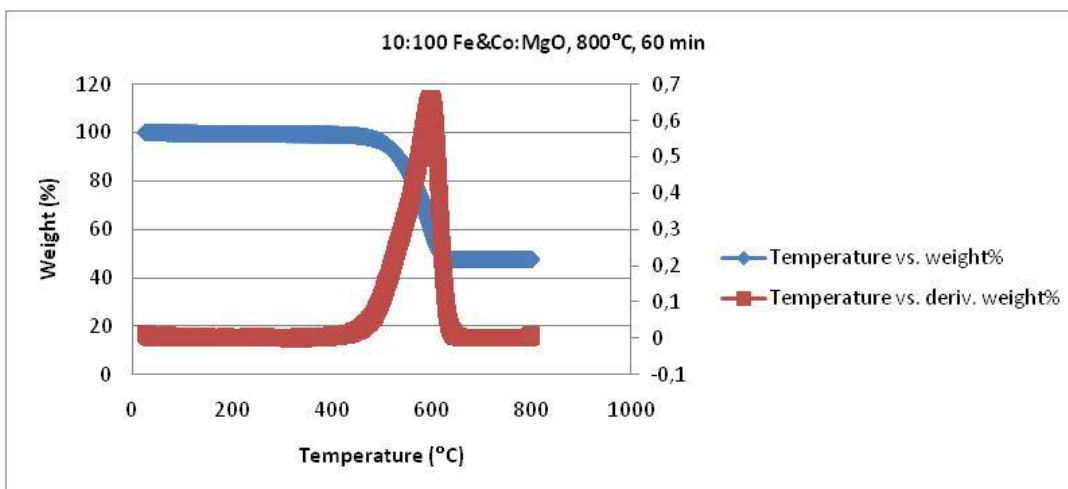**Figure A.3:**TG,DTG curves of CNT synt. at 1:100 Fe:MgO,800°C,35 min
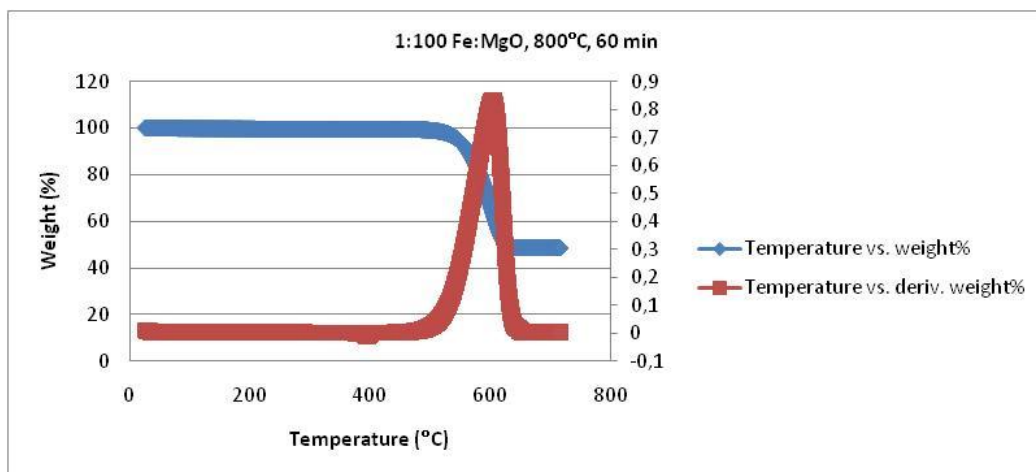
Figure A.4:TG,DTG curves of CNT synt. at 1:100 Fe:MgO,800°C,60 min
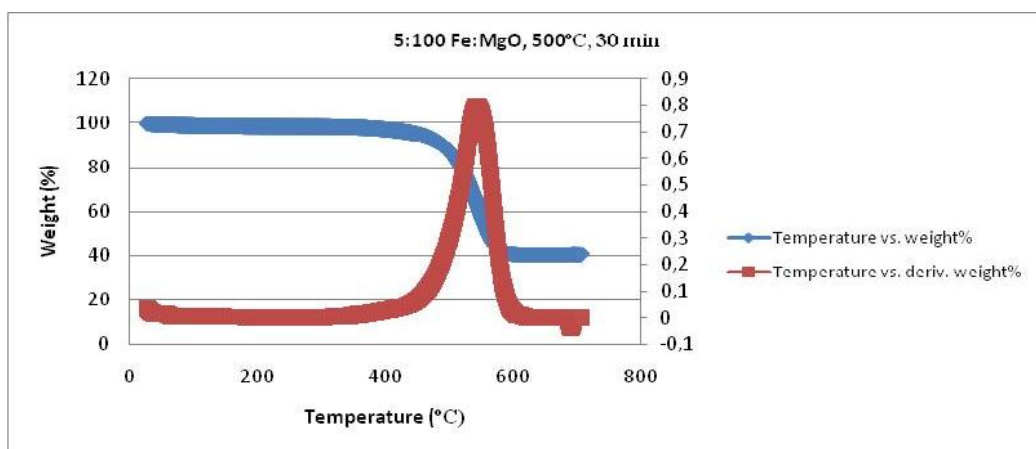
Figure A.5:TG,DTG curves of CNT synt. at 5:100 Fe:MgO,500°C,30 min
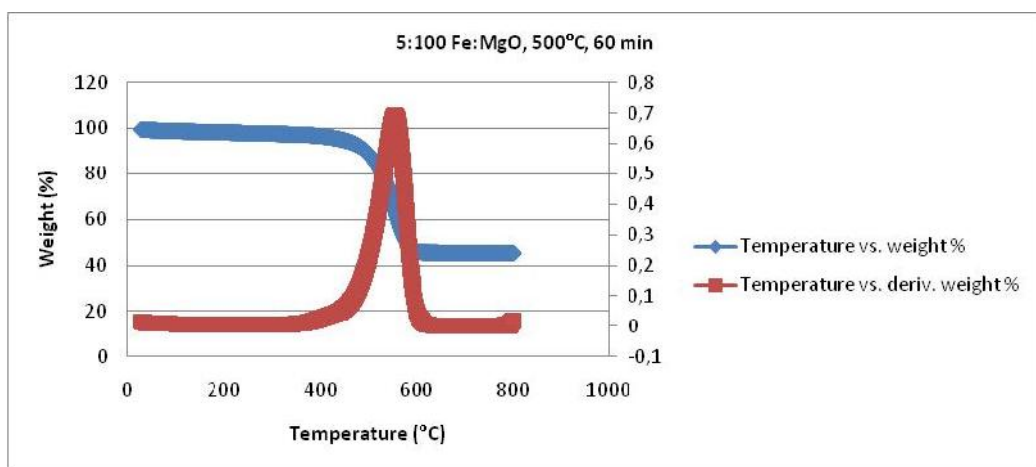
Figure A.6:TG,DTG curves of CNT synt. at 5:100 Fe:MgO,500°C,60 min
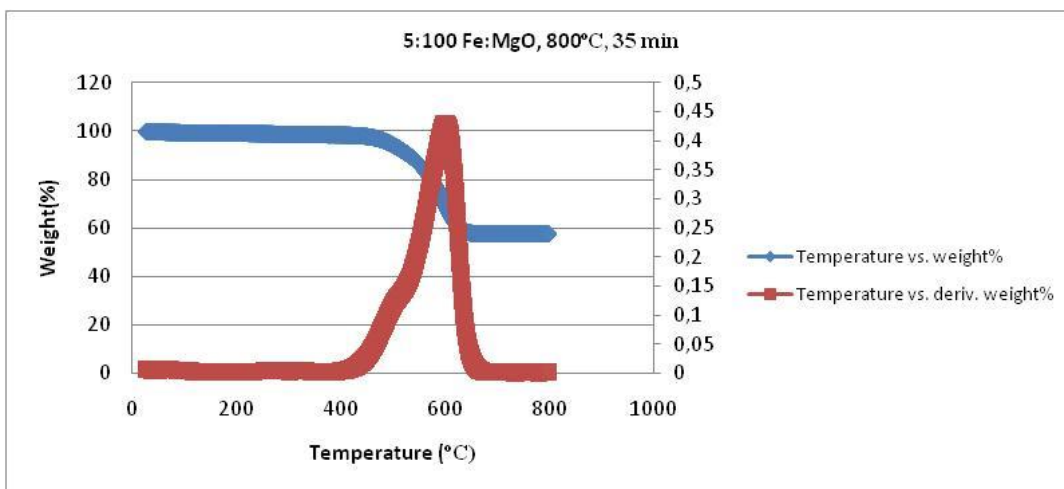
Figure A.7:TG,DTG curves of CNT synt.at 5:100 Fe:MgO,800°C,35 min
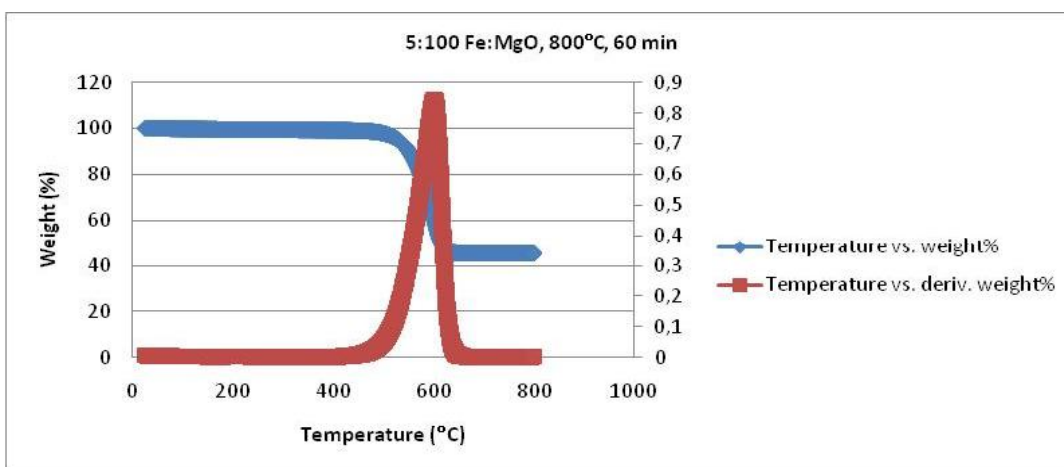
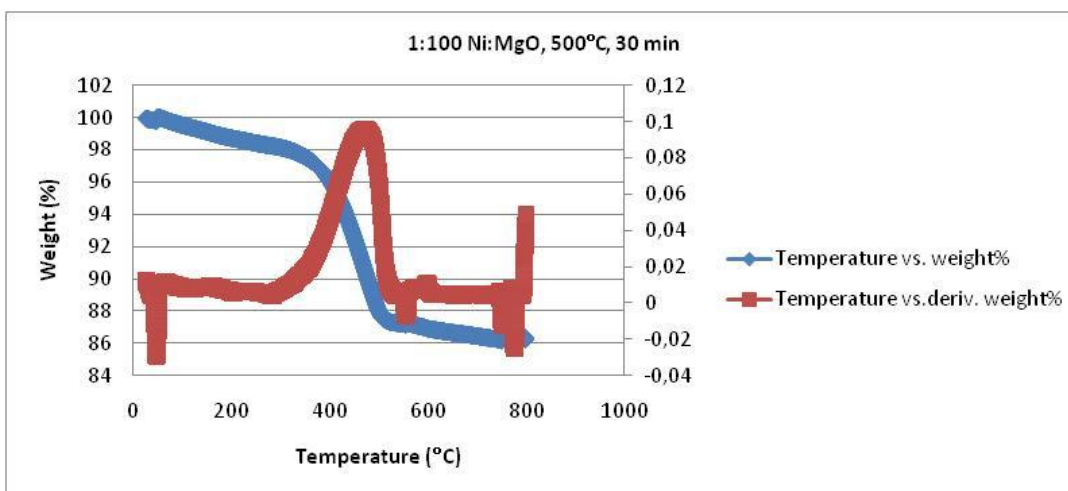**Figure A.8:**TG,DTG curves of CNT synt. at 5:100 Fe:MgO,800°C,60 min
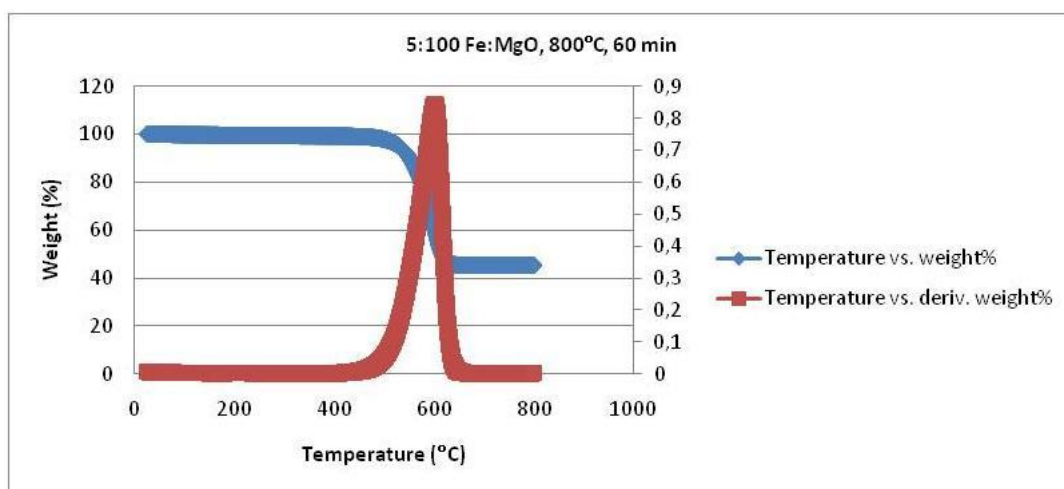
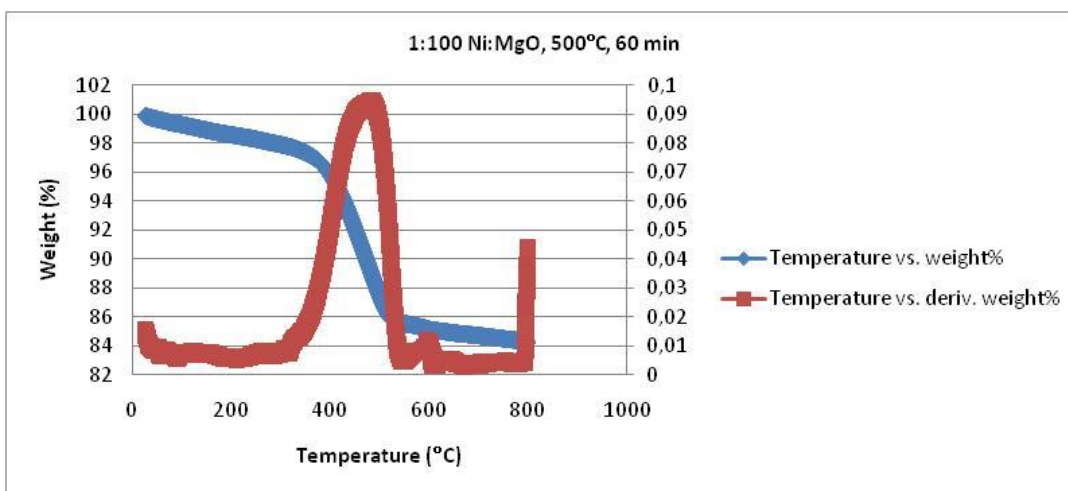**Figure A.9:**TG,DTG curves of CNT synt. at 5:100 Fe:MgO,800°C,60 min
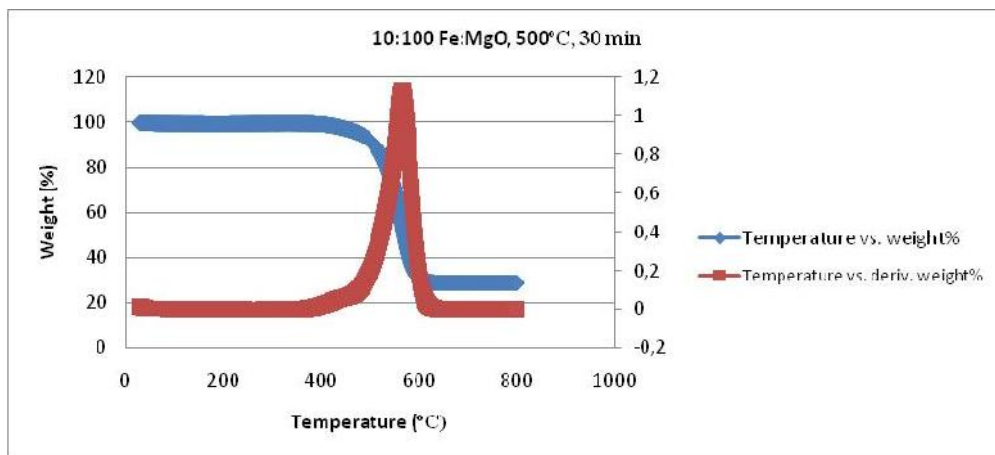
Figure A.10:TG,DTG curves of CNT synt. at 10:100 Fe:MgO,500°C,30 min
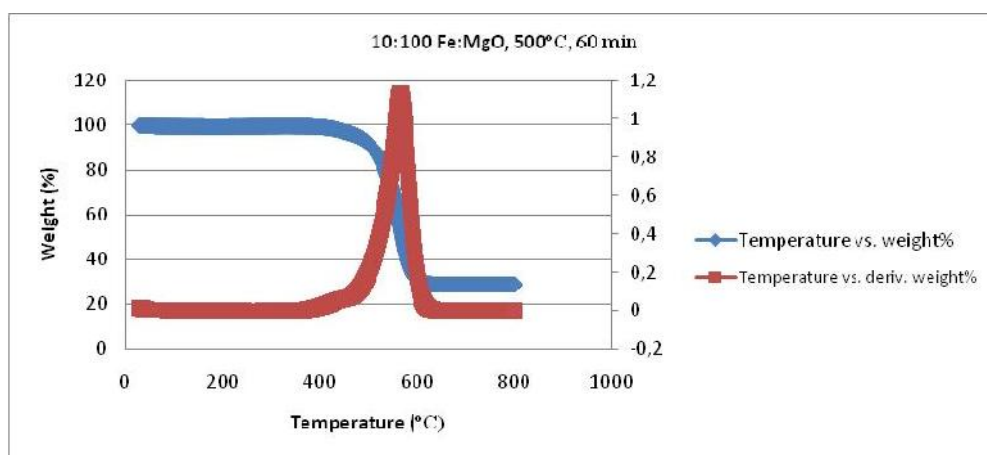
Figure A.11:TG,DTG curves of CNT synt. at 10:100 Fe:MgO,500°C,60 min
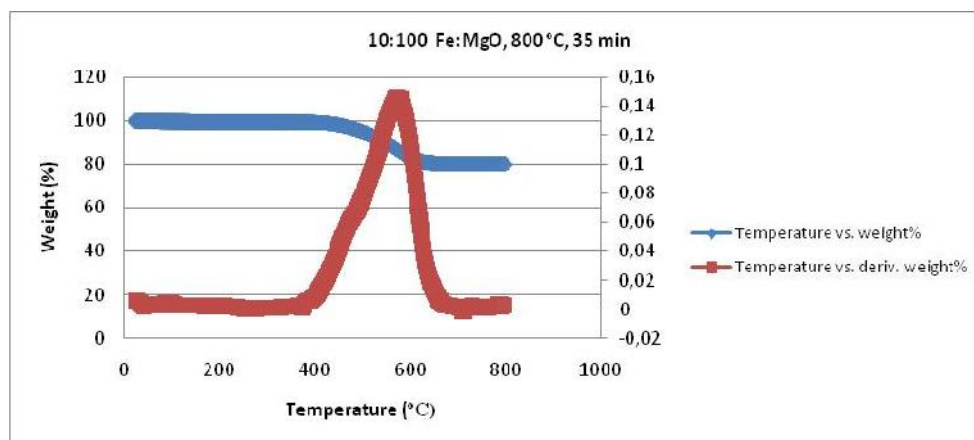
Figure A.12:TG,DTG curves of CNT synt. at 10:100 Fe:MgO,800°C,35 min
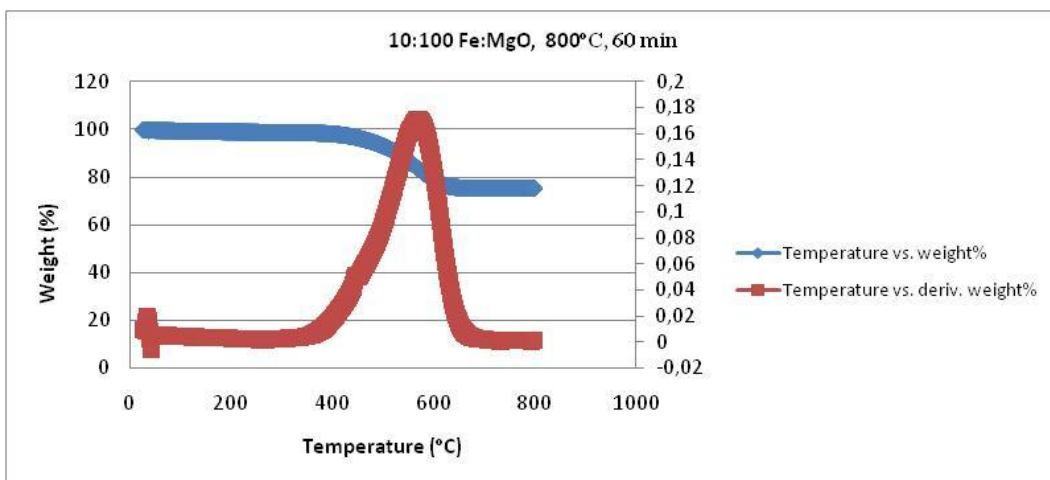
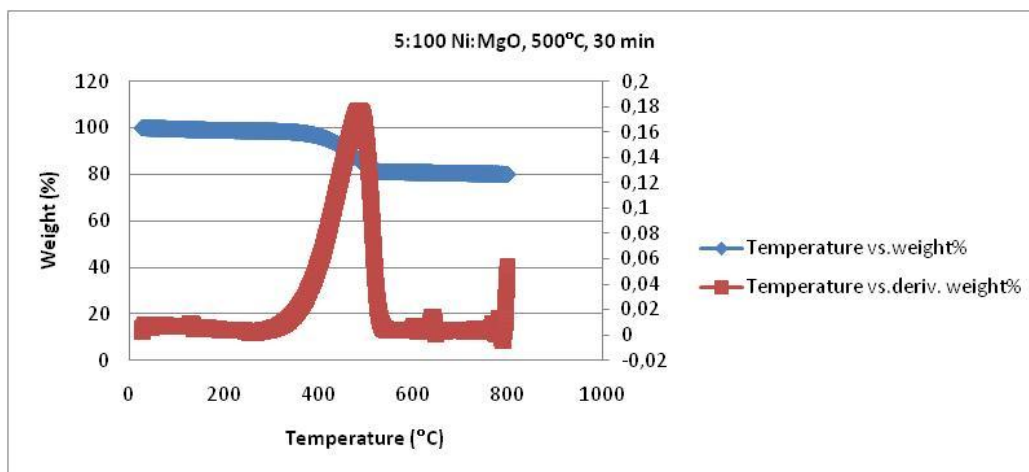**Figure A.13:**TG,DTG curves of CNT synt. at 10:100 Fe:MgO,800°C,60 min
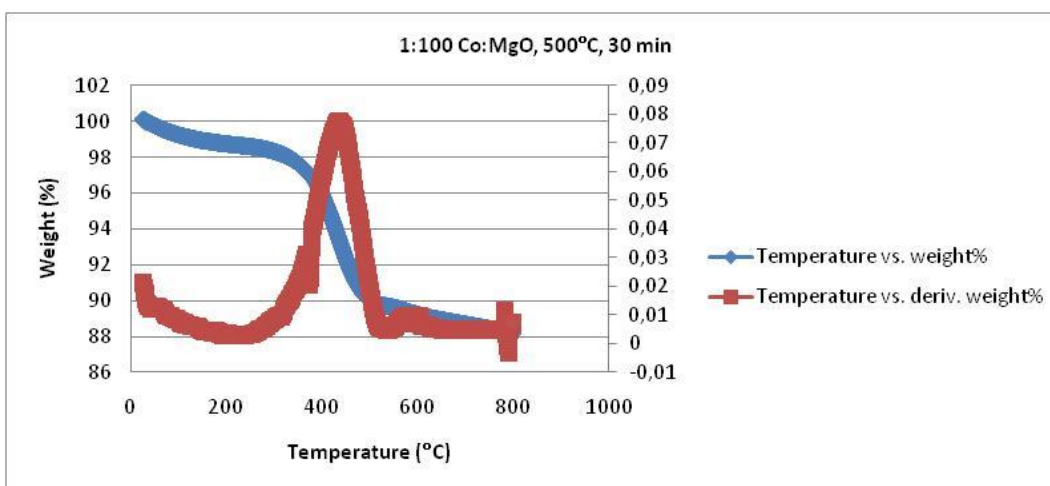
Figure A.14:TG,DTG curves of CNT synt. at 1:100 Co:MgO,500°C,30 min
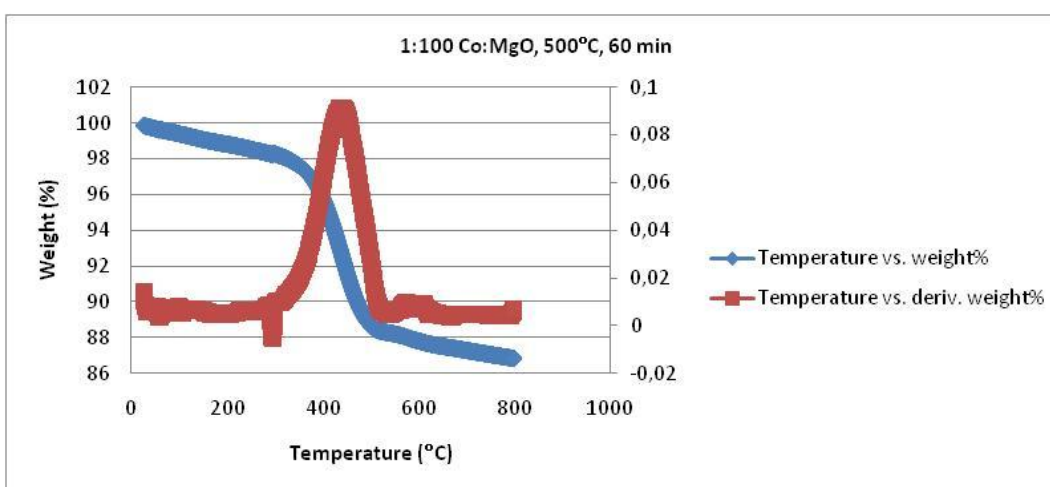
Figure A.15:TG,DTG curves of CNT synt. at 1:100 Co:MgO,500°C,60 min
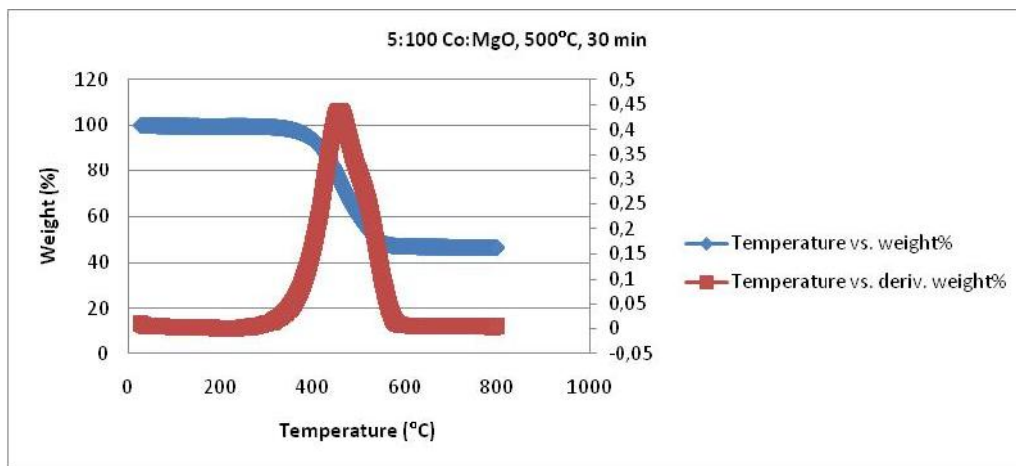
Figure A.16:TG,DTG curves of CNT synt. at 5:100 Co:MgO,500°C,30 min
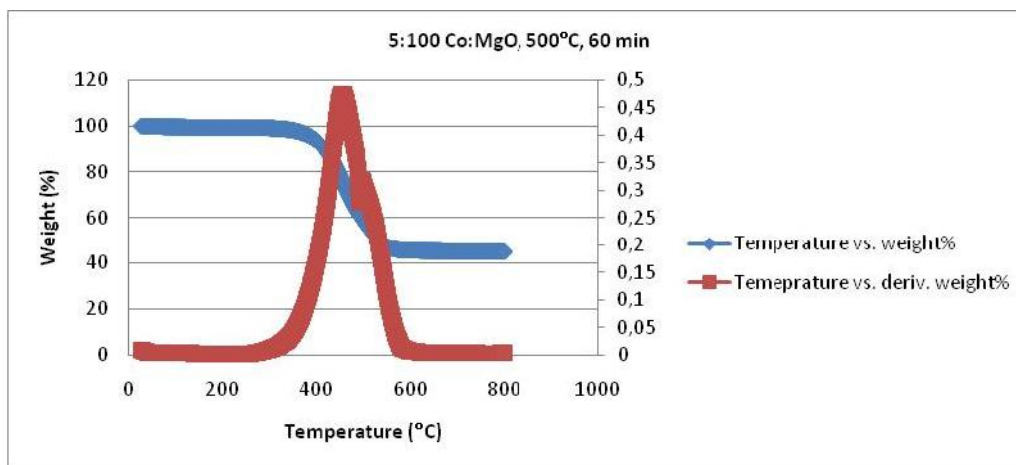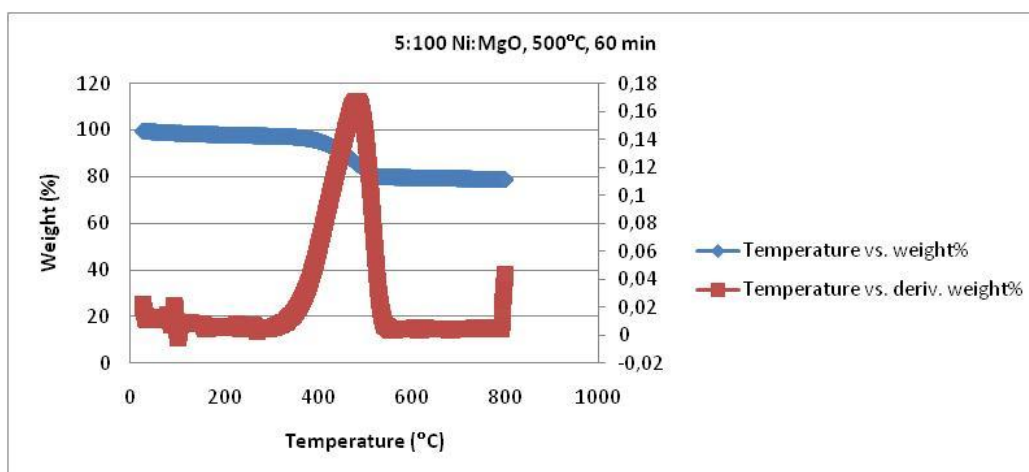

Figure A.17:TG,DTG curves of CNT synt. at 5:100 Co:MgO,500°C,60 min
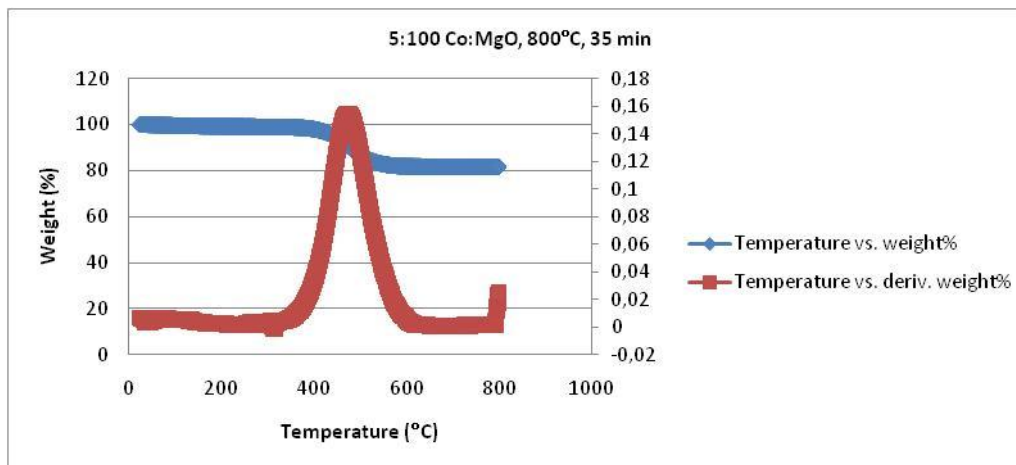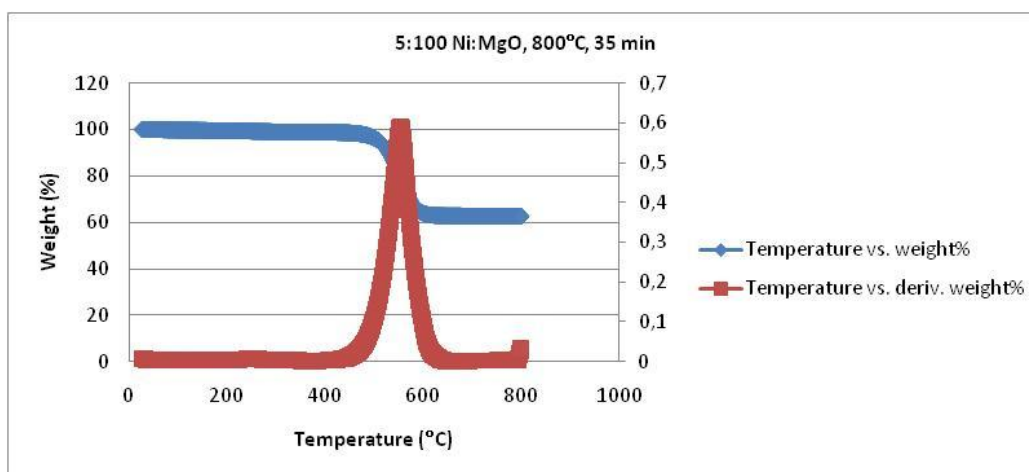

Figure A.18:TG,DTG curves of CNT synt. at 5:100 Co:MgO,800°C,35 min
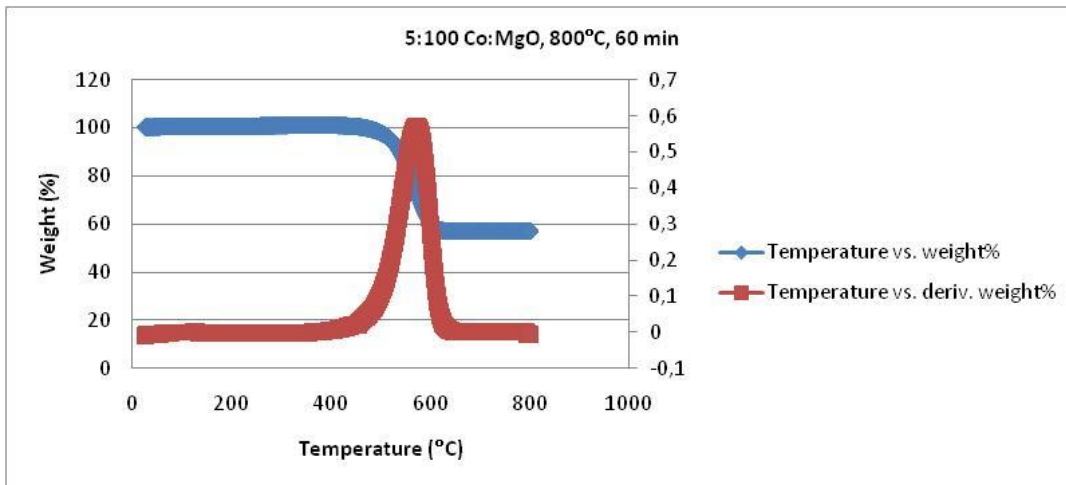
Figure A.19:TG,DTG curves of CNT synt. at 5:100 Co:MgO,800°C,60 min
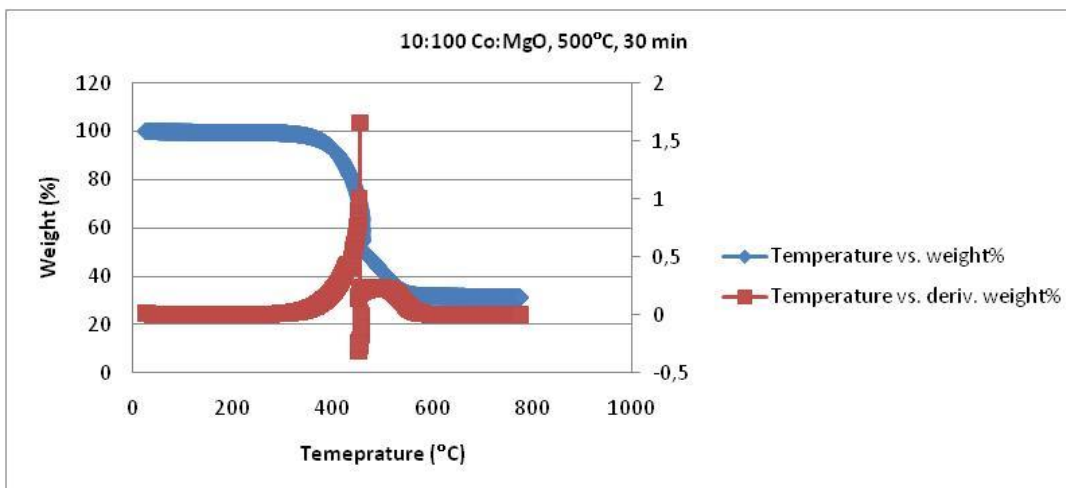
Figure A.20:TG,DTG curves of CNT synt. at 10:100 Co:MgO,500°C,30 min
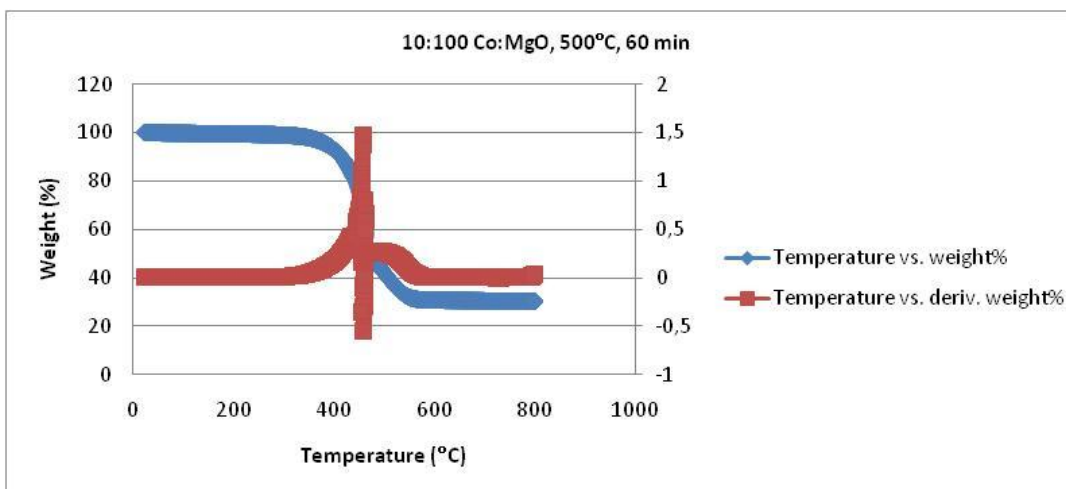
Figure A.21:TG,DTG curves of CNT synt. at 1:100 Co:MgO,500°C,30 min
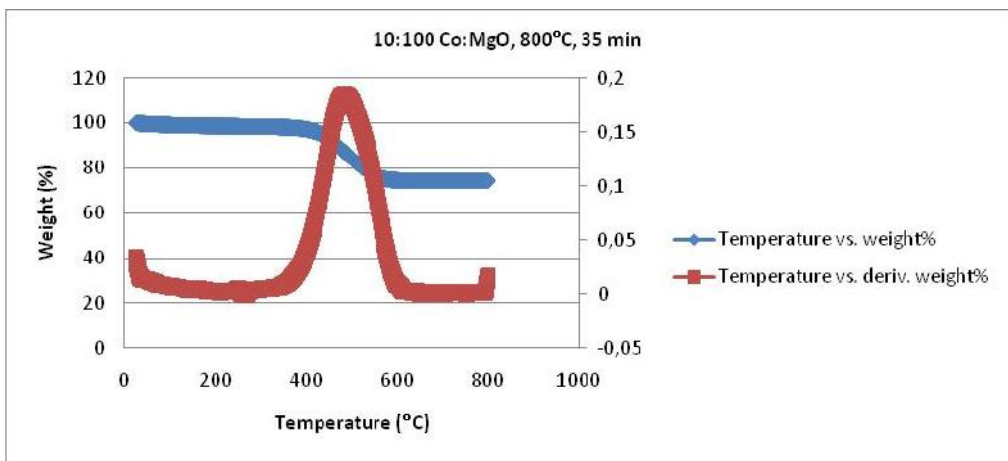
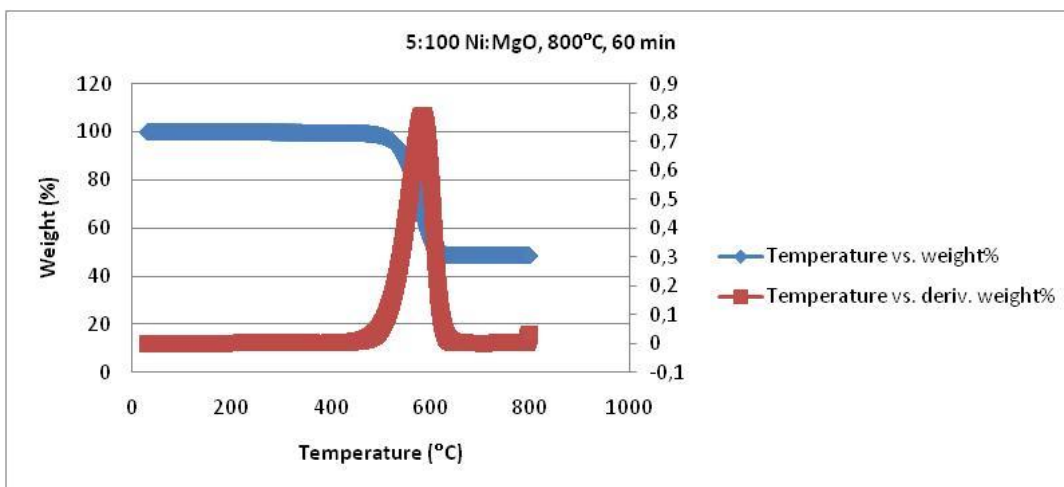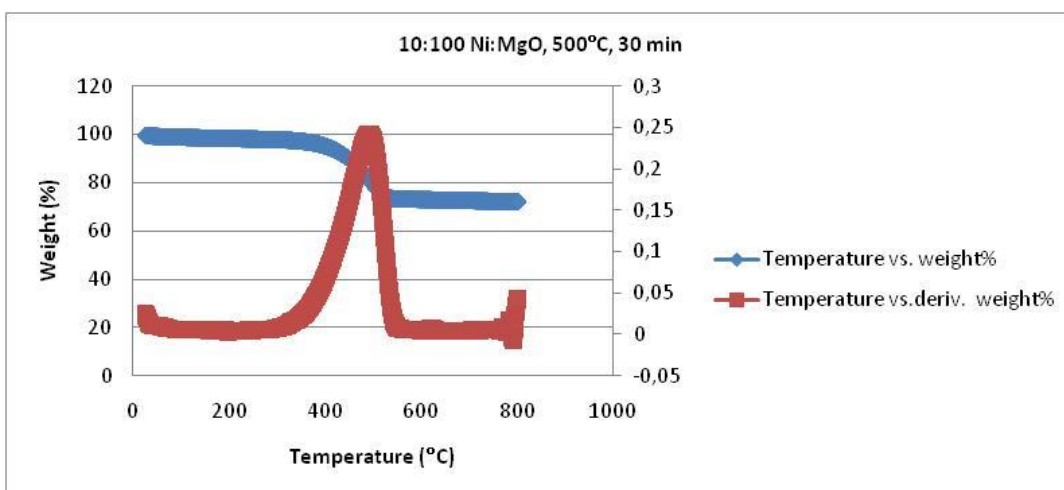**Figure A.22:**TG,DTG curves of CNT synt. at 10:100 Co:MgO,800°C,35 min
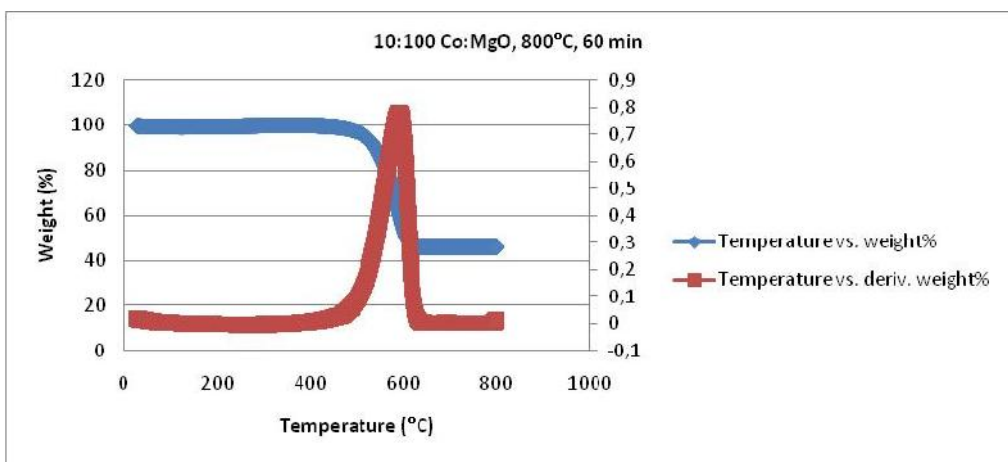
Figure A.23:TG,DTG curves of CNT synt. at 10:100 Co:MgO,800°C,60 min
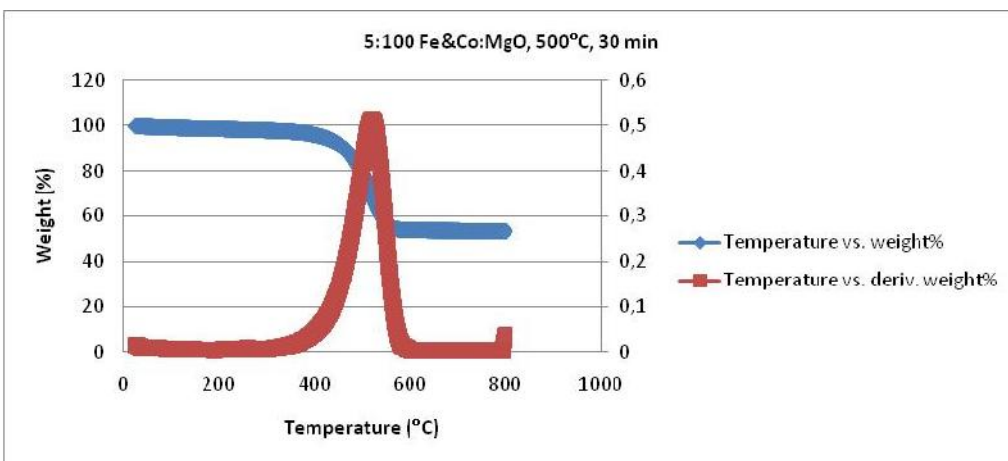
Figure A.24:TG,DTG curves of CNT synt. at 5:100 Fe&Co:MgO,500°C,30 min
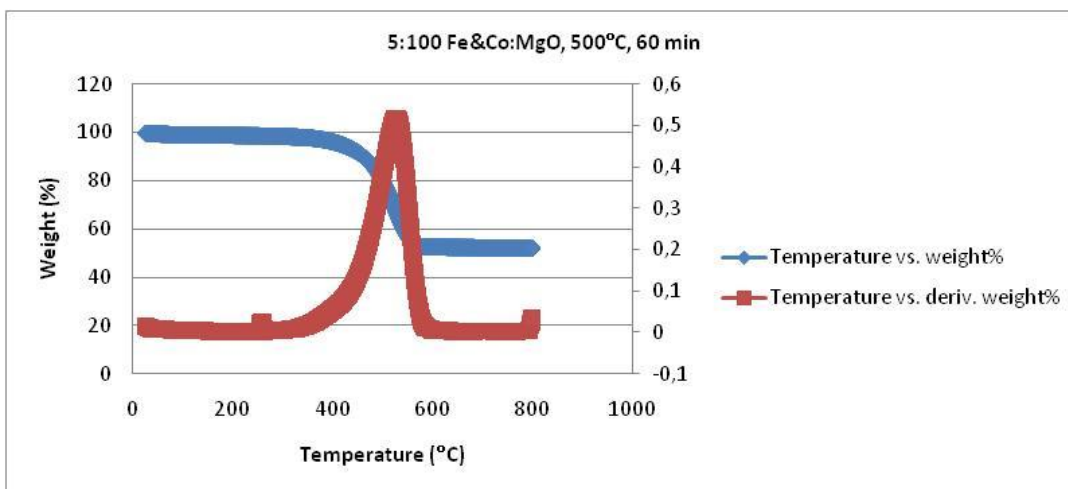
Figure A.25:TG, DTG curves of CNT synt. at 5:100 Fe&Co:MgO,500°C,60 min
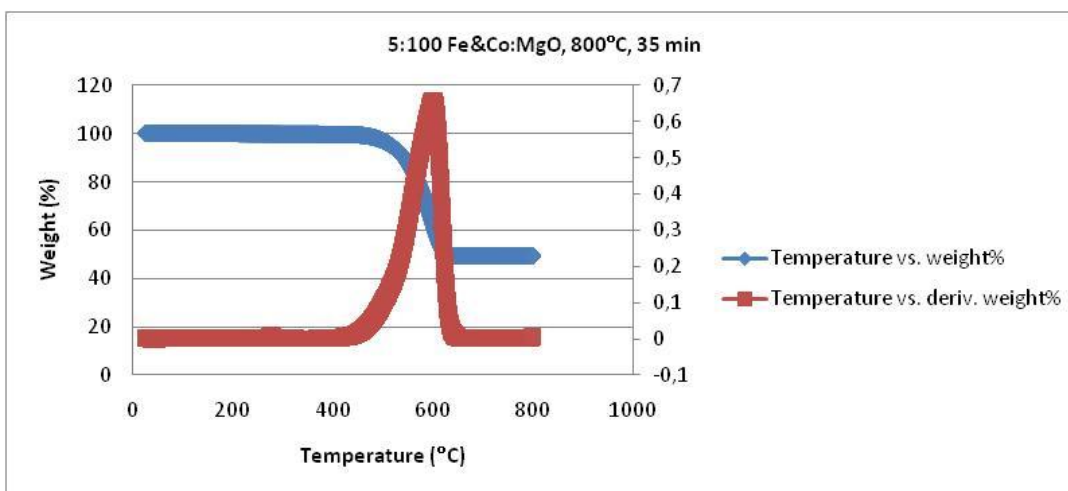
Figure A.26:TG,DTG curves of CNT synt.at 5:100 Fe&Co:MgO,800°C,35 min
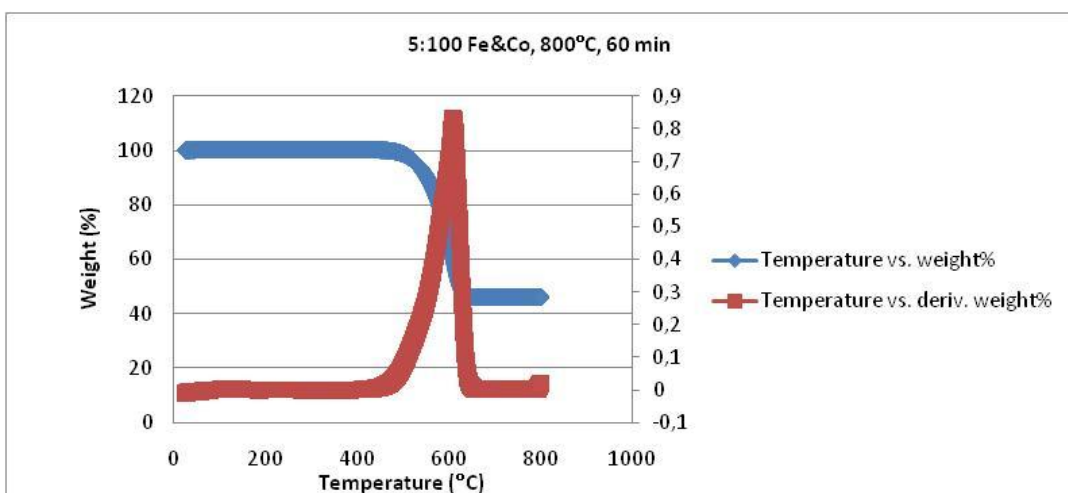
Figure A.27:TG,DTG curves of CNT synt. at 5:100 Fe&Co:MgO,800°C,60 min
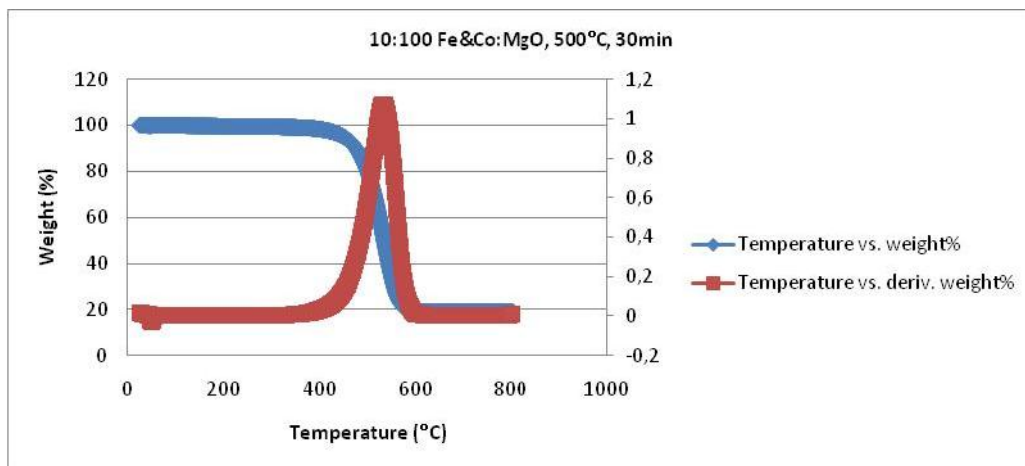
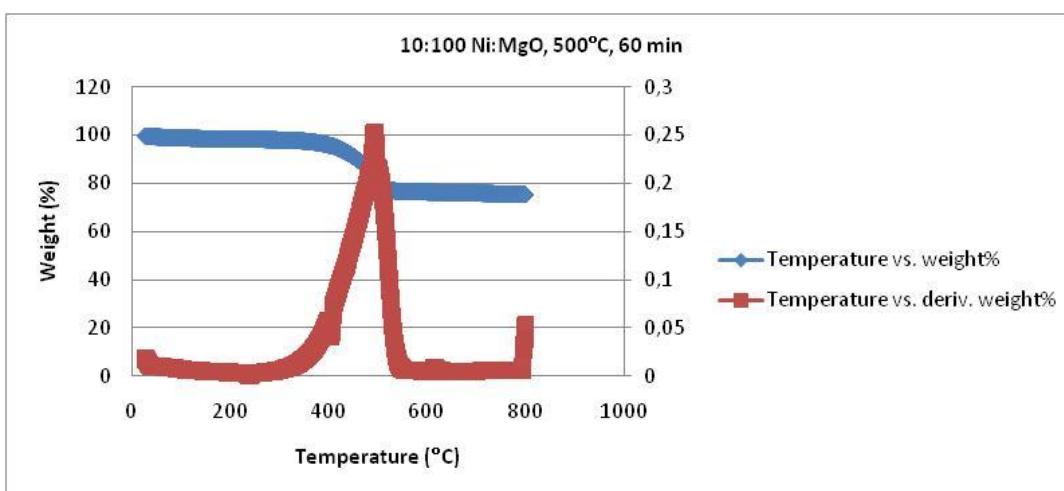**Figure A.28:**TG,DTG curves of CNT synt. at 10:100 Fe&Co:MgO,500°C,30 min

Figure A.29:TG,DTG curves of CNT synt. at 10:100 Fe&Co:MgO,500°C,60 min

Figure A.30:TG,DTG curves of CNT synt. at 10:100 Fe&Co:MgO,800°C,35 min

Figure A.31:TG,DTG curves of CNT synt. at 10:100 Fe&Co:MgO,800°C,60 min

Figure A.32:TG,DTG curves of CNT synt. at 1:100 Ni:MgO,500°C,30 min

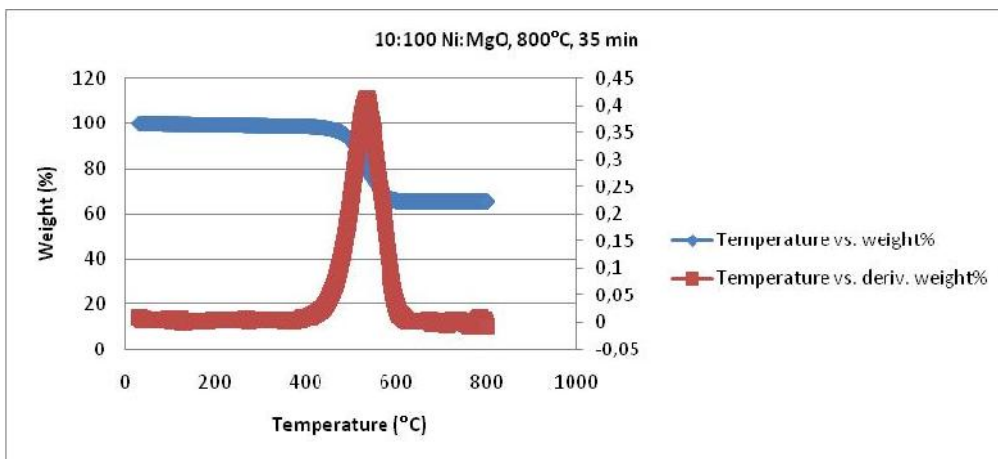**Figure A.33:**TG,DTG curves of CNT synt. at 1:100 Ni:MgO,500°C,60 min

Figure A.34:TG,DTG curves of CNT synt. at 5:100 Ni:MgO,500°C,30 min
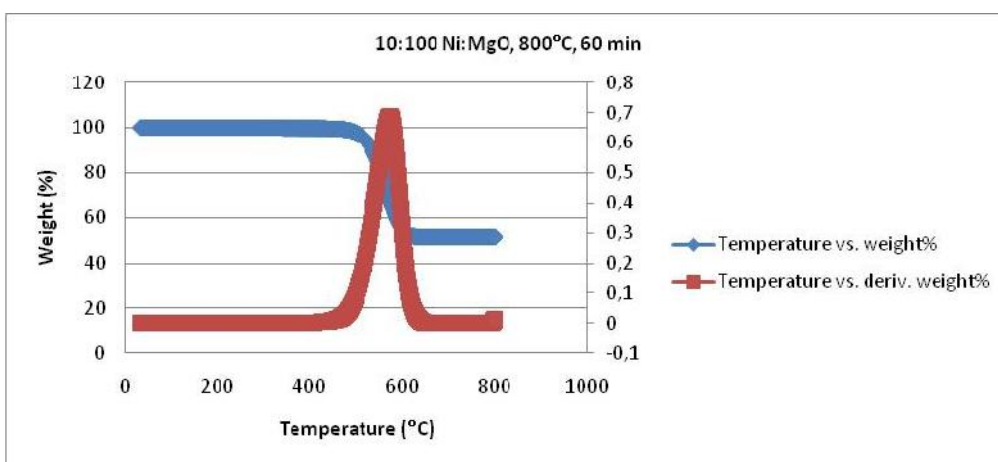

Figure A.35:TG,DTG curves of CNT synt. at 5:100 Ni:MgO,500°C,60 min

Figure A.36:TG,DTG curves of CNT synt. at 5:100 Ni:MgO,800°C,35 min

Figure A.37:TG,DTG curves of CNT synt. at 5:100 Ni:MgO,800°C,60 min

Figure A.38:TG,DTG curves of CNT synt. at 10:100 Ni:MgO,500°C,30 min

Figure A.39:TG,DTG curves of CNT synt. at 10:100 Ni:MgO,500°C,60 min

Figure A.40:TG,DTG curves of CNT synt. at 10:100 Ni:MgO,800°C,35 min

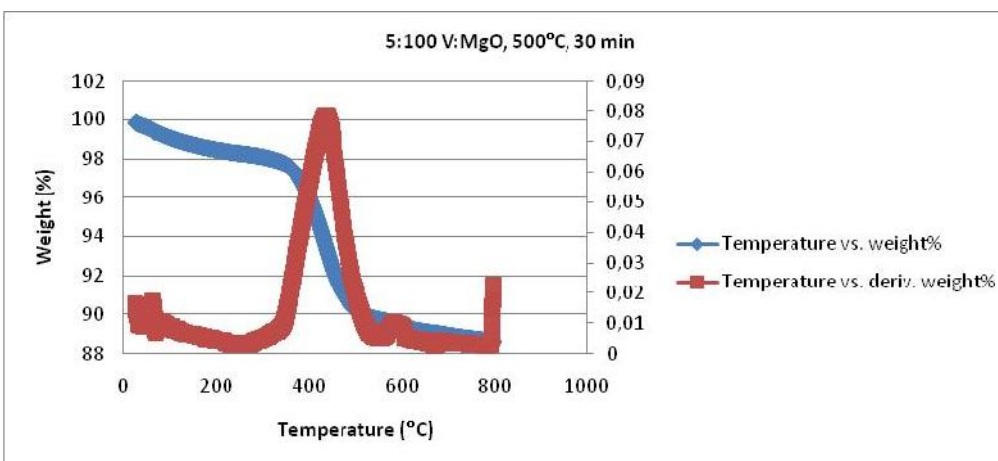**Figure A.41:**TG,DTG curves of CNT synt. at 10:100 Ni:MgO,800°C,60 min

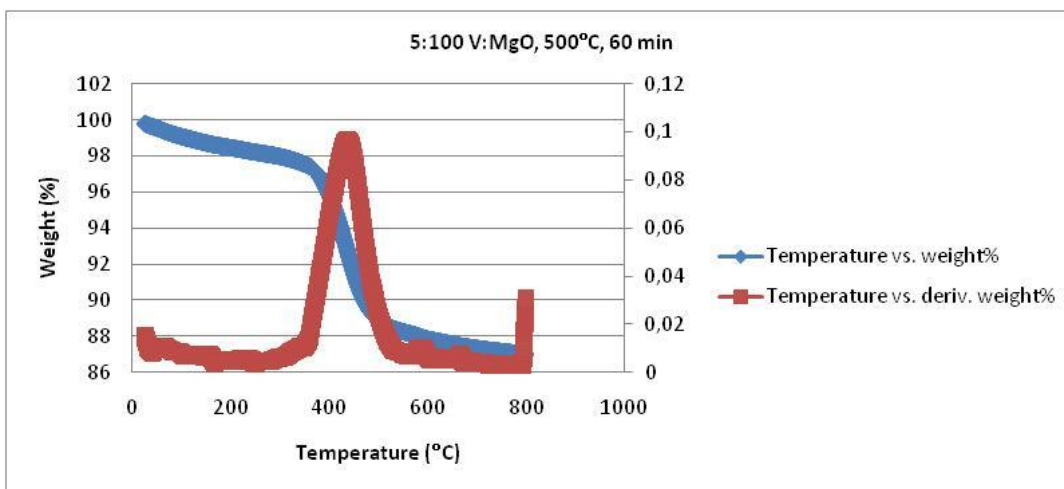**Figure A.42:**TG,DTG curves of CNT synt. at 5:100 V:MgO,500°C,30 min

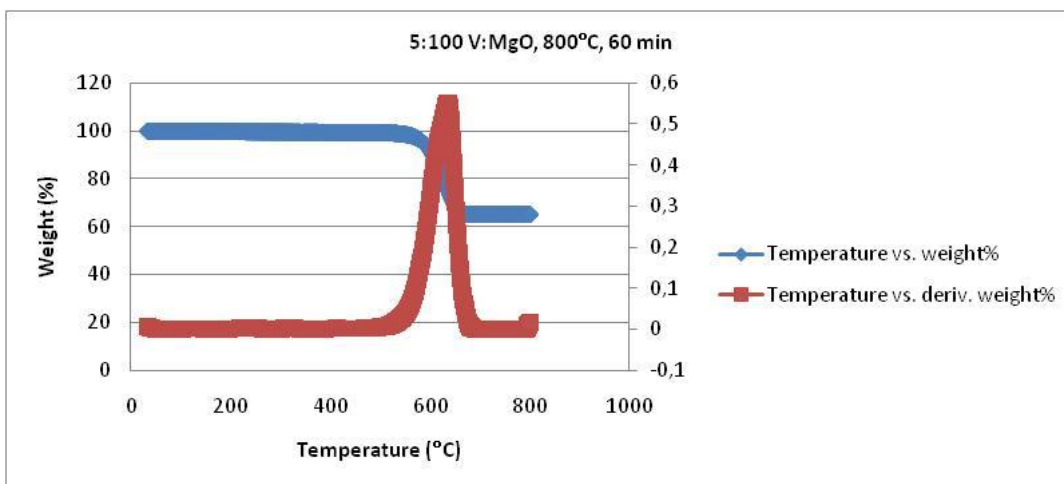**Figure A.43:**TG,DTG curves of CNT synt. at 5:100 V:MgO,500°C,60 min

Figure A.44:TG,DTG curves of CNT synt. at 5:100 V:MgO,800°C,60 min
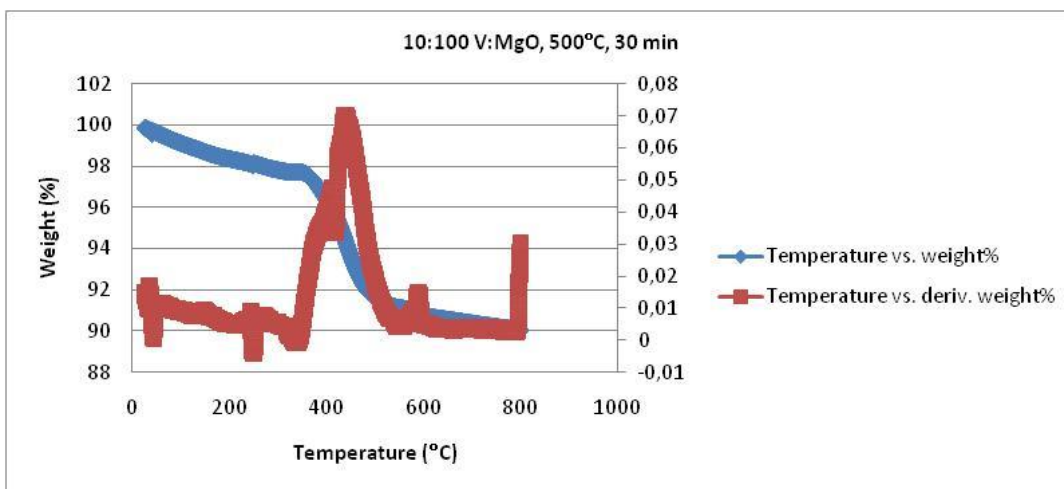

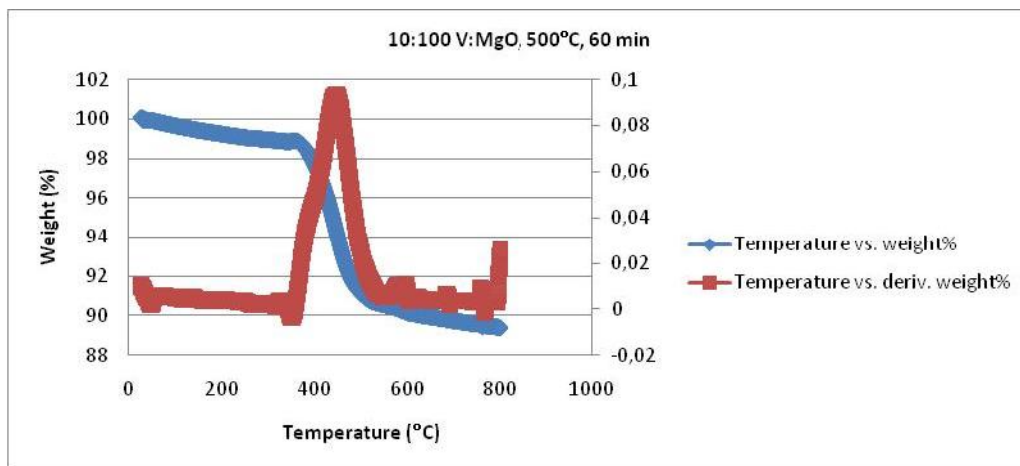**Figure A.45:**TG,DTG curves of CNT synt. at 10:100 V:MgO,500°C,30 min

Figure A.46:TG,DTG curves of CNT synt. at 10:100 V:MgO,500°C,60 min

CURRICULUM VITAE

Candidate's full name:	Ezgi DÜNDAR TEKKAYA
Place and date of birth:	Ankara, 1981
Universities and Colleges attended:	B.Sc. Metallurgical and Materials Engineering, Middle East Technical University
	M.A. International Business Administration, Northumbria University

Publications:

 Dundar E., 2006: The improvement of quality management in construction industry of Turkey after the earthquakes in 1999, Masters Dissertation.

Dundar-Tekkaya, E., Serincan, M. F., Yazıcı, M. S., 2010: Codes & Regulations on Hydrogen Production and Storage, *ICH2P-International Conference on Hydrogen Production*, June 16-18, 2010, İstanbul-Turkey